

A Simple Parameterization of Matter Effects on Neutrino Oscillations

Minako Honda,^{1,*} Yee Kao,^{2,†} Naotoshi Okamura,^{3,‡} and Tatsu Takeuchi^{2,§}

¹*Physics Department, Ochanomizu Women's University, Tokyo 112-8610, Japan.*

²*Institute for Particle Physics and Astrophysics,*

Physics Department, Virginia Tech, Blacksburg VA 24061, USA

³*Yukawa Institute for Theoretical Physics,*

Kyoto University, Kyoto 606-8502, Japan

(Dated: February 12, 2006)

Abstract

We present simple analytical approximations to matter-effect corrected effective neutrino mixing-angles and effective mass-squared-differences. The expressions clarify the dependence of oscillation probabilities in matter to the mixing angles and mass-squared-differences in vacuum, and are useful for analyzing long-baseline neutrino oscillation experiments.

PACS numbers: 13.15.+g, 14.60.Pq, 14.60.Lm

*Electronic address: minako@hep.phys.ocha.ac.jp

†Electronic address: ykao@vt.edu

‡Electronic address: okamura@yukawa.kyoto-u.ac.jp

§Electronic address: takeuchi@vt.edu

I. INTRODUCTION

The discovery of neutrino masses and mixings through solar [1, 2], atmospheric [3], and reactor [4] neutrino oscillation experiments has provided new clues to solving the mysteries of the Standard Model. Flavor mixing in the lepton-sector, together with the well-known mixing in the quark-sector, may lead to a new understanding of what ‘flavor’ is, why there are three generations of fermions, and where the quark- and lepton-mass hierarchies come from. CP violation in the neutrino-sector could potentially be large enough to account for the matter-antimatter asymmetry in the universe [5].

Due to these possibilities, several long-baseline (LBL) neutrino oscillation experiments are in progress [6, 7, 8, 9, 10] with many more being proposed [11, 12, 13, 14, 15, 16, 17] for the purpose of better determining the neutrino masses and mixing parameters. Since the neutrino beams of LBL experiments necessarily traverse the Earth, the understanding of matter effects [18] is crucial in extracting the masses and mixing parameters in vacuum from the measured oscillation probabilities in matter.

The calculation of matter effects requires the diagonalization of the effective Hamiltonian in matter, which is an energy- and matter-density-dependent 3×3 matrix. This can be done numerically on a computer with ease, but the dependence of the oscillation probabilities on the vacuum parameters is not transparent [19]. It is also possible to write down exact analytical expressions for the effective parameters in matter in terms of those in vacuum [20], but the expressions are too complicated to be illuminating. Approximate expressions for the oscillation probabilities have also been worked out, but were limited in their range of applicability [21], or still too complicated to be of practical use [22].

In this paper, we derive simple approximate expressions for the effective mass-squared-differences and mixing angles in matter, in terms of the corresponding parameters in vacuum. They are simple enough to be used by hand, yet accurate enough in a wide energy range.

This paper is organized as follows. In section II, we review the formalism of neutrino oscillations to fix our notation, and list the current experimental bounds on the mixing angles and mass-squared differences. In section III, we derive our approximate expressions for the effective mixing angles and mass-squared differences in matter, for both neutrinos and anti-neutrinos. In section IV, we provide sample calculations to illustrate the accuracy of our approximation. In section V, we present simple analytical approximations for the

oscillation probabilities and demonstrate their utility in understanding which parameters are best constrained at what baseline lengths. Section VI concludes.

II. BASICS

A. The MNS Matrix

Assuming three-generation neutrino mixing, the flavor eigenstates $|\nu_\alpha\rangle$ ($\alpha = e, \mu, \tau$) are related to the three mass eigenstates $|\nu_i\rangle$ ($i = 1, 2, 3$) via the Maki-Nakagawa-Sakata (MNS) matrix: [23]

$$(V_{\text{MNS}})_{\alpha i} \equiv \langle \nu_\alpha | \nu_i \rangle, \quad |\nu_i\rangle = \sum_{\alpha=e,\mu,\tau} (V_{\text{MNS}})_{\alpha i} |\nu_\alpha\rangle, \quad |\nu_\alpha\rangle = \sum_{i=1,2,3} (V_{\text{MNS}})_{\alpha i}^* |\nu_i\rangle. \quad (1)$$

A popular parametrization is given by [24]

$$V_{\text{MNS}} = U\mathcal{P}, \quad (2)$$

with

$$U = \begin{bmatrix} 1 & 0 & 0 \\ 0 & c_{23} & s_{23} \\ 0 & -s_{23} & c_{23} \end{bmatrix} \begin{bmatrix} c_{13} & 0 & s_{13}e^{-i\delta} \\ 0 & 1 & 0 \\ -s_{13}e^{i\delta} & 0 & c_{13} \end{bmatrix} \begin{bmatrix} c_{12} & s_{12} & 0 \\ -s_{12} & c_{12} & 0 \\ 0 & 0 & 1 \end{bmatrix} \\ = \begin{bmatrix} c_{12}c_{13} & s_{12}c_{13} & s_{13}e^{-i\delta} \\ -s_{12}c_{23} - c_{12}s_{13}s_{23}e^{i\delta} & c_{12}c_{23} - s_{12}s_{13}s_{23}e^{i\delta} & c_{13}s_{23} \\ s_{12}s_{23} - c_{12}s_{13}c_{23}e^{i\delta} & -c_{12}s_{23} - s_{12}s_{13}c_{23}e^{i\delta} & c_{13}c_{23} \end{bmatrix}, \quad (3)$$

$$\mathcal{P} = \text{diag}(e^{i\alpha_1/2}, e^{i\alpha_2/2}, 1),$$

where $s_{ij} \equiv \sin \theta_{ij}$, and $c_{ij} \equiv \cos \theta_{ij}$. Without loss of generality, we can adopt the convention $0 \leq \theta_{ij} \leq \pi/2$, $0 \leq \delta < 2\pi$ [25]. Of the six parameters in this expression and the three masses, which add up to a total of nine parameters, neutrino \rightarrow neutrino oscillations are only sensitive to six:

- the three mixing angles: $\theta_{12}, \theta_{23}, \theta_{13}$,
- two mass-squared differences: $\delta m_{21}^2, \delta m_{31}^2$, where $\delta m_{ij}^2 = m_i^2 - m_j^2$, and
- the CP-violating phase: δ .

The Majorana phases, α_1 and α_2 , only appear in lepton-number violating processes such as neutrinoless double beta decay, and cannot be determined via neutrino \rightarrow neutrino oscillations. The absolute scale of the neutrino masses also remain undetermined since neutrino oscillation is an interference effect.

B. Oscillations

If a neutrino of flavor α is created at $x = 0$ with energy E , then the state of the neutrino at $x = 0$ is

$$|\nu_{\alpha,0}(x = 0)\rangle = |\nu_{\alpha}\rangle = \sum_{i=1}^3 (V_{\text{MNS}})_{\alpha i}^* |\nu_i\rangle . \quad (4)$$

At $x = L$, the same state is

$$|\nu_{\alpha,0}(x = L)\rangle = \sum_{i=1}^3 e^{ip_i L} (V_{\text{MNS}})_{\alpha i}^* |\nu_i\rangle . \quad (5)$$

Using

$$p_i = \sqrt{E^2 - m_i^2} = E - \frac{m_i^2}{2E} + \dots , \quad (6)$$

we find

$$|\nu_{\alpha,0}(x = L)\rangle = e^{iEL} \sum_{i=1}^3 \exp\left(-i\frac{m_i^2}{2E}L\right) (V_{\text{MNS}})_{\alpha i}^* |\nu_i\rangle . \quad (7)$$

Therefore, the amplitude of observing the neutrino of flavor β at $x = L$ is given by (dropping the irrelevant overall phase)

$$\begin{aligned} & \langle \nu_{\beta} | \nu_{\alpha,0}(x = L) \rangle \\ &= \left[\sum_{j=1}^3 \langle \nu_j | (V_{\text{MNS}})_{\beta j} \right] \left[\sum_{i=1}^3 \exp\left(-i\frac{m_i^2}{2E}L\right) (V_{\text{MNS}})_{\alpha i}^* |\nu_i\rangle \right] \\ &= \sum_{j=1}^3 (V_{\text{MNS}})_{\beta j} \exp\left(-i\frac{m_j^2}{2E}L\right) (V_{\text{MNS}})_{\alpha j}^* , \end{aligned} \quad (8)$$

and the probability of oscillation from $|\nu_{\alpha}\rangle$ to $|\nu_{\beta}\rangle$ with neutrino energy E and baseline L is given by

$$\begin{aligned} P(\nu_{\alpha} \rightarrow \nu_{\beta}) &= \left| \sum_{j=1}^3 (V_{\text{MNS}})_{\beta j} \exp\left(-i\frac{m_j^2}{2E}L\right) (V_{\text{MNS}})_{\alpha j}^* \right|^2 \\ &= \delta_{\alpha\beta} - 4 \sum_{i>j} \Re(U_{\alpha i}^* U_{\beta i} U_{\alpha j} U_{\beta j}^*) \sin^2 \frac{\Delta_{ij}}{2} + 2 \sum_{i>j} \Im(U_{\alpha i}^* U_{\beta i} U_{\alpha j} U_{\beta j}^*) \sin \Delta_{ij} , \end{aligned}$$

(9)

where

$$\Delta_{ij} \equiv \frac{\delta m_{ij}^2}{2E} L = 2.534 \frac{\delta m_{ij}^2 (\text{eV}^2)}{E (\text{GeV})} L (\text{km}), \quad \delta m_{ij}^2 \equiv m_i^2 - m_j^2. \quad (10)$$

Since

$$\Delta_{32} = \Delta_{31} - \Delta_{21}, \quad (11)$$

only two of the three Δ_{ij} 's in Eq. (9) are independent. Eliminating Δ_{32} from Eq. (9), we obtain

$$\begin{aligned} P(\nu_\alpha \rightarrow \nu_\alpha) &= 1 - 4 |U_{\alpha 2}|^2 (1 - |U_{\alpha 2}|^2) \sin^2 \frac{\Delta_{21}}{2} - 4 |U_{\alpha 3}|^2 (1 - |U_{\alpha 3}|^2) \sin^2 \frac{\Delta_{31}}{2} \\ &\quad + 2 |U_{\alpha 2}|^2 |U_{\alpha 3}|^2 \left(4 \sin^2 \frac{\Delta_{21}}{2} \sin^2 \frac{\Delta_{31}}{2} + \sin \Delta_{21} \sin \Delta_{31} \right), \end{aligned} \quad (12)$$

for the $\alpha = \beta$ case, and

$$\begin{aligned} P(\nu_\alpha \rightarrow \nu_\beta) &= 4 |U_{\alpha 2}|^2 |U_{\beta 2}|^2 \sin^2 \frac{\Delta_{21}}{2} + 4 |U_{\alpha 3}|^2 |U_{\beta 3}|^2 \sin^2 \frac{\Delta_{31}}{2} \\ &\quad + 2 \Re(U_{\alpha 3}^* U_{\beta 3} U_{\alpha 2} U_{\beta 2}^*) \left(4 \sin^2 \frac{\Delta_{21}}{2} \sin^2 \frac{\Delta_{31}}{2} + \sin \Delta_{21} \sin \Delta_{31} \right) \\ &\quad + 4 J_{(\alpha, \beta)} \left(\sin^2 \frac{\Delta_{21}}{2} \sin \Delta_{31} - \sin^2 \frac{\Delta_{31}}{2} \sin \Delta_{21} \right), \end{aligned} \quad (13)$$

for the $\alpha \neq \beta$ case, where $J_{(\alpha, \beta)}$ is the Jarshog invariant:

$$\begin{aligned} J_{(\alpha, \beta)} &= +\Im(U_{\alpha 1}^* U_{\beta 1} U_{\alpha 2} U_{\beta 2}^*) = +\Im(U_{\alpha 2}^* U_{\beta 2} U_{\alpha 3} U_{\beta 3}^*) = +\Im(U_{\alpha 3}^* U_{\beta 3} U_{\alpha 1} U_{\beta 1}^*) \\ &= -\Im(U_{\alpha 2}^* U_{\beta 2} U_{\alpha 1} U_{\beta 1}^*) = -\Im(U_{\alpha 1}^* U_{\beta 1} U_{\alpha 3} U_{\beta 3}^*) = -\Im(U_{\alpha 3}^* U_{\beta 3} U_{\alpha 2} U_{\beta 2}^*) \\ &= -J_{(\beta, \alpha)}. \end{aligned} \quad (14)$$

In the parametrization given in Eq. (3), we have

$$J_{(\mu, e)} = -J_{(e, \mu)} = J_{(e, \tau)} = -J_{(\tau, e)} = J_{(\tau, \mu)} = -J_{(\mu, \tau)} = A \sin \delta, \quad (15)$$

with

$$A = s_{12} c_{12} s_{13} c_{13}^2 s_{23} c_{23}. \quad (16)$$

The oscillation probabilities for the anti-neutrinos are obtained by replacing $U_{\alpha i}$ with its complex conjugate, which only amounts to flipping the sign of δ in the parametrization of Eq. (3). It is clear from Eq. (12) that $P(\bar{\nu}_\alpha \rightarrow \bar{\nu}_\alpha) = P(\nu_\alpha \rightarrow \nu_\alpha)$, which is to be expected from the CPT theorem. For flavor changing oscillations, only the Jarshog term in Eq. (13) changes sign.

C. Current Experimental Bounds

When $|\Delta_{21}| \ll |\Delta_{31}| = O(1)$, the expressions given above can be expanded in Δ_{21} to yield

$$\begin{aligned}
P(\nu_\alpha \rightarrow \nu_\alpha) &= 1 - 4 |U_{\alpha 3}|^2 (1 - |U_{\alpha 3}|^2) \sin^2 \frac{\Delta_{31}}{2} + (2 |U_{\alpha 2}|^2 |U_{\alpha 3}|^2 \sin \Delta_{31}) \Delta_{21} \\
&\quad + |U_{\alpha 2}|^2 \left\{ 2 |U_{\alpha 3}|^2 \sin^2 \frac{\Delta_{31}}{2} - (1 - |U_{\alpha 2}|^2) \right\} \Delta_{21}^2 - \left(\frac{1}{3} |U_{\alpha 2}|^2 |U_{\alpha 3}|^2 \sin \Delta_{31} \right) \Delta_{21}^3 + O(\Delta_{21}^4) \\
&= 1 - 4 |U_{\alpha 3}|^2 (1 - |U_{\alpha 3}|^2) \sin^2 \left(\frac{\Delta_{31} - \kappa_{\alpha\alpha} \Delta_{21}}{2} \right) \\
&\quad - |U_{\alpha 1}|^2 |U_{\alpha 2}|^2 \left(1 + \frac{|U_{\alpha 3}|^2}{1 - |U_{\alpha 3}|^2} \cos \Delta_{31} \right) \Delta_{21}^2 \\
&\quad - |U_{\alpha 1}|^2 |U_{\alpha 2}|^2 |U_{\alpha 3}|^2 \left\{ \frac{1 + |U_{\alpha 2}|^2 - |U_{\alpha 3}|^2}{3(1 - |U_{\alpha 3}|^2)^2} \sin \Delta_{31} \right\} \Delta_{21}^3 + O(\Delta_{21}^4), \tag{17}
\end{aligned}$$

$$\begin{aligned}
P(\nu_\alpha \rightarrow \nu_\beta) &= 4 |U_{\alpha 3}|^2 |U_{\beta 3}|^2 \sin^2 \frac{\Delta_{31}}{2} \\
&\quad + \left\{ 2 \Re(U_{\alpha 3}^* U_{\beta 3} U_{\alpha 2} U_{\beta 2}^*) \sin \Delta_{31} - 4 J_{(\alpha,\beta)} \sin^2 \frac{\Delta_{31}}{2} \right\} \Delta_{21} \\
&\quad + \left\{ |U_{\alpha 2}|^2 |U_{\beta 2}|^2 + 2 \Re(U_{\alpha 3}^* U_{\beta 3} U_{\alpha 2} U_{\beta 2}^*) \sin^2 \frac{\Delta_{31}}{2} + J_{(\alpha,\beta)} \sin \Delta_{31} \right\} \Delta_{21}^2 \\
&\quad + \frac{1}{3} \left\{ 2 J_{(\alpha,\beta)} \sin^2 \frac{\Delta_{31}}{2} - \Re(U_{\alpha 3}^* U_{\beta 3} U_{\alpha 2} U_{\beta 2}^*) \sin \Delta_{31} \right\} \Delta_{21}^3 + O(\Delta_{21}^4) \\
&= 4 (|U_{\alpha 3}|^2 |U_{\beta 3}|^2 - J_{(\alpha,\beta)} \Delta_{21}) \sin^2 \left(\frac{\Delta_{31} - \kappa_{\alpha\beta} \Delta_{21}}{2} \right) \\
&\quad + \left\{ \frac{J_{(\alpha,\beta)}^2}{|U_{\alpha 3}|^2 |U_{\beta 3}|^2} - 2 |U_{\alpha 3}|^2 |U_{\beta 3}|^2 \kappa_{\alpha\beta} (1 - \kappa_{\alpha\beta}) \sin^2 \frac{\Delta_{31}}{2} - J_{(\alpha,\beta)} (1 - 2 \kappa_{\alpha\beta}) \sin \Delta_{31} \right\} \Delta_{21}^2 \\
&\quad - \frac{1}{3} \left\{ 3 J_{(\alpha,\beta)} \kappa_{\alpha\beta}^2 + 2 J_{(\alpha,\beta)} (1 - 3 \kappa_{\alpha\beta}^2) \sin^2 \frac{\Delta_{31}}{2} - |U_{\alpha 3}|^2 |U_{\beta 3}|^2 \kappa_{\alpha\beta} (1 - \kappa_{\alpha\beta}^2) \sin \Delta_{31} \right\} \Delta_{21}^3 \\
&\quad + O(\Delta_{21}^4), \tag{18}
\end{aligned}$$

where

$$\kappa_{\alpha\alpha} \equiv \frac{|U_{\alpha 2}|^2}{1 - |U_{\alpha 3}|^2}, \quad \kappa_{\alpha\beta} \equiv -\frac{\Re(U_{\alpha 3}^* U_{\beta 3} U_{\alpha 2} U_{\beta 2}^*)}{|U_{\alpha 3}|^2 |U_{\beta 3}|^2}. \tag{19}$$

Neglecting terms of order $O(\Delta_{21}^2)$ and higher, we obtain the following simplified expressions for a few specific processes:

$$\begin{aligned}
P(\nu_e \rightarrow \nu_e) &= 1 - 4 s_{13}^2 (1 - s_{13}^2) \sin^2 \left(\frac{\Delta_{31} - s_{12}^2 \Delta_{21}}{2} \right) \\
&= 1 - \sin^2(2\theta_{\text{rct}}) \sin^2 \left(\frac{\Delta_{31} - s_{12}^2 \Delta_{21}}{2} \right),
\end{aligned}$$

$$\begin{aligned}
P(\nu_\mu \rightarrow \nu_\mu) &= 1 - 4c_{13}^2 s_{23}^2 (1 - c_{13}^2 s_{23}^2) \sin^2 \left(\frac{\Delta_{31} - \kappa_{\mu\mu} \Delta_{21}}{2} \right) \\
&= 1 - \sin^2(2\theta_{\text{atm}}) \sin^2 \left(\frac{\Delta_{31} - \kappa_{\mu\mu} \Delta_{21}}{2} \right) , \\
P(\nu_\mu \rightarrow \nu_e) &= 4(c_{13}^2 s_{13}^2 s_{23}^2 - J_{(\mu,e)} \Delta_{21}) \sin^2 \left(\frac{\Delta_{31} - \kappa_{\mu e} \Delta_{21}}{2} \right) \\
&= 4(\sin^2 \theta_{\text{rct}} \sin^2 \theta_{\text{atm}} - A \sin \delta \Delta_{21}) \sin^2 \left(\frac{\Delta_{31} - \kappa_{\mu e} \Delta_{21}}{2} \right) , \tag{20}
\end{aligned}$$

where

$$\begin{aligned}
A &= \frac{1}{8} \sin(2\theta_{12}) \sin(2\theta_{\text{rct}}) \sin(2\theta_{\text{atm}}) \sqrt{1 - \tan^2 \theta_{\text{rct}} \tan^2 \theta_{\text{atm}}} , \\
\kappa_{\mu\mu} &= c_{12}^2 - (c_{12}^2 - s_{12}^2) \tan^2 \theta_{\text{rct}} \tan^2 \theta_{\text{atm}} - \left(\frac{2A}{\cos^2 \theta_{\text{rct}} \cos^2 \theta_{\text{atm}}} \right) \cos \delta , \\
\kappa_{\mu e} &= s_{12}^2 - \left(\frac{A}{\sin^2 \theta_{\text{rct}} \sin^2 \theta_{\text{atm}}} \right) \cos \delta . \tag{21}
\end{aligned}$$

We have made the identifications

$$\begin{aligned}
\sin \theta_{\text{atm}} &= s_{23} c_{13} = \sin \theta_{23} \cos \theta_{13} , \\
\sin \theta_{\text{rct}} &= s_{13} = \sin \theta_{13} , \tag{22}
\end{aligned}$$

where θ_{atm} and θ_{rct} are the mixing angles extracted from atmospheric [3] and reactor [4] neutrino oscillation experiments, respectively, based on two-flavor oscillation analyses. The current experimental bounds from atmospheric neutrinos at the 90% confidence level are

$$\begin{aligned}
|\delta m_{31}^2| &= (1.5 \sim 3.4) \times 10^{-3} \text{ eV}^2 , \\
\sin^2(2\theta_{\text{atm}}) &> 0.92 . \tag{23}
\end{aligned}$$

Only the absolute value of δm_{31}^2 is known since $P(\nu_\mu \rightarrow \nu_\mu) = 1 - \sin^2(2\theta_{\text{atm}}) \sin^2(\Delta_{31}/2)$ at leading order in Δ_{21} . The 90% confidence limit on $\theta_{\text{rct}} = \theta_{13}$ from the CHOOZ experiment, which measured $P(\bar{\nu}_e \rightarrow \bar{\nu}_e) = 1 - \sin^2(2\theta_{\text{rct}}) \sin^2(\Delta_{31}/2)$, depends on the not-yet-well-known value of $|\delta m_{31}^2|$:

$$\begin{aligned}
\sin^2(2\theta_{\text{rct}}) &< 0.20 && \text{for } |\delta m_{31}^2| = 2.0 \times 10^{-3} \text{ eV}^2 , \\
\sin^2(2\theta_{\text{rct}}) &< 0.16 && \text{for } |\delta m_{31}^2| = 2.5 \times 10^{-3} \text{ eV}^2 , \\
\sin^2(2\theta_{\text{rct}}) &< 0.14 && \text{for } |\delta m_{31}^2| = 3.0 \times 10^{-3} \text{ eV}^2 . \tag{24}
\end{aligned}$$

When $|\Delta_{31}| \gg |\Delta_{21}| = O(1)$, $P(\nu_e \rightarrow \nu_e)$ simplifies to

$$P(\nu_e \rightarrow \nu_e) = 1 - 2|U_{e3}|^2 (1 - |U_{e3}|^2) - 4|U_{e1}|^2 |U_{e2}|^2 \sin^2 \frac{\Delta_{21}}{2}$$

$ \delta m_{31}^2 $ (eV ²)	$\varepsilon = \sqrt{\frac{\delta m_{21}^2}{ \delta m_{31}^2 }}$	Upper bound on θ_{13}
2.0×10^{-3}	$0.20 \sim 0.21$	0.23
2.5×10^{-3}	$0.18 \sim 0.19$	0.21
3.0×10^{-3}	$0.16 \sim 0.17$	0.19

TABLE I: Comparison of the size of the ratio $\delta m_{21}^2/|\delta m_{31}^2|$ and the 90% confidence limit on θ_{13} .

$$\begin{aligned}
&= 1 - 2s_{13}^2(1 - s_{13}^2) - 4c_{12}^2s_{12}^2c_{13}^4 \sin^2 \frac{\Delta_{21}}{2} \\
&= 1 - \sin^2(2\theta_{12}) \sin^2 \frac{\Delta_{21}}{2} + O(s_{13}^2) .
\end{aligned} \tag{25}$$

Since s_{13} is known to be small from CHOOZ, we can identify θ_{12} with the 2-flavor solar mixing angle θ_{sol} . The current experimental bounds at the 90% confidence level from solar neutrinos are [1, 2]

$$\begin{aligned}
\delta m_{21}^2 &= 8.2_{-0.5}^{+0.6} \times 10^{-5} \text{ eV}^2 , \\
\tan^2 \theta_{\text{sol}} &= 0.40_{-0.07}^{+0.09} .
\end{aligned} \tag{26}$$

The sign of $\delta m_{21}^2 = m_2^2 - m_1^2$ is known to be positive since $m_2^2 > m_1^2$ is required for the MSW effect [18] to work.

D. The Sizes of θ_{13} , θ_{12} , and θ_{23}

If we allow both δm_{21}^2 and $|\delta m_{31}^2|$ to move within their respective 90% confidence limits given in Eqs. (23) and (26), the ratio of the two is in the range

$$\frac{\delta m_{21}^2}{|\delta m_{31}^2|} = 0.023 \sim 0.059 . \tag{27}$$

Thus, the approximation $\Delta_{21} \ll |\Delta_{31}|$ that was used above is justified. The square-root of this ratio, which we will call ε , is in the range

$$\varepsilon \equiv \sqrt{\frac{\delta m_{21}^2}{|\delta m_{31}^2|}} = 0.15 \sim 0.24 . \tag{28}$$

Note that ε is roughly in the same range as that of the 90% upper bound on θ_{13} which can be obtained from Eq. (24). In fact, the two numbers are positively correlated as shown in TABLE I.

While we currently have no experimental lower bound on θ_{13} , many analyses of LBL experiments only consider cases where $\sin^2(2\theta_{13}) > 0.04$, which corresponds to $\theta_{13} > 0.1$, since smaller values of θ_{13} would put $P(\nu_\mu \rightarrow \nu_e)$ below detectable range. Therefore, we will assume that θ_{13} is of order ε in the following. However, the formulae we derive below can be applied as is to cases in which θ_{13} is smaller, since we only use the size of θ_{13} to decide when terms containing s_{13} can be neglected. A smaller θ_{13} will simply make those terms even more negligible.

The 90% confidence limits on the solar mixing angle given in Eq. (26) translates into

$$\theta_{12} = 0.56_{-0.04}^{+0.05} = (0.18 \pm 0.01)\pi , \quad (29)$$

and

$$\begin{aligned} s_{12} &= 0.50 \sim 0.57 , \\ c_{12} &= 0.82 \sim 0.87 , \\ \sin(2\theta_{12}) &= 0.86 \sim 0.94 , \\ \cos(2\theta_{12}) &= 0.34 \sim 0.50 . \end{aligned} \quad (30)$$

Being sines and cosines, the upper end of these ranges are always smaller than one. However, s_{12} , c_{12} , and $\sin(2\theta_{12})$ are still much larger than ε so we will treat them, and also θ_{12} , as numbers of order 1. On the other hand, $\cos(2\theta_{12})$ is only slightly larger than ε . Its range is roughly equal to that of 2ε . Therefore, we can consider $\cos(2\theta_{12})/2$ as a number of order ε .

The 90% confidence limits on the atmospheric mixing angle given in Eq. (23) translates to

$$\theta_{\text{atm}} = 0.64 \sim 0.93 = (0.25 \pm 0.05)\pi . \quad (31)$$

Though we made the identification $\sin \theta_{\text{atm}} = s_{23}c_{13}$ in Eq. (22), the limits on θ_{23} are virtually identical to those of θ_{atm} due to the smallness of θ_{13} . We can therefore assume

$$\begin{aligned} s_{23} &= 0.60 \sim 0.80 , \\ c_{23} &= 0.60 \sim 0.80 , \\ \sin(2\theta_{23}) &> 0.96 , \\ |\cos(2\theta_{23})| &< 0.28 . \end{aligned} \quad (32)$$

As in the case of θ_{12} , we can assume s_{23} , c_{23} , $\sin(2\theta_{23})$, and θ_{23} to be numbers of order 1, while $\cos(2\theta_{23})$ is of order ε or smaller.

III. MATTER EFFECTS

A. Diagonalization of the Effective Neutrino Hamiltonian

If the matter density along the baseline is constant, matter effects on neutrino oscillations can be taken into account by simply replacing the MNS matrix elements and mass-squared differences with their “effective” values in matter:

$$\Delta_{ij} \rightarrow \tilde{\Delta}_{ij}, \quad U_{\alpha i} \rightarrow \tilde{U}_{\alpha i}, \quad (33)$$

where \tilde{U} is the unitary matrix that diagonalizes the modified Hamiltonian,

$$H = \tilde{U} \begin{bmatrix} \lambda_1 & 0 & 0 \\ 0 & \lambda_2 & 0 \\ 0 & 0 & \lambda_3 \end{bmatrix} \tilde{U}^\dagger = U \begin{bmatrix} 0 & 0 & 0 \\ 0 & \delta m_{21}^2 & 0 \\ 0 & 0 & \delta m_{31}^2 \end{bmatrix} U^\dagger + \begin{bmatrix} a & 0 & 0 \\ 0 & 0 & 0 \\ 0 & 0 & 0 \end{bmatrix}, \quad (34)$$

and

$$\tilde{\Delta}_{ij} = \frac{\delta\lambda_{ij}}{2E} L, \quad \delta\lambda_{ij} = \lambda_i - \lambda_j. \quad (35)$$

The factor a is due to the interaction of the $|\nu_e\rangle$ component of the neutrinos with the electrons in matter via W -exchange:

$$a = 2\sqrt{2} G_F N_e E = 7.63 \times 10^{-5} (\text{eV})^2 \left(\frac{\rho}{\text{g/cm}^3} \right) \left(\frac{E}{\text{GeV}} \right). \quad (36)$$

Note that a is E -dependent, which means that both \tilde{U} and $\tilde{\Delta}_{ij}$ are also E -dependent. It is also assumed that $E \ll M_W$ since the W -exchange interaction is approximated by a point-like four-fermion interaction in deriving this expression.

To see the effect of a , we introduce the matrix

$$\mathcal{Q} = \text{diag}(1, 1, e^{i\delta}), \quad (37)$$

and start with the partially diagonalized Hamiltonian:

$$\begin{aligned} H' &= \mathcal{Q}^\dagger U^\dagger H U \mathcal{Q} \\ &= \mathcal{Q}^\dagger \left\{ \begin{bmatrix} 0 & 0 & 0 \\ 0 & \delta m_{21}^2 & 0 \\ 0 & 0 & \delta m_{31}^2 \end{bmatrix} + U^\dagger \begin{bmatrix} a & 0 & 0 \\ 0 & 0 & 0 \\ 0 & 0 & 0 \end{bmatrix} U \right\} \mathcal{Q} \end{aligned}$$

$$\begin{aligned}
&= \mathcal{Q}^\dagger \begin{bmatrix} 0 & 0 & 0 \\ 0 & \delta m_{21}^2 & 0 \\ 0 & 0 & \delta m_{31}^2 \end{bmatrix} \mathcal{Q} + a \mathcal{Q}^\dagger \begin{bmatrix} U_{e1}^* U_{e1} & U_{e1}^* U_{e2} & U_{e1}^* U_{e3} \\ U_{e2}^* U_{e1} & U_{e2}^* U_{e2} & U_{e2}^* U_{e3} \\ U_{e3}^* U_{e1} & U_{e3}^* U_{e2} & U_{e3}^* U_{e3} \end{bmatrix} \mathcal{Q} \\
&= \begin{bmatrix} 0 & 0 & 0 \\ 0 & \delta m_{21}^2 & 0 \\ 0 & 0 & \delta m_{31}^2 \end{bmatrix} + a \begin{bmatrix} c_{12}^2 c_{13}^2 & c_{12} s_{12} c_{13}^2 & c_{12} c_{13} s_{13} \\ c_{12} s_{12} c_{13}^2 & s_{12}^2 c_{13}^2 & s_{12} c_{13} s_{13} \\ c_{12} c_{13} s_{13} & s_{12} c_{13} s_{13} & s_{13}^2 \end{bmatrix} \\
&= \begin{bmatrix} a c_{12}^2 c_{13}^2 & a c_{12} s_{12} c_{13}^2 & a c_{12} c_{13} s_{13} \\ a c_{12} s_{12} c_{13}^2 & a s_{12}^2 c_{13}^2 + \delta m_{21}^2 & a s_{12} c_{13} s_{13} \\ a c_{12} c_{13} s_{13} & a s_{12} c_{13} s_{13} & a s_{13}^2 + \delta m_{31}^2 \end{bmatrix}. \tag{38}
\end{aligned}$$

The matrix \mathcal{Q} serves to rid H' of any reference to the CP violating phase δ . Our strategy is to approximately diagonalize H' through the Jacobi method using $\varepsilon = \sqrt{\delta m_{21}^2 / |\delta m_{31}^2|}$ as the expansion parameter. We assume $\theta_{13} = O(\varepsilon)$ as discussed above. Corrections to the eigenvalues of H' of order $\varepsilon^3 |\delta m_{31}^2|$ and higher, and those to the elements of \tilde{U} of order ε^3 and higher will be neglected. For $\varepsilon = 0.15 \sim 0.24$, we have $\varepsilon^3 = 0.0034 \sim 0.014$.

Recall that for 2×2 real symmetric matrices, such as

$$M = \begin{bmatrix} \alpha & \beta \\ \beta & \gamma \end{bmatrix}, \quad \alpha, \beta, \gamma \in \mathbb{R}, \tag{39}$$

diagonalization is trivial. Just define

$$R = \begin{bmatrix} c_\omega & s_\omega \\ -s_\omega & c_\omega \end{bmatrix}, \quad \text{where} \quad c_\omega = \cos \omega, \quad s_\omega = \sin \omega, \quad \tan 2\omega \equiv \frac{2\beta}{\gamma - \alpha}, \tag{40}$$

and we obtain

$$R^\dagger M R = \begin{bmatrix} \Lambda_1 & 0 \\ 0 & \Lambda_2 \end{bmatrix}, \tag{41}$$

with

$$\Lambda_1 = \frac{\alpha c_\omega^2 - \gamma s_\omega^2}{c_\omega^2 - s_\omega^2}, \quad \Lambda_2 = \frac{\gamma c_\omega^2 - \alpha s_\omega^2}{c_\omega^2 - s_\omega^2}. \tag{42}$$

The Jacobi method entails iteratively diagonalizing 2×2 submatrices of a larger matrix in the order that requires the largest rotation angle at each step. In the case of H' , as we will show below, two iterations at most are sufficient to achieve approximate diagonalization to the order required, regardless of the size of a .

In the following, we will consider the five cases $a/|\delta m_{31}^2| = O(\varepsilon^3)$, $O(\varepsilon^2)$, $O(\varepsilon)$, $O(1)$, and $O(\varepsilon^{-1})$ separately. Values of $a/|\delta m_{31}^2|$ outside this range can be treated in a similar manner as the $O(\varepsilon^3)$ and $O(\varepsilon^{-1})$ cases. (For conditions on the Earth, however, $a/|\delta m_{31}^2| \geq O(\varepsilon^{-2})$ implies $E > M_W$, invalidating our approximation.)

A1. $a/|\delta m_{31}^2| = O(\varepsilon^3)$ case

We begin by considering the case $a/|\delta m_{31}^2| = O(\varepsilon^3)$. Treating both c_{12} and s_{12} as numbers of order 1, and s_{13} as a number of order ε , the relative sizes of the elements of H' are given by

$$H' = \begin{bmatrix} ac_{12}^2 c_{13}^2 & ac_{12} s_{12} c_{13}^2 & ac_{12} c_{13} s_{13} \\ ac_{12} s_{12} c_{13}^2 & as_{12}^2 c_{13}^2 + \delta m_{21}^2 & as_{12} c_{13} s_{13} \\ ac_{12} c_{13} s_{13} & as_{12} c_{13} s_{13} & as_{13}^2 + \delta m_{31}^2 \end{bmatrix} = |\delta m_{31}^2| \begin{bmatrix} O(\varepsilon^3) & O(\varepsilon^3) & O(\varepsilon^4) \\ O(\varepsilon^3) & O(\varepsilon^2) & O(\varepsilon^4) \\ O(\varepsilon^4) & O(\varepsilon^4) & O(1) \end{bmatrix}. \quad (43)$$

Of the three 2×2 submatrices of H' , the one which is farthest from diagonal is the (1, 2) submatrix since it requires an $O(\varepsilon)$ rotation to diagonalize, while the other two submatrices only require $O(\varepsilon^4)$ rotations. To diagonalize the (1, 2) submatrix of H' , we define

$$V = \begin{bmatrix} c_\varphi & s_\varphi & 0 \\ -s_\varphi & c_\varphi & 0 \\ 0 & 0 & 1 \end{bmatrix}, \quad (44)$$

where

$$c_\varphi = \cos \varphi, \quad s_\varphi = \sin \varphi, \quad \tan 2\varphi \equiv \frac{ac_{13}^2 \sin 2\theta_{12}}{\delta m_{21}^2 - ac_{13}^2 \cos 2\theta_{12}}, \quad \left(0 \leq \varphi < \frac{\pi}{2}\right). \quad (45)$$

Using V , we find

$$H'' = V^\dagger H' V = \begin{bmatrix} \lambda'_1 & 0 & ac'_{12} c_{13} s_{13} \\ 0 & \lambda'_2 & as'_{12} c_{13} s_{13} \\ ac'_{12} c_{13} s_{13} & as'_{12} c_{13} s_{13} & as_{13}^2 + \delta m_{31}^2 \end{bmatrix}, \quad (46)$$

where

$$c'_{12} = \cos \theta'_{12}, \quad s'_{12} = \sin \theta'_{12}, \quad \theta'_{12} = \theta_{12} + \varphi, \quad (47)$$

and

$$\lambda'_1 = \frac{(ac_{12}^2 c_{13}^2) c_\varphi^2 - (as_{12}^2 c_{13}^2 + \delta m_{21}^2) s_\varphi^2}{c_\varphi^2 - s_\varphi^2} = \lambda'_-,$$

$$\lambda'_2 = \frac{(as_{12}^2 c_{13}^2 + \delta m_{21}^2) c_\varphi^2 - (ac_{12}^2 c_{13}^2) s_\varphi^2}{c_\varphi^2 - s_\varphi^2} = \lambda'_+, \quad (48)$$

with

$$\lambda'_\pm = \frac{(ac_{13}^2 + \delta m_{21}^2) \pm \sqrt{(ac_{13}^2 - \delta m_{21}^2)^2 + 4ac_{13}^2 s_{12}^2 \delta m_{21}^2}}{2}. \quad (49)$$

Note that

$$\tan 2\theta'_{12} = \frac{\tan 2\theta_{12} + \tan 2\varphi}{1 - \tan 2\theta_{12} \tan 2\varphi} = \frac{\delta m_{21}^2 \sin 2\theta_{12}}{\delta m_{21}^2 \cos 2\theta_{12} - ac_{13}^2}, \quad (50)$$

which can be used to calculate θ'_{12} without calculating φ first.

Since $a/|\delta m_{31}^2| = O(\varepsilon^3)$, which means that $a/\delta m_{21}^2 = O(\varepsilon)$, we can expand λ'_1 , λ'_2 , and φ in powers of $a/\delta m_{21}^2$ and $s_{13} = O(\varepsilon)$. We find

$$\begin{aligned} \lambda'_1 &= ac_{12}^2 + O(\varepsilon^4 |\delta m_{31}^2|) = O(\varepsilon^3 |\delta m_{31}^2|), \\ \lambda'_2 &= \delta m_{21}^2 + as_{12}^2 + O(\varepsilon^4 |\delta m_{31}^2|) = \delta m_{21}^2 + O(\varepsilon^3 |\delta m_{31}^2|) = O(\varepsilon^2 |\delta m_{31}^2|), \end{aligned} \quad (51)$$

and,

$$\begin{aligned} \varphi &= \frac{1}{2} \left(\frac{ac_{13}^2}{\delta m_{21}^2} \right) \sin(2\theta_{12}) + \frac{1}{2} \left(\frac{ac_{13}^2}{\delta m_{21}^2} \right)^2 \sin(2\theta_{12}) \cos(2\theta_{12}) + \dots \\ &= \frac{a}{2\delta m_{21}^2} \sin(2\theta_{12}) + O(\varepsilon^3) = O(\varepsilon), \end{aligned}$$

$$\theta'_{12} = \theta_{12} + \varphi = \theta_{12} + \frac{a}{2\delta m_{21}^2} \sin(2\theta_{12}) + O(\varepsilon^3) = O(1). \quad (52)$$

Note that the second term in the expansion of φ can be considered to be of order ε^3 since $\cos(2\theta_{12})/2$ is of order ε as discussed in the previous section. Therefore, the sizes of the elements of H'' are

$$H'' = \begin{bmatrix} \lambda'_1 & 0 & ac'_{12} c_{13} s_{13} \\ 0 & \lambda'_2 & as'_{12} c_{13} s_{13} \\ ac'_{12} c_{13} s_{13} & as'_{12} c_{13} s_{13} & as_{13}^2 + \delta m_{31}^2 \end{bmatrix} = |\delta m_{31}^2| \begin{bmatrix} O(\varepsilon^3) & 0 & O(\varepsilon^4) \\ 0 & O(\varepsilon^2) & O(\varepsilon^4) \\ O(\varepsilon^4) & O(\varepsilon^4) & O(1) \end{bmatrix}. \quad (53)$$

The rotation angles required to diagonalize the (1, 3) or (2, 3) submatrices are of order ε^4 , which we will neglect. So in this case, the Hamiltonian is approximately diagonalized by one (1, 2) rotation of angle $O(\varepsilon)$, and the eigenvalues are

$$\begin{aligned} \lambda_1 &\approx \lambda'_1 \approx ac_{12}^2, \\ \lambda_2 &\approx \lambda'_2 \approx \delta m_{21}^2 + as_{12}^2, \\ \lambda_3 &\approx \delta m_{31}^2. \end{aligned} \quad (54)$$

We have kept terms up to $O(\varepsilon^3 |\delta m_{31}^2|)$ here to show how the eigenvalues are shifted away from their vacuum values.

A2. $a/|\delta m_{31}^2| = O(\varepsilon^2)$ case

Next, we consider the case $a/|\delta m_{31}^2| = O(\varepsilon^2)$. The relative sizes of the elements of H' in this case are

$$H' = \begin{bmatrix} ac_{12}^2 c_{13}^2 & ac_{12} s_{12} c_{13}^2 & ac_{12} c_{13} s_{13} \\ ac_{12} s_{12} c_{13}^2 & as_{12}^2 c_{13}^2 + \delta m_{21}^2 & as_{12} c_{13} s_{13} \\ ac_{12} c_{13} s_{13} & as_{12} c_{13} s_{13} & as_{13}^2 + \delta m_{31}^2 \end{bmatrix} = |\delta m_{31}^2| \begin{bmatrix} O(\varepsilon^2) & O(\varepsilon^2) & O(\varepsilon^3) \\ O(\varepsilon^2) & O(\varepsilon^2) & O(\varepsilon^3) \\ O(\varepsilon^3) & O(\varepsilon^3) & O(1) \end{bmatrix}, \quad (55)$$

and again we find that we must diagonalize the (1, 2) submatrix first. We define V and φ as in Eqs. (44) and (45), and the matrix will be partially diagonalized to H'' in Eq. (46), with λ'_1 , λ'_2 , and θ'_{12} defined as in Eqs. (47) and (48). Since a and δm_{21}^2 are of the same order in this case, both $\tan(2\varphi)$ of Eq. (45) and $\tan(2\theta'_{12})$ of Eq. (50) can be expected to be large. Therefore, both s'_{12} and c'_{12} can be considered to be numbers of order 1 in this case also, and the relative sizes of the elements of H'' are

$$H'' = \begin{bmatrix} \lambda'_1 & 0 & ac'_{12} c_{13} s_{13} \\ 0 & \lambda'_2 & as'_{12} c_{13} s_{13} \\ ac'_{12} c_{13} s_{13} & as'_{12} c_{13} s_{13} & as_{13}^2 + \delta m_{31}^2 \end{bmatrix} = |\delta m_{31}^2| \begin{bmatrix} O(\varepsilon^2) & 0 & O(\varepsilon^3) \\ 0 & O(\varepsilon^2) & O(\varepsilon^3) \\ O(\varepsilon^3) & O(\varepsilon^3) & O(1) \end{bmatrix}. \quad (56)$$

Further diagonalization requires rotations by angles of order ε^3 , which we will neglect.

In this case, we cannot expand φ , λ'_1 , and λ'_2 in powers of $a/\delta m_{21}^2$ or its inverse. However, we can still expand in $s_{13} = O(\varepsilon)$ and find

$$\lambda'_{\pm} = \frac{(a + \delta m_{21}^2) \pm \sqrt{(a - \delta m_{21}^2)^2 + 4a \delta m_{21}^2 s_{12}^2}}{2} + O(\varepsilon^4 |\delta m_{31}^2|), \quad (57)$$

and

$$\varphi = \frac{1}{2} \tan^{-1} \left(\frac{a \sin 2\theta_{12}}{\delta m_{21}^2 - a \cos 2\theta_{12}} \right) - \frac{a \delta m_{21}^2 s_{12} c_{12} s_{13}^2}{(a - \delta m_{21}^2)^2 + 4a \delta m_{21}^2 s_{12}^2} + O(\varepsilon^4). \quad (58)$$

The coefficient of s_{13}^2 in the second term is bounded from above by

$$\frac{a \delta m_{21}^2 s_{12} c_{12}}{(a - \delta m_{21}^2)^2 + 4a \delta m_{21}^2 s_{12}^2} \leq \frac{c_{12}}{4s_{12}} = 0.38 \sim 0.42 \approx 2\varepsilon. \quad (59)$$

Therefore, though this factor is formally of $O(1)$, we can consider it to be a number of order ε and approximate

$$\varphi \approx \frac{1}{2} \tan^{-1} \left(\frac{a \sin 2\theta_{12}}{\delta m_{21}^2 - a \cos 2\theta_{12}} \right), \quad \theta'_{12} \approx \frac{1}{2} \tan^{-1} \left(\frac{\delta m_{21}^2 \sin 2\theta_{12}}{\delta m_{21}^2 \cos 2\theta_{12} - a} \right). \quad (60)$$

The eigenvalues in this case are

$$\begin{aligned}
\lambda_1 &\approx \lambda'_- \approx \frac{(a + \delta m_{21}^2) - \sqrt{(a - \delta m_{21}^2)^2 + 4a \delta m_{21}^2 s_{12}^2}}{2}, \\
\lambda_2 &\approx \lambda'_+ \approx \frac{(a + \delta m_{21}^2) + \sqrt{(a - \delta m_{21}^2)^2 + 4a \delta m_{21}^2 s_{12}^2}}{2}, \\
\lambda_3 &\approx \delta m_{31}^2.
\end{aligned} \tag{61}$$

A3. $a/|\delta m_{31}^2| = O(\varepsilon)$ case

The relative sizes of the elements of H' in this case are

$$H' = \begin{bmatrix} ac_{12}^2 c_{13}^2 & ac_{12} s_{12} c_{13}^2 & ac_{12} c_{13} s_{13} \\ ac_{12} s_{12} c_{13}^2 & as_{12}^2 c_{13}^2 + \delta m_{21}^2 & as_{12} c_{13} s_{13} \\ ac_{12} c_{13} s_{13} & as_{12} c_{13} s_{13} & as_{13}^2 + \delta m_{31}^2 \end{bmatrix} = |\delta m_{31}^2| \begin{bmatrix} O(\varepsilon) & O(\varepsilon) & O(\varepsilon^2) \\ O(\varepsilon) & O(\varepsilon) & O(\varepsilon^2) \\ O(\varepsilon^2) & O(\varepsilon^2) & O(1) \end{bmatrix}. \tag{62}$$

As in the previous two cases, the $(1, 2)$ submatrix is diagonalized by V defined as in Eq. (44) with φ defined as in (45). The partially diagonalized form is H'' in Eq. (46), with λ'_1 , λ'_2 , and θ'_{12} defined as in Eqs. (47) and (48).

Since $\delta m_{21}^2/a = O(\varepsilon)$ in this case, we can expand λ'_1 , λ'_2 , and φ in powers of $\delta m_{21}^2/a$ and find

$$\begin{aligned}
\lambda'_1 &= \delta m_{21}^2 c_{12}^2 + O(\varepsilon^3 \delta m_{31}^2) = O(\varepsilon^2 |\delta m_{31}^2|), \\
\lambda'_2 &= a + \delta m_{21}^2 s_{12}^2 + O(\varepsilon^3 \delta m_{31}^2) = O(\varepsilon |\delta m_{31}^2|),
\end{aligned} \tag{63}$$

and

$$\begin{aligned}
\varphi &= \left(\frac{\pi}{2} - \theta_{12}\right) - \frac{1}{2} \left(\frac{\delta m_{21}^2}{ac_{13}^2}\right) \sin(2\theta_{12}) - \frac{1}{2} \left(\frac{\delta m_{21}^2}{ac_{13}^2}\right)^2 \sin(2\theta_{12}) \cos(2\theta_{12}) + \dots, \\
&= \left(\frac{\pi}{2} - \theta_{12}\right) - \frac{\delta m_{21}^2}{2a} \sin(2\theta_{12}) + O(\varepsilon^3), \\
\theta'_{12} &= \theta_{12} + \varphi = \frac{\pi}{2} - \frac{\delta m_{21}^2}{2a} \sin(2\theta_{12}) + O(\varepsilon^3),
\end{aligned} \tag{64}$$

which shows that

$$\begin{aligned}
c'_{12} &\approx \cos\left(\frac{\pi}{2} - \frac{\delta m_{21}^2}{2a} \sin(2\theta_{12})\right) = \sin\left(\frac{\delta m_{21}^2}{2a} \sin(2\theta_{12})\right) = O(\varepsilon), \\
s'_{12} &\approx \sin\left(\frac{\pi}{2} - \frac{\delta m_{21}^2}{2a} \sin(2\theta_{12})\right) = \cos\left(\frac{\delta m_{21}^2}{2a} \sin(2\theta_{12})\right) = O(1).
\end{aligned} \tag{65}$$

Note that

$$ac'_{12} \approx a \left(\frac{\delta m_{21}^2}{2a} \sin(2\theta_{12}) \right) = |\delta m_{31}^2| \left(\frac{\delta m_{21}^2}{2|\delta m_{31}^2|} \sin(2\theta_{12}) \right) = |\delta m_{31}^2| O(\varepsilon^2), \quad (66)$$

for all $a \gg \delta m_{21}^2$. We will use this relation repeatedly in the following.

Thus, we find the sizes of the elements of H'' in this case to be

$$H'' = \begin{bmatrix} \lambda'_1 & 0 & ac'_{12}c_{13}s_{13} \\ 0 & \lambda'_2 & as'_{12}c_{13}s_{13} \\ ac'_{12}c_{13}s_{13} & as'_{12}c_{13}s_{13} & as_{13}^2 + \delta m_{31}^2 \end{bmatrix} = |\delta m_{31}^2| \begin{bmatrix} O(\varepsilon^2) & 0 & O(\varepsilon^3) \\ 0 & O(\varepsilon) & O(\varepsilon^2) \\ O(\varepsilon^3) & O(\varepsilon^2) & O(1) \end{bmatrix}. \quad (67)$$

This time, the (2, 3) submatrix requires an $O(\varepsilon^2)$ rotation to be diagonalized. We define

$$W = \begin{bmatrix} 1 & 0 & 0 \\ 0 & c_\phi & s_\phi \\ 0 & -s_\phi & c_\phi \end{bmatrix}, \quad (68)$$

where

$$c_\phi = \cos \phi, \quad s_\phi = \sin \phi, \quad \tan 2\phi \equiv \frac{as'_{12} \sin 2\theta_{13}}{\delta m_{31}^2 + as_{13}^2 - \lambda'_2}. \quad (69)$$

The angle ϕ is in the first quadrant when $\delta m_{31}^2 > 0$, and in the fourth quadrant when $\delta m_{31}^2 < 0$. Then,

$$H''' = W^\dagger H'' W = \begin{bmatrix} \lambda'_1 & -ac'_{12}c_{13}s_{13}s_\phi & ac'_{12}c_{13}s_{13}c_\phi \\ -ac'_{12}c_{13}s_{13}s_\phi & \lambda''_2 & 0 \\ ac'_{12}c_{13}s_{13}c_\phi & 0 & \lambda''_3 \end{bmatrix}, \quad (70)$$

where

$$\lambda''_2 = \frac{\lambda'_2 c_\phi^2 - (as_{13}^2 + \delta m_{31}^2) s_\phi^2}{c_\phi^2 - s_\phi^2}, \quad \lambda''_3 = \frac{(as_{13}^2 + \delta m_{31}^2) c_\phi^2 - \lambda'_2 s_\phi^2}{c_\phi^2 - s_\phi^2}. \quad (71)$$

If we define

$$\lambda''_{\pm} \equiv \frac{[\lambda'_2 + (as_{13}^2 + \delta m_{31}^2)] \pm \sqrt{[\lambda'_2 - (as_{13}^2 + \delta m_{31}^2)]^2 + 4a^2 s_{12}'^2 c_{13}^2 s_{13}^2}}{2}, \quad (72)$$

then

$$\lambda''_2 = \lambda''_-, \quad \lambda''_3 = \lambda''_+, \quad \text{if } \delta m_{31}^2 > 0,$$

$$\lambda_2'' = \lambda_+'' , \quad \lambda_3'' = \lambda_-'' , \quad \text{if } \delta m_{31}^2 < 0 . \quad (73)$$

Expanding λ_2'' , λ_3'' , and ϕ in powers of $a/\delta m_{31}^2 = O(\varepsilon)$, we find

$$\begin{aligned} \lambda_2'' &= \lambda_2' + O(\varepsilon^4 |\delta m_{31}^2|) = a + \delta m_{21}^2 s_{12}^2 + O(\varepsilon^3 |\delta m_{31}^2|) = O(\varepsilon |\delta m_{31}^2|) , \\ \lambda_3'' &= (\delta m_{31}^2 + a s_{13}^2) + O(\varepsilon^4 |\delta m_{31}^2|) = \delta m_{31}^2 + O(\varepsilon^3 |\delta m_{31}^2|) = O(|\delta m_{31}^2|) , \end{aligned} \quad (74)$$

and

$$\phi = \frac{a}{2 \delta m_{31}^2} \sin(2\theta_{13}) + \dots = \frac{a}{\delta m_{31}^2} \theta_{13} + O(\varepsilon^3) = O(\varepsilon^2) , \quad (75)$$

which means that $s_\phi = O(\varepsilon^2)$, $c_\phi = O(1)$, and

$$H''' = \begin{bmatrix} \lambda_1' & -ac'_{12}c_{13}s_{13}s_\phi & ac'_{12}c_{13}s_{13}c_\phi \\ -ac'_{12}c_{13}s_{13}s_\phi & \lambda_2'' & 0 \\ ac'_{12}c_{13}s_{13}c_\phi & 0 & \lambda_3'' \end{bmatrix} = |\delta m_{31}^2| \begin{bmatrix} O(\varepsilon^2) & O(\varepsilon^5) & O(\varepsilon^3) \\ O(\varepsilon^5) & O(\varepsilon) & 0 \\ O(\varepsilon^3) & 0 & O(1) \end{bmatrix} . \quad (76)$$

Further diagonalization require rotations of order $O(\varepsilon^3)$ and higher, which we neglect. So in this case, the Hamiltonian is approximately diagonalized by a (1, 2) rotation of angle $O(1)$ followed by a (2, 3) rotation of angle $O(\varepsilon^2)$, and the eigenvalues are

$$\begin{aligned} \lambda_1 &\approx \lambda_1' \approx \delta m_{21}^2 c_{12}^2 , \\ \lambda_2 &\approx \lambda_2'' \approx a + \delta m_{21}^2 s_{12}^2 , \\ \lambda_3 &\approx \lambda_3'' \approx \delta m_{31}^2 . \end{aligned} \quad (77)$$

A4. $a/|\delta m_{31}^2| = O(1)$ case

The relative sizes of the elements of H' in this case are

$$H' = \begin{bmatrix} ac_{12}^2 c_{13}^2 & ac_{12}s_{12}c_{13}^2 & ac_{12}c_{13}s_{13} \\ ac_{12}s_{12}c_{13}^2 & as_{12}^2 c_{13}^2 + \delta m_{21}^2 & as_{12}c_{13}s_{13} \\ ac_{12}c_{13}s_{13} & as_{12}c_{13}s_{13} & as_{13}^2 + \delta m_{31}^2 \end{bmatrix} = |\delta m_{31}^2| \begin{bmatrix} O(1) & O(1) & O(\varepsilon) \\ O(1) & O(1) & O(\varepsilon) \\ O(\varepsilon) & O(\varepsilon) & O(1) \end{bmatrix} . \quad (78)$$

As in the three previous cases, the (1, 2) submatrix is diagonalized by V defined as in Eq. (44) with φ defined as in (45). The partially diagonalized form is H'' in Eq. (46), with λ_1' , λ_2' , and θ'_{12} defined as in Eqs. (47) and (48). The expansions of λ_1' and λ_2' in powers of $\delta m_{21}^2/a$ yield

$$\lambda_1' = \delta m_{21}^2 c_{12}^2 + O(\varepsilon^4 |\delta m_{31}^2|) = O(\varepsilon^2 |\delta m_{31}^2|) ,$$

$$\lambda'_2 = ac_{13}^2 + \delta m_{21}^2 s_{12}^2 + O(\varepsilon^4 |\delta m_{31}^2|) = O(|\delta m_{31}^2|). \quad (79)$$

Note that we cannot replace c_{13} in this expression with 1 without introducing an error of order $\varepsilon^2 |\delta m_{31}^2|$ which is the same order as the second term. The expansions of φ and θ'_{12} are

$$\begin{aligned} \varphi &= \left(\frac{\pi}{2} - \theta_{12} \right) - \frac{\delta m_{21}^2}{2a} \sin(2\theta_{12}) + O(\varepsilon^4), \\ \theta'_{12} &= \theta_{12} + \varphi = \frac{\pi}{2} - \frac{\delta m_{21}^2}{2a} \sin(2\theta_{12}) + O(\varepsilon^4). \end{aligned} \quad (80)$$

From Eqs. (65) and (66), we can tell that $s'_{12} = O(1)$, and $ac'_{12} = O(\varepsilon^2 |\delta m_{31}^2|)$. Therefore,

$$H'' = \begin{bmatrix} \lambda'_1 & 0 & ac'_{12} c_{13} s_{13} \\ 0 & \lambda'_2 & as'_{12} c_{13} s_{13} \\ ac'_{12} c_{13} s_{13} & as'_{12} c_{13} s_{13} & as_{13}^2 + \delta m_{31}^2 \end{bmatrix} = |\delta m_{31}^2| \begin{bmatrix} O(\varepsilon^2) & 0 & O(\varepsilon^3) \\ 0 & O(1) & O(\varepsilon) \\ O(\varepsilon^3) & O(\varepsilon) & O(1) \end{bmatrix}. \quad (81)$$

Again, we need to diagonalize the (2, 3) submatrix with the matrix W defined in Eq. (68) with the angle ϕ defined in Eq.(69). The resulting matrix is H''' given in Eq. (70). From this point on, we must treat the $\delta m_{31}^2 > 0$ and $\delta m_{31}^2 < 0$ cases separately since level crossing between a and δm_{31}^2 occurs for the $\delta m_{31}^2 > 0$ case but not for the $\delta m_{31}^2 < 0$ case.

When $\delta m_{31}^2 > 0$, we can use $1 - s'_{12} = O(\varepsilon^4)$, and $\lambda'_2 = ac_{13}^2 + O(\varepsilon^2 |\delta m_{31}^2|)$ to approximate

$$\tan 2\phi = \frac{a \sin 2\theta_{13}}{\delta m_{31}^2 - a \cos 2\theta_{13}} + O(\varepsilon^3). \quad (82)$$

In this case, we expect $\phi = O(1)$, $s_\phi = O(1)$, and $c_\phi = O(1)$. The λ'' 's can also be expanded in $\delta m_{21}^2/a = O(\varepsilon^2)$ and we find

$$\begin{aligned} \lambda''_2 &= \lambda''_- \\ &\approx \frac{(a + \delta m_{31}^2) - \sqrt{(a - \delta m_{31}^2)^2 + 4a \delta m_{31}^2 s_{13}^2}}{2} + \Theta(\delta m_{31}^2 - a) \delta m_{21}^2 s_{12}^2 + O(\varepsilon^4 |\delta m_{31}^2|), \\ \lambda''_3 &= \lambda''_+ \\ &\approx \frac{(a + \delta m_{31}^2) + \sqrt{(a - \delta m_{31}^2)^2 + 4a \delta m_{31}^2 s_{13}^2}}{2} + \Theta(a - \delta m_{31}^2) \delta m_{21}^2 s_{12}^2 + O(\varepsilon^4 |\delta m_{31}^2|), \end{aligned} \quad (83)$$

where Θ is the Heaviside step function.

For the $\delta m_{31}^2 < 0$ case, the denominator in the definition of $\tan 2\phi$ in Eq. (69) is always negative and never crosses zero for any value of a . Therefore, the smallness of $\sin 2\theta_{13}$ in the numerator is never cancelled by an equally small denominator. This allows us to expand ϕ in θ_{13} and we find

$$\phi = \left(\frac{a}{\delta m_{31}^2 - a} \right) \theta_{13} + O(\varepsilon^3) = O(\varepsilon), \quad (84)$$

which is actually valid for all values of a when $\delta m_{31}^2 < 0$. Therefore, $s_\phi = O(\varepsilon)$ and $c_\phi = O(1)$. The λ'' s are expanded as

$$\begin{aligned}\lambda_2'' &= \lambda_+'' \approx ac_{13}^2 + \delta m_{21}^2 s_{12}^2 + O(\varepsilon^4 |\delta m_{31}^2|), \\ \lambda_3'' &= \lambda_-'' \approx \delta m_{31}^2 + as_{13}^2 + O(\varepsilon^6 |\delta m_{31}^2|).\end{aligned}\quad (85)$$

For both the $\delta m_{31}^2 > 0$ and $\delta m_{31}^2 < 0$ cases, both λ_2'' and λ_3'' are of the same order as $|\delta m_{31}^2|$. Therefore,

$$H''' = \begin{bmatrix} \lambda_1' & -ac'_{12}c_{13}s_{13}s_\phi & ac'_{12}c_{13}s_{13}c_\phi \\ -ac'_{12}c_{13}s_{13}s_\phi & \lambda_2'' & 0 \\ ac'_{12}c_{13}s_{13}c_\phi & 0 & \lambda_3'' \end{bmatrix} = |\delta m_{31}^2| \begin{bmatrix} O(\varepsilon^2) & O(\varepsilon^{3,4}) & O(\varepsilon^3) \\ O(\varepsilon^{3,4}) & O(1) & 0 \\ O(\varepsilon^3) & 0 & O(1) \end{bmatrix}, \quad (86)$$

where the sizes of the (1, 2) and (2, 1) elements depend on whether $\phi = O(\varepsilon)$ ($\delta m_{31}^2 < 0$) or $\phi = O(1)$ ($\delta m_{31}^2 > 0$). In either case, further diagonalization is not necessary.

If we relax our accuracy requirement and allow for errors of $O(\varepsilon^2 |\delta m_{31}^2|)$, then the λ'' s for both the $\delta m_{31}^2 > 0$ and $\delta m_{31}^2 < 0$ cases can be approximated by

$$\lambda_\pm'' \approx \frac{(a + \delta m_{31}^2) \pm \sqrt{(a - \delta m_{31}^2)^2 + 4a \delta m_{31}^2 s_{13}^2}}{2}. \quad (87)$$

We will argue that this approximation is sufficient later. The eigenvalues are then:

$$\begin{aligned}\lambda_1 &\approx \lambda_1' \approx \delta m_{21}^2 c_{12}^2, \\ \lambda_2 &\approx \lambda_\mp'' \approx \frac{(a + \delta m_{31}^2) \mp \sqrt{(a - \delta m_{31}^2)^2 + 4a \delta m_{31}^2 s_{13}^2}}{2}, \\ \lambda_3 &\approx \lambda_\pm'' \approx \frac{(a + \delta m_{31}^2) \pm \sqrt{(a - \delta m_{31}^2)^2 + 4a \delta m_{31}^2 s_{13}^2}}{2},\end{aligned}\quad (88)$$

where the upper sign corresponds to the $\delta m_{31}^2 > 0$ case, and the lower sign corresponds to the $\delta m_{31}^2 < 0$ case.

A5. $a/|\delta m_{31}^2| = O(\varepsilon^{-1})$

The relative sizes of the elements of H' in this case are

$$H' = \begin{bmatrix} ac_{12}^2 c_{13}^2 & ac_{12} s_{12} c_{13}^2 & ac_{12} c_{13} s_{13} \\ ac_{12} s_{12} c_{13}^2 & as_{12}^2 c_{13}^2 + \delta m_{21}^2 & as_{12} c_{13} s_{13} \\ ac_{12} c_{13} s_{13} & as_{12} c_{13} s_{13} & as_{13}^2 + \delta m_{31}^2 \end{bmatrix} = |\delta m_{31}^2| \begin{bmatrix} O(\varepsilon^{-1}) & O(\varepsilon^{-1}) & O(1) \\ O(\varepsilon^{-1}) & O(\varepsilon^{-1}) & O(1) \\ O(1) & O(1) & O(1) \end{bmatrix}. \quad (89)$$

As in all the previous cases, the (1, 2) submatrix is diagonalized by V defined as in Eq. (44) with φ defined as in (45). The partially diagonalized form is H'' in Eq. (46), with λ'_1 , λ'_2 , and θ'_{12} defined as in Eqs. (47) and (48). The expansions of these quantities are:

$$\begin{aligned}\lambda'_1 &= \delta m_{21}^2 c_{12}^2 + O(\varepsilon^5 |\delta m_{31}^2|) = O(\varepsilon^2 |\delta m_{31}^2|), \\ \lambda'_2 &= ac_{13}^2 + \delta m_{21}^2 s_{12}^2 + O(\varepsilon^5 |\delta m_{31}^2|) = O(\varepsilon^{-1} |\delta m_{31}^2|),\end{aligned}\quad (90)$$

and

$$\begin{aligned}\varphi &= \left(\frac{\pi}{2} - \theta_{12}\right) - \frac{\delta m_{21}^2}{2a} \sin(2\theta_{12}) + O(\varepsilon^5), \\ \theta'_{12} &= \theta_{12} + \varphi = \frac{\pi}{2} - \frac{\delta m_{21}^2}{2a} \sin(2\theta_{12}) + O(\varepsilon^5).\end{aligned}\quad (91)$$

Since $s'_{12} = O(1)$, and $ac'_{12} = O(\varepsilon^2 |\delta m_{31}^2|)$, we find

$$H'' = \begin{bmatrix} \lambda'_1 & 0 & ac'_{12}c_{13}s_{13} \\ 0 & \lambda'_2 & as'_{12}c_{13}s_{13} \\ ac'_{12}c_{13}s_{13} & as'_{12}c_{13}s_{13} & as_{13}^2 + \delta m_{31}^2 \end{bmatrix} = |\delta m_{31}^2| \begin{bmatrix} O(\varepsilon^2) & 0 & O(\varepsilon^3) \\ 0 & O(\varepsilon^{-1}) & O(1) \\ O(\varepsilon^3) & O(1) & O(1) \end{bmatrix}. \quad (92)$$

We diagonalize the (2, 3) submatrix with the matrix W defined in Eq. (68) with the angle ϕ defined in Eq.(69). The resulting matrix is H''' given in Eq. (70).

Recall that 2ϕ is in the second quadrant if $\delta m_{31}^2 > 0$ (level crossing occurs), and in the fourth quadrant if $\delta m_{31}^2 < 0$ (no level crossing). The expansions of λ''_2 , λ''_3 , and ϕ in powers of $\delta m_{31}^2/a = O(\varepsilon)$ differ accordingly. For the $\delta m_{31}^2 > 0$ case, we find

$$\begin{aligned}\lambda''_2 &= \lambda''_- = \delta m_{31}^2 c_{13}^2 + O(\varepsilon^3 |\delta m_{31}^2|) = O(|\delta m_{31}^2|), \\ \lambda''_3 &= \lambda''_+ = a + \delta m_{31}^2 s_{13}^2 + \delta m_{21}^2 s_{12}^2 + O(\varepsilon^3 |\delta m_{31}^2|) = O(\varepsilon^{-1} |\delta m_{31}^2|),\end{aligned}\quad (93)$$

and

$$\phi = \left(\frac{\pi}{2} - \theta_{13}\right) - \frac{\delta m_{31}^2}{a} \theta_{13} + O(\varepsilon^3) = O(1), \quad (94)$$

in which case both s_ϕ and c_ϕ are of order 1 and

$$H''' = \begin{bmatrix} \lambda'_1 & -ac'_{12}c_{13}s_{13}s_\phi & ac'_{12}c_{13}s_{13}c_\phi \\ -ac'_{12}c_{13}s_{13}s_\phi & \lambda''_2 & 0 \\ ac'_{12}c_{13}s_{13}c_\phi & 0 & \lambda''_3 \end{bmatrix} = |\delta m_{31}^2| \begin{bmatrix} O(\varepsilon^2) & O(\varepsilon^3) & O(\varepsilon^3) \\ O(\varepsilon^3) & O(1) & 0 \\ O(\varepsilon^3) & 0 & O(\varepsilon^{-1}) \end{bmatrix}. \quad (95)$$

For the $\delta m_{31}^2 < 0$ case, we have

$$\lambda''_2 = \lambda''_+ = a + \delta m_{31}^2 s_{13}^2 + \delta m_{21}^2 s_{12}^2 + O(\varepsilon^3 |\delta m_{31}^2|) = O(\varepsilon^{-1} |\delta m_{31}^2|),$$

$$\lambda_3'' = \lambda_-'' = \delta m_{31}^2 c_{13}^2 + O(\varepsilon^3 |\delta m_{31}^2|) = O(|\delta m_{31}^2|), \quad (96)$$

and

$$\phi = -\theta_{13} - \frac{\delta m_{31}^2}{a} \theta_{13} + O(\varepsilon^3) = O(\varepsilon), \quad (97)$$

which is just Eq. (84) expanded in powers of $\delta m_{31}^2/a$. In this case, $s_\phi = O(\varepsilon)$ and $c_\phi = O(1)$.

Therefore,

$$H''' = \begin{bmatrix} \lambda_1' & -ac'_{12}c_{13}s_{13}s_\phi & ac'_{12}c_{13}s_{13}c_\phi \\ -ac'_{12}c_{13}s_{13}s_\phi & \lambda_2'' & 0 \\ ac'_{12}c_{13}s_{13}c_\phi & 0 & \lambda_3'' \end{bmatrix} = |\delta m_{31}^2| \begin{bmatrix} O(\varepsilon^2) & O(\varepsilon^4) & O(\varepsilon^3) \\ O(\varepsilon^4) & O(\varepsilon^{-1}) & 0 \\ O(\varepsilon^3) & 0 & O(1) \end{bmatrix}. \quad (98)$$

In either case, the Hamiltonian has been approximately diagonalized. The eigenvalues for the $\delta m_{31}^2 > 0$ case are

$$\begin{aligned} \lambda_1 &\approx \lambda_1' \approx \delta m_{21}^2 c_{12}^2, \\ \lambda_2 &\approx \lambda_-'' \approx \delta m_{31}^2 c_{13}^2, \\ \lambda_3 &\approx \lambda_+'' \approx a + \delta m_{31}^2 s_{13}^2 + \delta m_{21}^2 s_{12}^2, \end{aligned} \quad (99)$$

while for the $\delta m_{31}^2 < 0$ case, they are

$$\begin{aligned} \lambda_1 &\approx \lambda_1' \approx \delta m_{21}^2 c_{12}^2, \\ \lambda_2 &\approx \lambda_+'' \approx a + \delta m_{31}^2 s_{13}^2 + \delta m_{21}^2 s_{12}^2, \\ \lambda_3 &\approx \lambda_-'' \approx \delta m_{31}^2 c_{13}^2. \end{aligned} \quad (100)$$

B. Effective Mixing Angles

To summarize what we have learned above, when $a/|\delta m_{31}^2| = O(\varepsilon^2)$ or smaller, H' can be approximately diagonalized by a single (1, 2) rotation using the matrix

$$V = \begin{bmatrix} c_\varphi & s_\varphi & 0 \\ -s_\varphi & c_\varphi & 0 \\ 0 & 0 & 1 \end{bmatrix}, \quad (101)$$

where

$$c_\varphi = \cos \varphi, \quad s_\varphi = \sin \varphi, \quad \tan 2\varphi \equiv \frac{ac_{13}^2 \sin 2\theta_{12}}{\delta m_{21}^2 - ac_{13}^2 \cos 2\theta_{12}} \approx \frac{a \sin 2\theta_{12}}{\delta m_{21}^2 - a \cos 2\theta_{12}}, \quad (102)$$

with $0 \leq \varphi < \frac{\pi}{2}$. When $a/|\delta m_{31}^2| = O(\varepsilon)$ or larger, this must be followed by a (2, 3) rotation using the matrix

$$W = \begin{bmatrix} 1 & 0 & 0 \\ 0 & c_\phi & s_\phi \\ 0 & -s_\phi & c_\phi \end{bmatrix}, \quad (103)$$

where

$$c_\phi = \cos \phi, \quad s_\phi = \sin \phi, \quad \tan 2\phi \equiv \frac{as'_{12} \sin 2\theta_{13}}{\delta m_{31}^2 + as_{13}^2 - \lambda'_2} \approx \frac{a \sin 2\theta_{13}}{\delta m_{31}^2 - a \cos 2\theta_{13}}, \quad (104)$$

with s'_{12} and λ'_2 defined in Eqs. (47) and (48). If $\delta m_{31}^2 > 0$, then $0 < \phi < \frac{\pi}{2}$. If $\delta m_{31}^2 < 0$, then $-\frac{\pi}{4} < \phi < 0$.

Note that the first case is encompassed in the second, since in the first case the second rotation angle ϕ becomes negligibly small. Therefore, the matrix which approximately diagonalizes the effective Hamiltonian is

U'

$$\begin{aligned} &= UQVW \\ &= \begin{bmatrix} 1 & 0 & 0 \\ 0 & c_{23} & s_{23} \\ 0 & -s_{23} & c_{23} \end{bmatrix} \begin{bmatrix} c_{13} & 0 & s_{13}e^{-i\delta} \\ 0 & 1 & 0 \\ -s_{13}e^{i\delta} & 0 & c_{13} \end{bmatrix} \begin{bmatrix} c_{12} & s_{12} & 0 \\ -s_{12} & c_{12} & 0 \\ 0 & 0 & 1 \end{bmatrix} \begin{bmatrix} 1 & 0 & 0 \\ 0 & 1 & 0 \\ 0 & 0 & e^{i\delta} \end{bmatrix} \begin{bmatrix} c_\phi & s_\phi & 0 \\ -s_\phi & c_\phi & 0 \\ 0 & 0 & 1 \end{bmatrix} W \\ &= \begin{bmatrix} 1 & 0 & 0 \\ 0 & c_{23} & s_{23} \\ 0 & -s_{23} & c_{23} \end{bmatrix} \begin{bmatrix} c_{13} & 0 & s_{13}e^{-i\delta} \\ 0 & 1 & 0 \\ -s_{13}e^{i\delta} & 0 & c_{13} \end{bmatrix} \begin{bmatrix} c_{12} & s_{12} & 0 \\ -s_{12} & c_{12} & 0 \\ 0 & 0 & 1 \end{bmatrix} \begin{bmatrix} c_\phi & s_\phi & 0 \\ -s_\phi & c_\phi & 0 \\ 0 & 0 & 1 \end{bmatrix} \begin{bmatrix} 1 & 0 & 0 \\ 0 & 1 & 0 \\ 0 & 0 & e^{i\delta} \end{bmatrix} W \\ &= \begin{bmatrix} 1 & 0 & 0 \\ 0 & c_{23} & s_{23} \\ 0 & -s_{23} & c_{23} \end{bmatrix} \begin{bmatrix} c_{13} & 0 & s_{13}e^{-i\delta} \\ 0 & 1 & 0 \\ -s_{13}e^{i\delta} & 0 & c_{13} \end{bmatrix} \begin{bmatrix} c'_{12} & s'_{12} & 0 \\ -s'_{12} & c'_{12} & 0 \\ 0 & 0 & 1 \end{bmatrix} \begin{bmatrix} 1 & 0 & 0 \\ 0 & 1 & 0 \\ 0 & 0 & e^{i\delta} \end{bmatrix} \begin{bmatrix} 1 & 0 & 0 \\ 0 & c_\phi & s_\phi \\ 0 & -s_\phi & c_\phi \end{bmatrix} \\ &= \begin{bmatrix} c_{13}c'_{12} & c_{13}s'_{12}c_\phi - s_{13}s_\phi & c_{13}s'_{12}s_\phi + s_{13}c_\phi \\ -c_{23}s'_{12} - s_{23}s_{13}c'_{12}e^{i\delta} & c_{23}c'_{12}c_\phi - s_{23}(s_{13}s'_{12}c_\phi + c_{13}s_\phi)e^{i\delta} & c_{23}c'_{12}s_\phi - s_{23}(s_{13}s'_{12}s_\phi - c_{13}c_\phi)e^{i\delta} \\ s_{23}s'_{12} - c_{23}s_{13}c'_{12}e^{i\delta} & -s_{23}c'_{12}c_\phi - c_{23}(s_{13}s'_{12}c_\phi + c_{13}s_\phi)e^{i\delta} & -s_{23}c'_{12}s_\phi - c_{23}(s_{13}s'_{12}s_\phi - c_{13}c_\phi)e^{i\delta} \end{bmatrix} \quad (105) \end{aligned}$$

We would like to identify this matrix with

$$\tilde{U} = \begin{bmatrix} 1 & 0 & 0 \\ 0 & \tilde{c}_{23} & \tilde{s}_{23} \\ 0 & -\tilde{s}_{23} & \tilde{c}_{23} \end{bmatrix} \begin{bmatrix} \tilde{c}_{13} & 0 & \tilde{s}_{13}e^{-i\tilde{\delta}} \\ 0 & 1 & 0 \\ -\tilde{s}_{13}e^{i\tilde{\delta}} & 0 & \tilde{c}_{13} \end{bmatrix} \begin{bmatrix} \tilde{c}_{12} & \tilde{s}_{12} & 0 \\ -\tilde{s}_{12} & \tilde{c}_{12} & 0 \\ 0 & 0 & 1 \end{bmatrix}$$

$\frac{a}{ \delta m_{31}^2 }$	δm_{31}^2	c'_{12}	$(1 - s'_{12})$	s_ϕ	c'_{13}	$\frac{(1 - s'_{12})s_\phi}{c'_{13}}$	$\frac{s_{13}c'_{12}(1 - s'_{12})s_\phi}{c'_{13}}$	$c'_{12} \left(1 - \frac{c'_{13}}{c_{13}}\right)$	$c'_{12}s_\phi$	$c'_{12}s_\phi/c'_{13}$
$O(\varepsilon^3)$	\pm	$O(1)$	$O(1)$	$O(\varepsilon^4)$	$O(1)$	$O(\varepsilon^4)$	$O(\varepsilon^5)$	$O(\varepsilon^5)$	$O(\varepsilon^4)$	$O(\varepsilon^4)$
$O(\varepsilon^2)$	\pm	$O(1)$	$O(1)$	$O(\varepsilon^3)$	$O(1)$	$O(\varepsilon^3)$	$O(\varepsilon^4)$	$O(\varepsilon^4)$	$O(\varepsilon^3)$	$O(\varepsilon^3)$
$O(\varepsilon)$	\pm	$O(\varepsilon)$	$O(\varepsilon^2)$	$O(\varepsilon^2)$	$O(1)$	$O(\varepsilon^4)$	$O(\varepsilon^6)$	$O(\varepsilon^4)$	$O(\varepsilon^3)$	$O(\varepsilon^3)$
$O(1)$	$-$	$O(\varepsilon^2)$	$O(\varepsilon^4)$	$O(\varepsilon)$	$O(1)$	$O(\varepsilon^5)$	$O(\varepsilon^8)$	$O(\varepsilon^4)$	$O(\varepsilon^3)$	$O(\varepsilon^3)$
	$+$	$O(\varepsilon^2)$	$O(\varepsilon^4)$	$O(1)$	$O(1)$	$O(\varepsilon^4)$	$O(\varepsilon^7)$	—	$O(\varepsilon^2)$	$O(\varepsilon^2)$
$O(\varepsilon^{-1})$	$-$	$O(\varepsilon^3)$	$O(\varepsilon^6)$	$O(\varepsilon)$	$O(1)$	$O(\varepsilon^7)$	$O(\varepsilon^{11})$	$O(\varepsilon^5)$	$O(\varepsilon^4)$	$O(\varepsilon^4)$
	$+$	$O(\varepsilon^3)$	$O(\varepsilon^6)$	$O(1)$	$O(\varepsilon^2)$	$O(\varepsilon^4)$	$O(\varepsilon^8)$	—	$O(\varepsilon^3)$	$O(\varepsilon)$

TABLE II: The sizes of the factors $(1 - s'_{12})s_\phi/c'_{13}$, $s_{13}c'_{12}(1 - s'_{12})s_\phi/c'_{13}$, $c'_{12}(1 - c'_{13}/c_{13})$, $c'_{12}s_\phi$, and $c'_{12}s_\phi/c'_{13}$.

$$= \begin{bmatrix} \tilde{c}_{12}\tilde{c}_{13} & \tilde{s}_{12}\tilde{c}_{13} & \tilde{s}_{13}e^{-i\tilde{\delta}} \\ -\tilde{s}_{12}\tilde{c}_{23} - \tilde{c}_{12}\tilde{s}_{13}\tilde{s}_{23}e^{i\tilde{\delta}} & \tilde{c}_{12}\tilde{c}_{23} - \tilde{s}_{12}\tilde{s}_{13}\tilde{s}_{23}e^{i\tilde{\delta}} & \tilde{c}_{13}\tilde{s}_{23} \\ \tilde{s}_{12}\tilde{s}_{23} - \tilde{c}_{12}\tilde{s}_{13}\tilde{c}_{23}e^{i\tilde{\delta}} & -\tilde{c}_{12}\tilde{s}_{23} - \tilde{s}_{12}\tilde{s}_{13}\tilde{c}_{23}e^{i\tilde{\delta}} & \tilde{c}_{13}\tilde{c}_{23} \end{bmatrix}, \quad (106)$$

up to phases that can be absorbed into the Majorana phases of the neutrinos and redefinitions of the charged lepton fields. Comparing the $(1, 3)$ elements of the matrices, we can make the identification

$$\begin{aligned} \tilde{s}_{13} &= c_{13}s'_{12}s_\phi + s_{13}c_\phi \\ &= (c_{13}s_\phi + s_{13}c_\phi) - (1 - s'_{12})s_\phi c_{13} \\ &= s'_{13} + c'_{13} \left\{ -\frac{(1 - s'_{12})s_\phi c_{13}}{c'_{13}} \right\}, \end{aligned} \quad (107)$$

where we have defined

$$s'_{13} = \sin \theta'_{13}, \quad c'_{13} = \cos \theta'_{13}, \quad \theta'_{13} = \theta_{13} + \phi. \quad (108)$$

Note that the factor $(1 - s'_{12})s_\phi/c'_{13}$ is of order ε^3 or smaller regardless of the value of a , as shown in Table II. Therefore,

$$\sin \tilde{\theta}_{13} = \sin [\theta'_{13} + O(\varepsilon^3)], \quad (109)$$

which implies

$$\tilde{\theta}_{13} = \theta'_{13} + O(\varepsilon^3). \quad (110)$$

Next, looking at the $(1, 1)$ and $(1, 2)$ elements, we find

$$\tan \tilde{\theta}_{12} = \frac{\tilde{s}_{12}\tilde{c}_{13}}{\tilde{c}_{12}\tilde{c}_{13}}$$

$$\begin{aligned}
&= \frac{c_{13}s'_{12}c_\phi - s_{13}s_\phi}{c_{13}c'_{12}} \\
&= \frac{(c_{13}c_\phi - s_{13}s_\phi)s'_{12} - s_{13}(1 - s'_{12})s_\phi}{c_{13}c'_{12}} \\
&= \left(\frac{c'_{13}}{c_{13}}\right) \left[\tan \theta'_{12} + \frac{1}{\cos^2 \theta'_{12}} \left\{ -\frac{s_{13}c'_{12}(1 - s'_{12})s_\phi}{c'_{13}} \right\} \right]. \tag{111}
\end{aligned}$$

From Table II, we find that the factor $s_{13}c'_{12}(1 - s'_{12})s_\phi/c'_{13}$ is of order ε^4 or smaller for all a . Therefore,

$$\tan \tilde{\theta}_{12} = \left(\frac{c'_{13}}{c_{13}}\right) \tan [\theta'_{12} + O(\varepsilon^4)]. \tag{112}$$

Since $\theta'_{13} = \theta_{13} + \phi$, we can expect the ratio c'_{13}/c_{13} to be roughly equal to one when ϕ is small, and consequently, $\tilde{\theta}_{12} \approx \theta'_{12}$. Indeed, if $\delta m_{31}^2 > 0$ with $a/|\delta m_{31}^2| \leq O(\varepsilon)$, or $\delta m_{31}^2 < 0$ with any a , then $s_\phi \leq O(\varepsilon)$, and we find

$$1 - \frac{c'_{13}}{c_{13}} = (1 - c_\phi) + s_\phi \tan \theta_{13} \leq O(\varepsilon^2). \tag{113}$$

In these cases, we can treat $(1 - c'_{13}/c_{13})$ as a small quantity and expand

$$\tilde{\theta}_{12} = \theta'_{12} + s'_{12}c'_{12} \left(1 - \frac{c'_{13}}{c_{13}}\right) + \dots = \theta'_{12} + O(\varepsilon^4). \tag{114}$$

The $\delta m_{31}^2 > 0$ case with $a/|\delta m_{31}^2| = O(1)$ or $a/|\delta m_{31}^2| = O(\varepsilon^{-1})$ must be considered separately. First, taking the reciprocal of both sides of Eq. (112), we obtain

$$\cot \tilde{\theta}_{12} = \frac{c_{13}}{c'_{13}} \cot \theta'_{12}, \tag{115}$$

where we have dropped the shift in θ'_{12} on the right hand side which is of order $\varepsilon^{7,8}$ in these particular cases. (cf. Table II.) Recall that when $a/|\delta m_{31}^2| = O(\varepsilon^{0,-1})$, we have

$$\theta'_{12} = \frac{\pi}{2} - \frac{\delta m_{21}^2}{2a} \sin(2\theta_{12}) + O(\varepsilon^{4,5}), \tag{116}$$

while

$$\frac{c_{13}}{c'_{13}} = O(\varepsilon^{0,-2}). \tag{117}$$

Therefore, from Eq. (115) we find

$$\begin{aligned}
\tan \left(\frac{\pi}{2} - \tilde{\theta}_{12}\right) &= \frac{c_{13}}{c'_{13}} \tan \left(\frac{\pi}{2} - \theta'_{12}\right) \\
&= \frac{c_{13}}{c'_{13}} \tan \left(\frac{\delta m_{21}^2}{2a} \sin(2\theta_{12}) + O(\varepsilon^{4,5})\right) \\
&= \frac{c_{13}}{c'_{13}} \left(\frac{\delta m_{21}^2}{2a} \sin(2\theta_{12})\right) + O(\varepsilon^{4,3})
\end{aligned}$$

$$= \tan \left(\frac{c_{13}}{c'_{13}} \frac{\delta m_{21}^2}{2a} \sin(2\theta_{12}) + O(\varepsilon^{4,3}) \right), \quad (118)$$

from which we can conclude

$$\tilde{\theta}_{12} = \frac{\pi}{2} - \frac{c_{13}}{c'_{13}} \left(\frac{\delta m_{21}^2}{2a} \right) \sin(2\theta_{12}) + O(\varepsilon^{4,3}). \quad (119)$$

Next, using the relation

$$s_{13}s'_{12}s_\phi - c_{13}c_\phi = -(c_{13}c_\phi - s_{13}s_\phi) - s_{13}(1 - s'_{12})s_\phi = -c'_{13} + O(\varepsilon^4), \quad (120)$$

we simplify the (2, 3) and (3, 3) elements of U' as

$$\begin{aligned} c_{23}c'_{12}s_\phi - s_{23}(s_{13}s'_{12}s_\phi - c_{13}c_\phi)e^{i\delta} &= c_{23}c'_{12}s_\phi + s_{23}c'_{13}e^{i\delta} + O(\varepsilon^4), \\ -s_{23}c'_{12}s_\phi - c_{23}(s_{13}s'_{12}s_\phi - c_{13}c_\phi)e^{i\delta} &= -s_{23}c'_{12}s_\phi + c_{23}c'_{13}e^{i\delta} + O(\varepsilon^4). \end{aligned} \quad (121)$$

Then, using the fact that $c'_{12}s_\phi = O(\varepsilon^2)$ or smaller, we find

$$\begin{aligned} &|c_{23}c'_{12}s_\phi - s_{23}(s_{13}s'_{12}s_\phi - c_{13}c_\phi)e^{i\delta}| \\ &= \sqrt{s_{23}^2 c_{13}'^2 + 2s_{23}c_{23}c'_{13}c'_{12}s_\phi \cos \delta + c_{23}^2 c_{12}'^2 s_\phi^2} + O(\varepsilon^4) \\ &= \sqrt{s_{23}^2 c_{13}'^2 + 2s_{23}c_{23}c'_{13}c'_{12}s_\phi \cos \delta} + O(\varepsilon^4) \\ &= s_{23}c'_{13} + c_{23}c'_{12}s_\phi \cos \delta + O(\varepsilon^4) \\ &|-s_{23}c'_{12}s_\phi - c_{23}(s_{13}s'_{12}s_\phi - c_{13}c_\phi)e^{i\delta}| \\ &= \sqrt{c_{23}^2 c_{13}'^2 - 2s_{23}c_{23}c'_{13}c'_{12}s_\phi \cos \delta + s_{23}^2 c_{12}'^2 s_\phi^2} + O(\varepsilon^4) \\ &= \sqrt{c_{23}^2 c_{13}'^2 - 2s_{23}c_{23}c'_{13}c'_{12}s_\phi \cos \delta} + O(\varepsilon^4) \\ &= c_{23}c'_{13} - s_{23}c'_{12}s_\phi \cos \delta + O(\varepsilon^4) \end{aligned} \quad (122)$$

Therefore, we can make the identification

$$\begin{aligned} \tan \tilde{\theta}_{23} &= \frac{\tilde{c}_{13}\tilde{s}_{23}}{\tilde{c}_{13}\tilde{c}_{23}} \\ &= \frac{s_{23}c'_{13} + c_{23}c'_{12}s_\phi \cos \delta}{c_{23}c'_{13} - s_{23}c'_{12}s_\phi \cos \delta} + O(\varepsilon^4) \\ &= \frac{t_{23} + \left(\frac{c'_{12}s_\phi}{c'_{13}} \right) \cos \delta}{1 - t_{23} \left(\frac{c'_{12}s_\phi}{c'_{13}} \right) \cos \delta} + O(\varepsilon^4) \\ &= \tan \left[\theta_{23} + \left(\frac{c'_{12}s_\phi}{c'_{13}} \right) \cos \delta \right] + O(\varepsilon^4), \end{aligned} \quad (123)$$

and we obtain

$$\tilde{\theta}_{23} = \theta_{23} + \left(\frac{c'_{12}s_\phi}{c'_{13}} \right) \cos \delta + O(\varepsilon^4). \quad (124)$$

The factor $c'_{12}s_\phi/c'_{13}$ is of order ε^3 or smaller if $\delta m_{31}^2 > 0$ with $a/|\delta m_{31}^2| \leq O(\varepsilon)$, or $\delta m_{31}^2 < 0$ with any a . In those cases, we have

$$\tilde{\theta}_{23} = \theta_{23} + O(\varepsilon^3). \quad (125)$$

For the case of $\delta m_{31}^2 > 0$ with $a/|\delta m_{31}^2| \geq O(1)$, we can expand c'_{12} and approximate

$$\tilde{\theta}_{23} = \theta_{23} + \frac{s_\phi}{c'_{13}} \left(\frac{\delta m_{21}^2}{2a} \right) \sin(2\theta_{12}) \cos \delta + O(\varepsilon^4). \quad (126)$$

Finally, we calculate the CP violating phase. The Jaroskog invariant of U' is

$$\begin{aligned} J' &= (c_{13}s'_{12}s_\phi + s_{13}c_\phi)(c_{13}s'_{12}c_\phi - s_{13}s_\phi)(c_{13}c'_{12})s_{23}c_{23} \sin \delta \\ &= \tilde{s}_{13}(\tilde{c}_{13}\tilde{s}_{12})(\tilde{c}_{13}\tilde{c}_{12})s_{23}c_{23} \sin \delta \\ &= (\tilde{s}_{13}\tilde{c}_{13}^2\tilde{s}_{12}\tilde{c}_{12})s_{23}c_{23} \sin \delta. \end{aligned} \quad (127)$$

On the other hand, the Jaroskog invariant of \tilde{U} is

$$\tilde{J} = \tilde{s}_{13}\tilde{c}_{13}^2\tilde{s}_{12}\tilde{c}_{12}\tilde{s}_{23}\tilde{c}_{23} \sin \tilde{\delta}. \quad (128)$$

Comparison with J' shows that

$$\sin(2\tilde{\theta}_{23}) \sin \tilde{\delta} = \sin(2\theta_{23}) \sin \delta, \quad (129)$$

which is actually an exact relation as discussed in Ref. [22]. Since $\tilde{\theta}_{23} = \theta_{23} + O(\varepsilon^3)$ when $\delta m_{31}^2 > 0$ with $a/|\delta m_{31}^2| \leq O(\varepsilon)$, or $\delta m_{31}^2 < 0$ with any a , for these cases we have

$$\tilde{\delta} = \delta + O(\varepsilon^3). \quad (130)$$

For the case $\delta m_{31}^2 > 0$ with $a/|\delta m_{31}^2| \geq O(1)$, we can use Eq. (126) to obtain

$$\tilde{\delta} = \delta - \frac{s_\phi}{c'_{13}} \left(\frac{\delta m_{21}^2}{a} \right) \frac{\sin(2\theta_{12})}{\tan(2\theta_{23})} \sin \delta + O(\varepsilon^6). \quad (131)$$

C. Summary of Neutrino Results and Sample Calculation

Let us summarize the results of the two previous subsections.

Approximate values of the effective mixing angles in matter can be obtained from the relations

$$\begin{aligned}
\tilde{\theta}_{13} &\approx \theta'_{13} , \\
\tan \tilde{\theta}_{12} &\approx \frac{c'_{13}}{c_{13}} \tan \theta'_{12} , \\
\tilde{\theta}_{23} &\approx \theta_{23} + \left(\frac{c'_{12} s_\phi}{c'_{13}} \right) \cos \delta , \\
\sin(2\tilde{\theta}_{23}) \sin \tilde{\delta} &= \sin(2\theta_{23}) \sin \delta ,
\end{aligned} \tag{132}$$

where

$$\begin{aligned}
\theta'_{12} &= \theta_{12} + \varphi , \\
\theta'_{13} &= \theta_{13} + \phi ,
\end{aligned} \tag{133}$$

and the angles φ and ϕ were defined in Eqs. (45) and (69), respectively. The a -dependence of φ and ϕ for the sample case of $\tan^2 \theta_{12} = 0.4$, $\sin^2(2\theta_{13}) = 0.16$, $\delta m_{21}^2 = 8.2 \times 10^{-5} \text{eV}^2$, and $|\delta m_{31}^2| = 2.5 \times 10^{-3} \text{eV}^2$ is shown in Fig 1 with gray solid lines. In the figure, the angles are in units of π , and they are plotted against the variable α defined as:

$$\alpha \equiv \log_{1/\varepsilon} \frac{a}{|\delta m_{31}^2|} , \quad \frac{a}{|\delta m_{31}^2|} = \varepsilon^{-\alpha} . \tag{134}$$

$\alpha = 0$ corresponds to $a = |\delta m_{31}^2|$, and $\alpha = -2$ corresponds to $a = \delta m_{21}^2$.

When either $\delta m_{31}^2 > 0$ (normal hierarchy) with $\alpha \lesssim -1$, which corresponds to $a/|\delta m_{31}^2| \leq O(\varepsilon)$, or $\delta m_{31}^2 < 0$ (inverted hierarchy) with any α , the angle ϕ is small, and Eq. (132) reduces to

$$\begin{aligned}
\tilde{\theta}_{13} &\approx \theta'_{13} = \theta_{13} + \phi , \\
\tilde{\theta}_{12} &\approx \theta'_{12} = \theta_{12} + \varphi , \\
\tilde{\theta}_{23} &\approx \theta_{23} , \\
\tilde{\delta} &\approx \delta .
\end{aligned} \tag{135}$$

For the $\delta m_{31}^2 > 0$ case (normal hierarchy) with $\alpha \gtrsim 0$, which corresponds to $a/|\delta m_{31}^2| \geq O(1)$, the angles can be approximated as

$$\begin{aligned}
\tilde{\theta}_{13} &\approx \theta'_{13} , \\
\tilde{\theta}_{12} &\approx \frac{\pi}{2} - \frac{c_{13}}{c'_{13}} \left(\frac{\delta m_{21}^2}{2a} \right) \sin(2\theta_{12}) ,
\end{aligned}$$

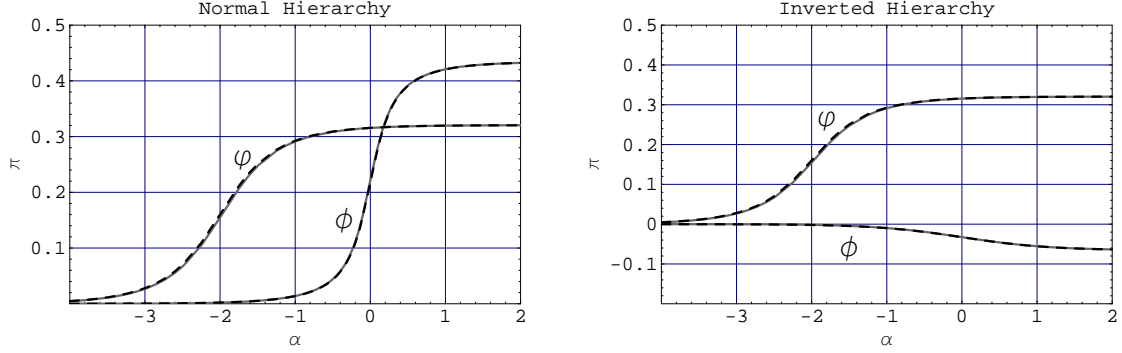


FIG. 1: The exact (gray solid line) and approximate (black dashed line) values of φ and ϕ plotted against $\alpha = \log_{1/\varepsilon}(a/|\delta m_{31}^2|)$. The parameter choice was $\tan^2 \theta_{12} = 0.4$, $\sin^2(2\theta_{13}) = 0.16$, $\delta m_{21}^2 = 8.2 \times 10^{-5} \text{eV}^2$ and $|\delta m_{31}^2| = 2.5 \times 10^{-3} \text{eV}^2$.

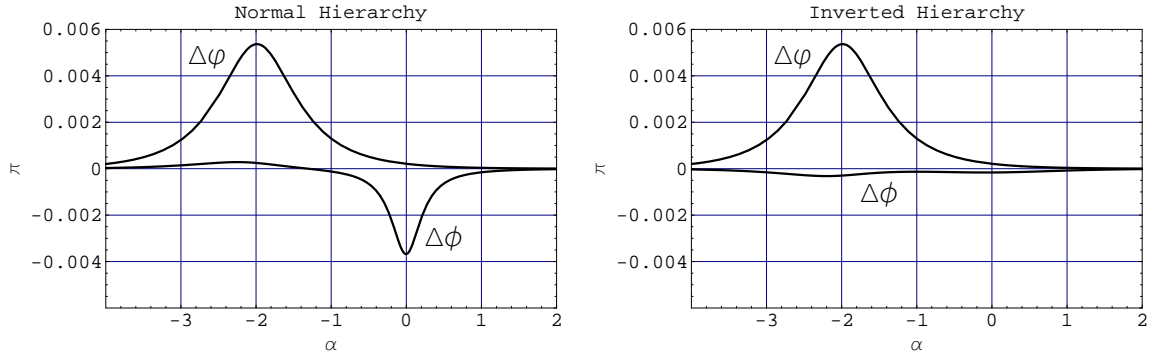


FIG. 2: $\Delta\varphi = \varphi_{\text{approx}} - \varphi_{\text{exact}}$ and $\Delta\phi = \phi_{\text{approx}} - \phi_{\text{exact}}$ plotted against $\alpha = \log_{1/\varepsilon}(a/|\delta m_{31}^2|)$ for the same parameter choice as Fig. 1.

$$\begin{aligned}
\tilde{\theta}_{23} &\approx \theta_{23} + \frac{s_\phi}{c'_{13}} \left(\frac{\delta m_{21}^2}{2a} \right) \sin(2\theta_{12}) \cos \delta , \\
\tilde{\delta} &\approx \delta - \frac{s_\phi}{c'_{13}} \left(\frac{\delta m_{21}^2}{a} \right) \frac{\sin(2\theta_{12})}{\tan(2\theta_{23})} \sin \delta .
\end{aligned} \tag{136}$$

To make use of these expressions, we must first calculate φ and ϕ , and then $\theta'_{12} = \theta_{12} + \varphi$ and $\theta'_{13} = \theta_{13} + \phi$. Simple approximations to φ and ϕ are provided by

$$\tan 2\varphi \approx \frac{a \sin 2\theta_{12}}{\delta m_{21}^2 - a \cos 2\theta_{12}} , \quad \tan 2\phi \approx \frac{a \sin 2\theta_{13}}{\delta m_{31}^2 - a \cos 2\theta_{13}} . \tag{137}$$

The approximate values of φ and ϕ obtained from these expressions are also shown in Fig. 1 with black dashed lines. As is clear from the figure, the graphs of the exact and approximate values are virtually indistinguishable at this scale. In Fig. 2 we plot the differences between the approximate and exact values of φ and ϕ :

$$\Delta\varphi \equiv \varphi_{\text{approx}} - \varphi_{\text{exact}} , \quad \Delta\phi \equiv \phi_{\text{approx}} - \phi_{\text{exact}} . \tag{138}$$

The maximum deviation from the exact values occur at the level-crossing points $\alpha = -2$ and $\alpha = 0$ (there is no level-crossing at $\alpha = 0$ when $\delta m_{31}^2 < 0$) but even then, it is a mere fraction of a percent of π . Using Eq. (137), we can also obtain simple approximate formulae for $\theta'_{12} = \theta_{12} + \varphi$ and $\theta'_{13} = \theta_{13} + \phi$:

$$\tan 2\theta'_{12} \approx \frac{\delta m_{21}^2 \sin 2\theta_{12}}{\delta m_{21}^2 \cos 2\theta_{12} - a} , \quad \tan 2\theta'_{13} \approx \frac{\delta m_{31}^2 \sin 2\theta_{13}}{\delta m_{31}^2 \cos 2\theta_{13} - a} . \tag{139}$$

These allow us to calculate θ'_{12} and θ'_{13} directly without going through φ and ϕ . Eqs. (137) and (139) provide a quick and easy way to obtain the input angles necessary to utilize Eqs. (132), (135), and (136).

To demonstrate the accuracy of these approximations, we present a sample calculation using the following parameter choice:

$$\begin{aligned}
\delta m_{21}^2 &= 8.2 \times 10^{-5} \text{ eV}^2 , \\
|\delta m_{31}^2| &= 2.5 \times 10^{-3} \text{ eV}^2 , \\
\tan^2 \theta_{12} &= 0.4 , \\
\sin^2(2\theta_{13}) &= 0.16 , \\
\theta_{23} &= 0.2 \pi , \\
\delta &= 0.25 \pi .
\end{aligned} \tag{140}$$

The values of δm_{21}^2 , $|\delta m_{31}^2|$, and $\tan^2 \theta_{12}$ are the experimental central values. The value of $\sin^2(2\theta_{13})$ is taken to be the 90% upper limit corresponding to our choice of $|\delta m_{31}^2|$ so that

the $O(\theta_{13})$ terms that we neglect are maximized. The value of θ_{23} is also chosen to be one of the 90% confidence limits since if we set θ_{23} to the experimentally preferred central value of 0.25π , then the shift of $\tilde{\delta}$ away from δ would be suppressed. Similarly, we chose $\delta = 0.25\pi$ so that both $\tilde{\theta}_{23}$ and $\tilde{\delta}$ will be shifted from their vacuum values.

We first consider the normal hierarchy case ($\delta m_{31}^2 > 0$). In Fig. 3a, we plot the exact values of $\tilde{\theta}_{12}$, $\tilde{\theta}_{13}$, $\tilde{\theta}_{23}$, and $\tilde{\delta}$ calculated numerically with gray solid lines, together with the approximate values obtained from Eq. (132), using Eqs. (137) and (139) to calculate the input angles, with dashed black lines. Fig. 3b shows the errors:

$$\Delta\theta_{ij} \equiv \tilde{\theta}_{ij,\text{approx}} - \tilde{\theta}_{ij,\text{exact}} , \quad \Delta\delta \equiv \tilde{\delta}_{\text{approx}} - \tilde{\delta}_{\text{exact}} . \quad (141)$$

$\Delta\theta_{12}$ and $\Delta\theta_{13}$ are indicated with solid gray lines, while $\Delta\theta_{23}$ and $\Delta\delta$ are indicated with dashed black lines. The errors are never larger than a fraction of a percent of π , and comparison with Fig. 2 makes it apparent that the majority of it was inherited from having calculated φ and ϕ using Eq. (137). In Figs. 4a and 5a, we plot the exact values against the approximate values obtained using Eqs. (135) and (136), respectively, together with the errors in Figs. 4b and 5b. Clearly, the approximations using Eqs. (135) and (136) are good in their respective ranges of applicability.

For the inverted hierarchy case ($\delta m_{31}^2 < 0$), we only need to consider Eq. (135). In Fig. 6a, we show the comparison between the numerically calculated exact values and the approximate values obtained from Eq. (135). The errors are shown in Fig. 6b.

The approximate values for the mass-squared eigenvalues are given by

$$\begin{aligned} \lambda_1 &\approx \lambda'_- , \\ \lambda_2 &\approx \lambda''_- , \\ \lambda_3 &\approx \lambda''_+ , \end{aligned} \quad (142)$$

for $\delta m_{31}^2 > 0$ (normal hierarchy), and by

$$\begin{aligned} \lambda_1 &\approx \lambda'_- , \\ \lambda_2 &\approx \lambda''_+ , \\ \lambda_3 &\approx \lambda''_- , \end{aligned} \quad (143)$$

for $\delta m_{31}^2 < 0$ (inverted hierarchy), where λ'_\pm and λ''_\pm are defined in Eqs. (49) and (72), respectively. The accuracy of this approximation is illustrated in Fig 7 using the parameter

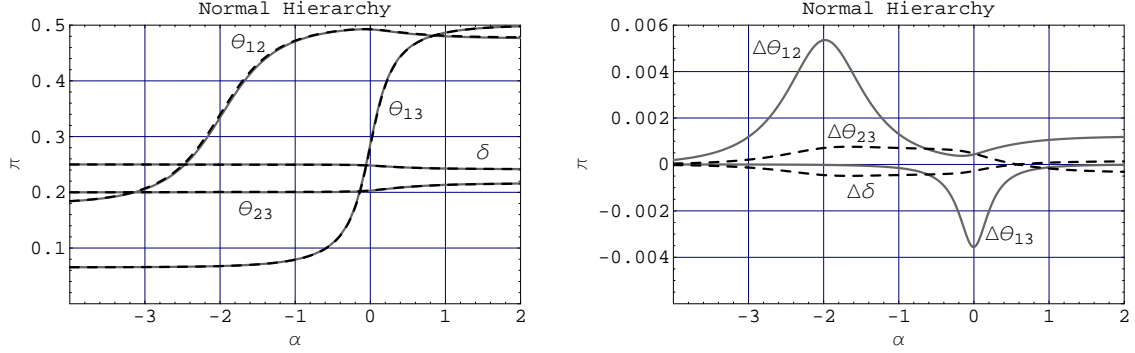


FIG. 3: (a) The exact values of $\tilde{\theta}_{12}$, $\tilde{\theta}_{13}$, $\tilde{\theta}_{23}$, and $\tilde{\delta}$ (solid gray lines) plotted against their approximate values (black dashed lines) obtained using Eq. (132), with Eqs. (137) and (139), as functions of $\alpha = \log_{1/\epsilon}(a/|\delta m_{31}^2|)$. (b) The differences $\Delta\theta_{12} = \tilde{\theta}_{12,\text{approx}} - \tilde{\theta}_{12,\text{exact}}$ and $\Delta\theta_{13} = \tilde{\theta}_{13,\text{approx}} - \tilde{\theta}_{13,\text{exact}}$ (solid gray lines), and the differences $\Delta\theta_{23} = \tilde{\theta}_{23,\text{approx}} - \tilde{\theta}_{23,\text{exact}}$ and $\Delta\delta = \tilde{\delta}_{\text{approx}} - \tilde{\delta}_{\text{exact}}$ (black dashed lines) of this approximation plotted against α .

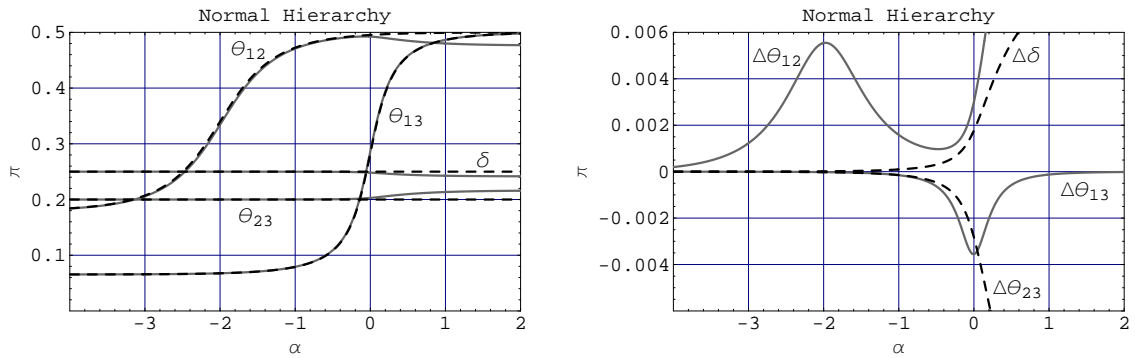


FIG. 4: (a) The exact values of $\tilde{\theta}_{12}$, $\tilde{\theta}_{13}$, $\tilde{\theta}_{23}$, and $\tilde{\delta}$ (solid gray lines) plotted against their approximate values (black dashed lines) obtained using Eq. (135) as functions of $\alpha = \log_{1/\epsilon}(a/|\delta m_{31}^2|)$. (b) $\Delta\theta_{12}$ and $\Delta\theta_{13}$ (solid gray lines), and $\Delta\theta_{23}$ and $\Delta\delta$ (black dashed lines) of this approximation plotted as functions of α . This approximation is applicable when $\alpha \lesssim -1$.

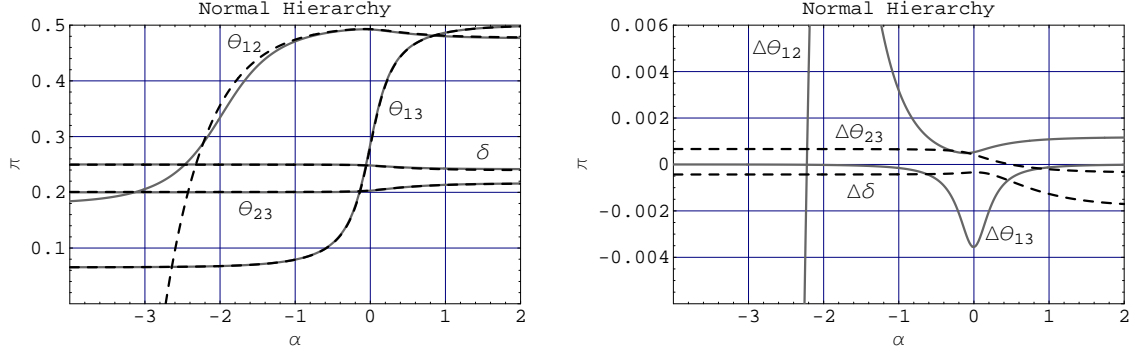


FIG. 5: (a) The exact values of $\tilde{\theta}_{12}$, $\tilde{\theta}_{13}$, $\tilde{\theta}_{23}$, and $\tilde{\delta}$ (solid gray lines) plotted against their approximate values (black dashed lines) obtained using Eq. (136) as functions of $\alpha = \log_{1/\varepsilon}(a/|\delta m_{31}^2|)$. (b) $\Delta\theta_{12}$ and $\Delta\theta_{13}$ (solid gray lines), and $\Delta\theta_{23}$ and $\Delta\delta$ (black dashed lines) of this approximation plotted as functions of α . This approximation is applicable when $\alpha \gtrsim 0$.

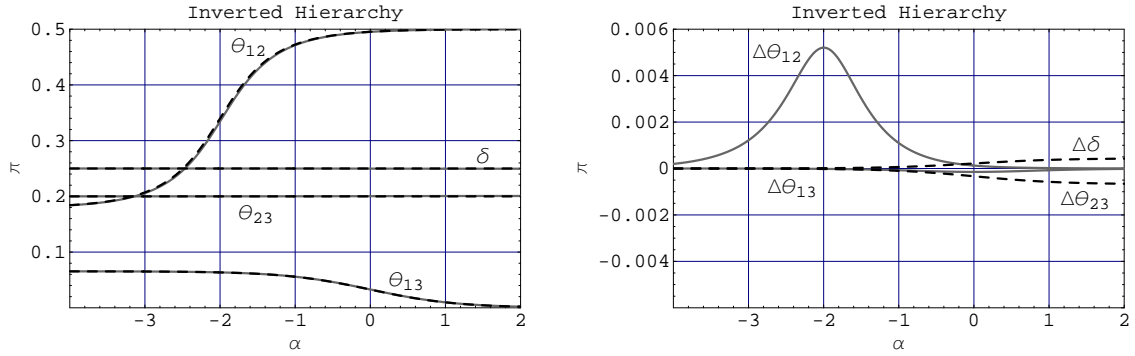


FIG. 6: (a) The exact values of $\tilde{\theta}_{12}$, $\tilde{\theta}_{13}$, $\tilde{\theta}_{23}$, and $\tilde{\delta}$ (solid gray lines) plotted against their approximate values (black dashed lines) obtained using Eq. (135) as functions of $\alpha = \log_{1/\varepsilon}(a/|\delta m_{31}^2|)$ for the inverted hierarchy case ($\delta m_{31}^2 < 0$). (b) $\Delta\theta_{12}$ and $\Delta\theta_{13}$ (solid gray lines), and $\Delta\theta_{23}$ and $\Delta\delta$ (black dashed lines) of this approximation plotted as functions of α .

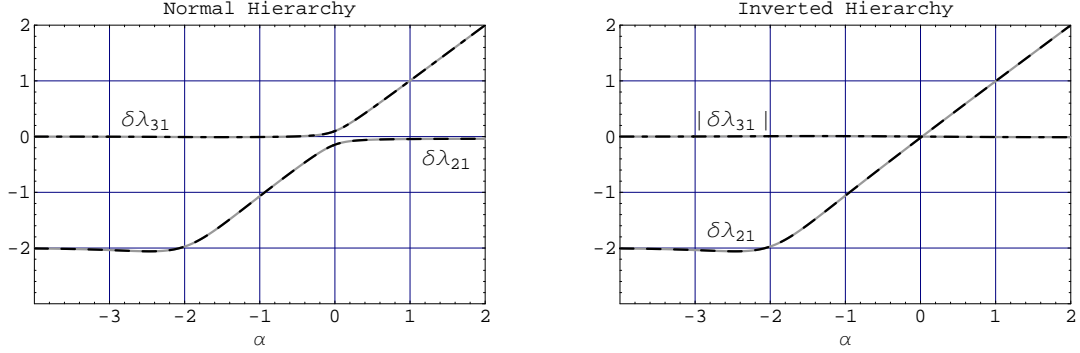


FIG. 7: The exact and approximate values of $\log_{1/\epsilon}(\delta\lambda_{21}/|\delta m_{31}^2|)$ and $\log_{1/\epsilon}(|\delta\lambda_{31}|/|\delta m_{31}^2|)$ for the parameter set of Eq. (140) plotted against $\alpha = \log_{1/\epsilon}(a/|\delta m_{31}^2|)$. The exact values are in gray solid lines, whereas the approximate values are in black dashed ($\delta\lambda_{21}$) and black dot-dashed ($|\delta\lambda_{31}|$) lines.

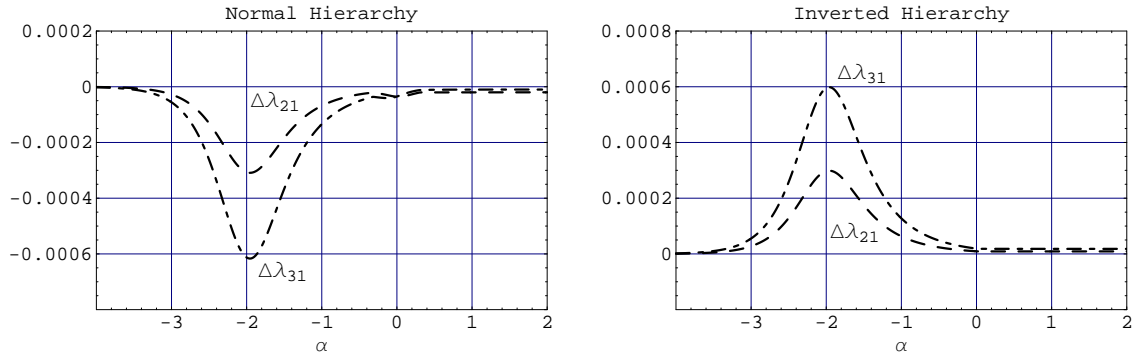


FIG. 8: The rescaled errors $\Delta\lambda_{21}$ (dashed) and $\Delta\lambda_{31}$ (dot-dashed), as defined in Eq. (144), for the approximation of Fig. 7.

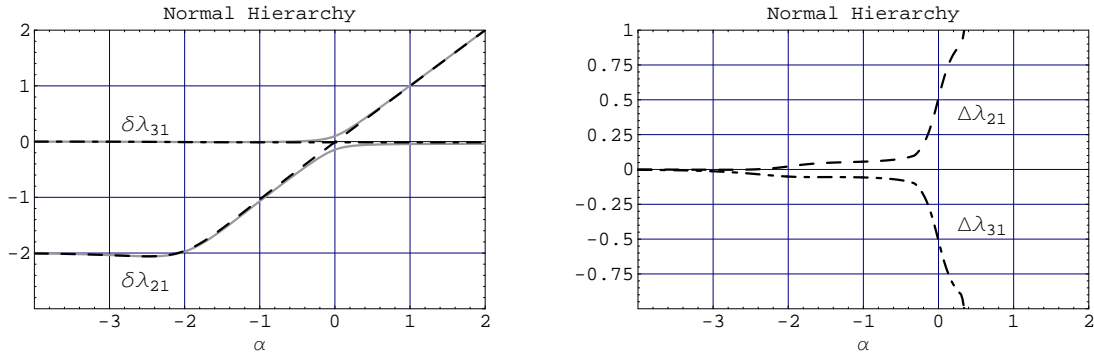


FIG. 9: Comparison of exact and approximate values using Eq. (146) for the normal hierarchy case. The approximation is applicable when $\alpha \lesssim -1$.

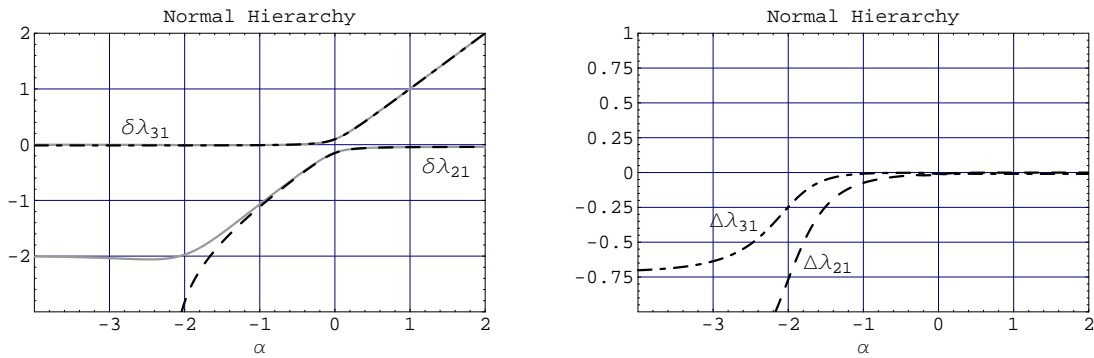


FIG. 10: Comparison of exact and approximate values using Eq. (147) for the normal hierarchy case. The approximation is applicable when $\alpha \gtrsim -1$.

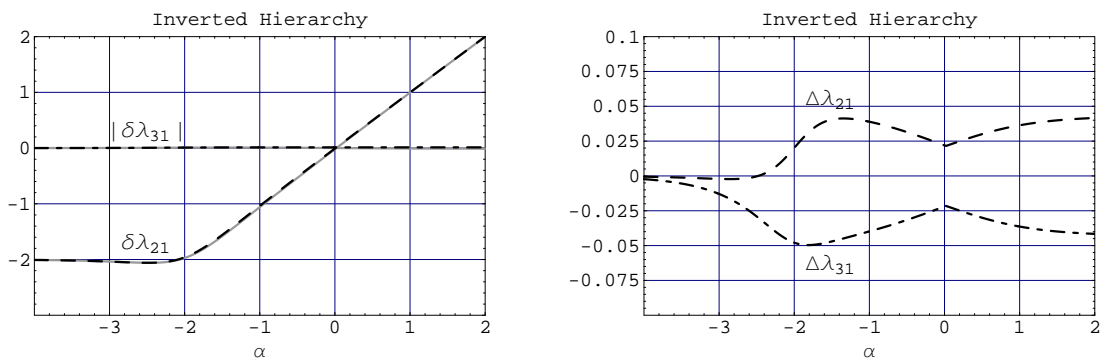


FIG. 11: Comparison of exact and approximate values using Eq. (146) for the inverted hierarchy case.

values of Eq. (140), where the exact numerically calculated values of $\delta\lambda_{21} = \lambda_2 - \lambda_1$ and $|\delta\lambda_{31}| = |\lambda_3 - \lambda_1|$ are plotted against those obtained from the above approximate expressions. The vertical axis is plotted using the same log-scale as the horizontal axis where $|\delta m_{31}^2|$ corresponds to 0 and δm_{21}^2 corresponds to -2 . Since a log-scale plot does not reflect the absolute accuracy of each $\delta\lambda_{ij}$, in Fig. 8 we plot the difference between the exact and approximate values of $\delta\lambda_{ij}$ normalized to $\delta\lambda_{\min,\text{exact}}$:

$$\Delta\lambda_{i1} \equiv \frac{\delta\lambda_{i1,\text{approx}} - \delta\lambda_{i1,\text{exact}}}{\delta\lambda_{\min,\text{exact}}}, \quad (i = 2, 3), \quad (144)$$

where

$$\delta\lambda_{\min,\text{exact}} \equiv \min(\delta\lambda_{21,\text{exact}}, |\delta\lambda_{31,\text{exact}}|, |\delta\lambda_{32,\text{exact}}|). \quad (145)$$

This tells us how large the errors are compared to $\delta\lambda_{\min}$, which is typically used to expand the oscillation probabilities in. As is evident from the figures, the approximation is excellent.

When either $\delta m_{31}^2 > 0$ (normal hierarchy) with $\alpha \lesssim -1$, *i.e.* $a/|\delta m_{31}^2| \leq O(\varepsilon)$, or $\delta m_{31}^2 < 0$ (inverted hierarchy) with any a , the λ 's can be further approximated by

$$\begin{aligned} \lambda_1 &\approx \frac{(a + \delta m_{21}^2) - \sqrt{(a - \delta m_{21}^2)^2 + 4a \delta m_{21}^2 s_{12}^2}}{2}, \\ \lambda_2 &\approx \frac{(a + \delta m_{21}^2) + \sqrt{(a - \delta m_{21}^2)^2 + 4a \delta m_{21}^2 s_{12}^2}}{2}, \\ \lambda_3 &\approx \delta m_{31}^2. \end{aligned} \quad (146)$$

For the $\delta m_{31}^2 > 0$ (normal hierarchy) case with $\alpha \gtrsim -1$, *i.e.* $a/|\delta m_{31}^2| \geq O(\varepsilon)$, we can use

$$\begin{aligned} \lambda_1 &\approx \delta m_{21}^2 c_{12}^2, \\ \lambda_2 &\approx \frac{(a + \delta m_{31}^2) - \sqrt{(a - \delta m_{31}^2)^2 + 4a \delta m_{31}^2 s_{13}^2}}{2}, \\ \lambda_3 &\approx \frac{(a + \delta m_{31}^2) + \sqrt{(a - \delta m_{31}^2)^2 + 4a \delta m_{31}^2 s_{13}^2}}{2}. \end{aligned} \quad (147)$$

This second approximation introduces errors of $O(\varepsilon^2|\delta m_{31}^2|)$ in the λ 's. However, since $\delta\lambda_{21} \geq O(\varepsilon|\delta m_{31}^2|)$ in this range, an error of this size is tolerable. The accuracy of these approximations is illustrated in Figs. 9 and 10 for the $\delta m_{31}^2 > 0$ case, and Fig. 11 for the $\delta m_{31}^2 < 0$ case. Though the accuracy is not as good as when Eqs. (142) and (143), with Eqs. (49) and (72), are used, it is sufficient for most practical purposes.

D. Anti-Neutrino Case

Matter effects for anti-neutrinos can be treated in an analogous fashion. We will therefore omit the details and give only an outline of the derivation and results.

The effective Hamiltonian for anti-neutrinos in matter is

$$\bar{H} = \tilde{U}^* \begin{bmatrix} \bar{\lambda}_1 & 0 & 0 \\ 0 & \bar{\lambda}_2 & 0 \\ 0 & 0 & \bar{\lambda}_3 \end{bmatrix} \tilde{U}^T = U^* \begin{bmatrix} 0 & 0 & 0 \\ 0 & \delta m_{21}^2 & 0 \\ 0 & 0 & \delta m_{31}^2 \end{bmatrix} U^T + \begin{bmatrix} -a & 0 & 0 \\ 0 & 0 & 0 \\ 0 & 0 & 0 \end{bmatrix}, \quad (148)$$

We denote the effective mass-squared eigenvalues as $\bar{\lambda}_i$, ($i = 1, 2, 3$), and the diagonalization matrix as \tilde{U} to distinguish them from those for the neutrinos. (Note the mirror image of the tilde on top of \tilde{U} .) This matrix can be partially diagonalized as

$$\begin{aligned} \bar{H}' &= \mathcal{Q} U^T \bar{H} U^* \mathcal{Q}^* \\ &= \mathcal{Q} \left\{ \begin{bmatrix} 0 & 0 & 0 \\ 0 & \delta m_{21}^2 & 0 \\ 0 & 0 & \delta m_{31}^2 \end{bmatrix} + U^T \begin{bmatrix} -a & 0 & 0 \\ 0 & 0 & 0 \\ 0 & 0 & 0 \end{bmatrix} U^* \right\} \mathcal{Q}^* \\ &= \mathcal{Q} \begin{bmatrix} 0 & 0 & 0 \\ 0 & \delta m_{21}^2 & 0 \\ 0 & 0 & \delta m_{31}^2 \end{bmatrix} \mathcal{Q}^* - a \mathcal{Q} \begin{bmatrix} U_{e1} U_{e1}^* & U_{e1} U_{e2}^* & U_{e1} U_{e3}^* \\ U_{e2} U_{e1}^* & U_{e2} U_{e2}^* & U_{e2} U_{e3}^* \\ U_{e3} U_{e1}^* & U_{e3} U_{e2}^* & U_{e3} U_{e3}^* \end{bmatrix} \mathcal{Q}^* \\ &= \begin{bmatrix} 0 & 0 & 0 \\ 0 & \delta m_{21}^2 & 0 \\ 0 & 0 & \delta m_{31}^2 \end{bmatrix} - a \begin{bmatrix} c_{12}^2 c_{13}^2 & c_{12} s_{12} c_{13}^2 & c_{12} c_{13} s_{13} \\ c_{12} s_{12} c_{13}^2 & s_{12}^2 c_{13}^2 & s_{12} c_{13} s_{13} \\ c_{12} c_{13} s_{13} & s_{12} c_{13} s_{13} & s_{13}^2 \end{bmatrix} \\ &= \begin{bmatrix} -a c_{12}^2 c_{13}^2 & -a c_{12} s_{12} c_{13}^2 & -a c_{12} c_{13} s_{13} \\ -a c_{12} s_{12} c_{13}^2 & -a s_{12}^2 c_{13}^2 + \delta m_{21}^2 & -a s_{12} c_{13} s_{13} \\ -a c_{12} c_{13} s_{13} & -a s_{12} c_{13} s_{13} & -a s_{13}^2 + \delta m_{31}^2 \end{bmatrix}. \end{aligned} \quad (149)$$

The only difference from the effective Hamiltonian H' for the neutrinos, Eq. (38), is in the sign in front of the matter-effect term a .

Following the general procedure we employed for the neutrinos, we begin by diagonalizing the 1-2 submatrix of \bar{H}' . Let

$$\bar{V} = \begin{bmatrix} \bar{c}_\varphi & \bar{s}_\varphi & 0 \\ -\bar{s}_\varphi & \bar{c}_\varphi & 0 \\ 0 & 0 & 1 \end{bmatrix}, \quad (150)$$

where

$$\bar{c}_\varphi = \cos \bar{\varphi}, \quad \bar{s}_\varphi = \sin \bar{\varphi}, \quad \tan 2\bar{\varphi} \equiv -\frac{ac_{13}^2 \sin 2\theta_{12}}{\delta m_{21}^2 + ac_{13}^2 \cos 2\theta_{12}}, \quad \left(-\frac{\pi}{2} < \bar{\varphi} \leq 0\right). \quad (151)$$

Using \bar{V} , we find

$$\bar{H}'' = \bar{V}^\dagger \bar{H}' \bar{V} = \begin{bmatrix} \bar{\lambda}'_1 & 0 & -a\bar{c}'_{12}c_{13}s_{13} \\ 0 & \bar{\lambda}'_2 & -a\bar{s}'_{12}c_{13}s_{13} \\ -a\bar{c}'_{12}c_{13}s_{13} & -a\bar{s}'_{12}c_{13}s_{13} & -as_{13}^2 + \delta m_{31}^2 \end{bmatrix}, \quad (152)$$

where

$$\bar{c}'_{12} = \cos \bar{\theta}'_{12}, \quad \bar{s}'_{12} = \sin \bar{\theta}'_{12}, \quad \bar{\theta}'_{12} = \theta_{12} + \bar{\varphi}, \quad \tan 2\bar{\theta}'_{12} = \frac{\delta m_{21}^2 \sin 2\theta_{12}}{\delta m_{21}^2 \cos 2\theta_{12} + ac_{13}^2}, \quad (153)$$

and $\bar{\lambda}'_1 = \bar{\lambda}'_-, \bar{\lambda}'_2 = \bar{\lambda}'_+$, with

$$\bar{\lambda}'_{\pm} = \frac{(\delta m_{21}^2 - ac_{13}^2) \pm \sqrt{(\delta m_{21}^2 + ac_{13}^2)^2 - 4ac_{13}^2 \delta m_{21}^2 s_{12}^2}}{2}. \quad (154)$$

Next, unlike the neutrino case, we diagonalize the 1-3 submatrix of \bar{H}'' . Let

$$\bar{W} = \begin{bmatrix} \bar{c}_\phi & 0 & \bar{s}_\phi \\ 0 & 1 & 0 \\ -\bar{s}_\phi & 0 & \bar{c}_\phi \end{bmatrix} \quad (155)$$

where

$$\bar{c}_\phi = \cos \bar{\phi}, \quad \bar{s}_\phi = \sin \bar{\phi}, \quad \tan 2\bar{\phi} \equiv -\frac{a\bar{c}'_{12} \sin 2\theta_{13}}{\delta m_{31}^2 - as_{13}^2 - \bar{\lambda}'_1}. \quad (156)$$

The angle $\bar{\phi}$ is in the fourth quadrant when $\delta m_{31}^2 > 0$, and the first quadrant when $\delta m_{31}^2 < 0$.

Using \bar{W} , we find

$$\bar{H}''' = \bar{W}^\dagger \bar{H}'' \bar{W} = \begin{bmatrix} \bar{\lambda}''_1 & a\bar{s}'_{12}c_{13}s_{13}\bar{s}_\phi & 0 \\ a\bar{s}'_{12}c_{13}s_{13}\bar{s}_\phi & \bar{\lambda}''_2 & -a\bar{s}'_{12}c_{13}s_{13}\bar{c}_\phi \\ 0 & -a\bar{s}'_{12}c_{13}s_{13}\bar{c}_\phi & \bar{\lambda}''_3 \end{bmatrix}, \quad (157)$$

where

$$\begin{aligned} \bar{\lambda}''_1 &= \bar{\lambda}''_-, & \bar{\lambda}''_3 &= \bar{\lambda}''_+, & \text{if } \delta m_{31}^2 > 0, \\ \bar{\lambda}''_1 &= \bar{\lambda}''_+, & \bar{\lambda}''_3 &= \bar{\lambda}''_-, & \text{if } \delta m_{31}^2 < 0. \end{aligned} \quad (158)$$

with

$$\bar{\lambda}''_{\pm} \equiv \frac{[(\delta m_{31}^2 - as_{13}^2) + \bar{\lambda}'_1] \pm \sqrt{[(\delta m_{31}^2 - as_{13}^2) - \bar{\lambda}'_1]^2 + 4a^2\bar{c}'_{12}{}^2c_{13}^2s_{13}^2}}{2}. \quad (159)$$

Evaluation of the off-diagonal terms of \bar{H}''' reveals that it is approximately diagonalized, and the diagonalization matrix is given approximately by

$$\bar{U}'^* \equiv U^* Q^* \bar{V} \bar{W} = U^* \bar{V} Q^* \bar{W} , \quad (160)$$

or taking the complex conjugate,

$$\begin{aligned} & \bar{U}' \\ &= U \bar{V} Q \bar{W} \\ &= \begin{bmatrix} 1 & 0 & 0 \\ 0 & c_{23} & s_{23} \\ 0 & -s_{23} & c_{23} \end{bmatrix} \begin{bmatrix} c_{13} & 0 & s_{13} e^{-i\delta} \\ 0 & 1 & 0 \\ -s_{13} e^{i\delta} & 0 & c_{13} \end{bmatrix} \begin{bmatrix} c_{12} & s_{12} & 0 \\ -s_{12} & c_{12} & 0 \\ 0 & 0 & 1 \end{bmatrix} \begin{bmatrix} \bar{c}_\varphi & \bar{s}_\varphi & 0 \\ -\bar{s}_\varphi & \bar{c}_\varphi & 0 \\ 0 & 0 & 1 \end{bmatrix} Q \bar{W} \\ &= \begin{bmatrix} 1 & 0 & 0 \\ 0 & c_{23} & s_{23} \\ 0 & -s_{23} & c_{23} \end{bmatrix} \begin{bmatrix} c_{13} & 0 & s_{13} e^{-i\delta} \\ 0 & 1 & 0 \\ -s_{13} e^{i\delta} & 0 & c_{13} \end{bmatrix} \begin{bmatrix} \bar{c}'_{12} & \bar{s}'_{12} & 0 \\ -\bar{s}'_{12} & \bar{c}'_{12} & 0 \\ 0 & 0 & 1 \end{bmatrix} \begin{bmatrix} 1 & 0 & 0 \\ 0 & 1 & 0 \\ 0 & 0 & e^{i\delta} \end{bmatrix} \begin{bmatrix} \bar{c}_\phi & 0 & \bar{s}_\phi \\ 0 & 1 & 0 \\ -\bar{s}_\phi & 0 & \bar{c}_\phi \end{bmatrix} \\ &= \begin{bmatrix} c_{13} \bar{c}'_{12} \bar{c}_\phi - s_{13} \bar{s}_\phi & c_{13} \bar{s}'_{12} & s_{13} \bar{c}_\phi + c_{13} \bar{c}'_{12} \bar{s}_\phi \\ -c_{23} \bar{s}'_{12} \bar{c}_\phi - s_{23} (c_{13} \bar{s}_\phi + s_{13} \bar{c}'_{12} \bar{c}_\phi) e^{i\delta} & c_{23} \bar{c}'_{12} - s_{23} s_{13} \bar{s}'_{12} e^{i\delta} & -c_{23} \bar{s}'_{12} \bar{s}_\phi + s_{23} (c_{13} \bar{c}_\phi - s_{13} \bar{c}'_{12} \bar{s}_\phi) e^{i\delta} \\ s_{23} \bar{s}'_{12} \bar{c}_\phi - c_{23} (c_{13} \bar{s}_\phi + s_{13} \bar{c}'_{12} \bar{c}_\phi) e^{i\delta} & -s_{23} \bar{c}'_{12} - c_{23} s_{13} \bar{s}'_{12} e^{i\delta} & s_{23} \bar{s}'_{12} \bar{s}_\phi + c_{23} (c_{13} \bar{c}_\phi - s_{13} \bar{c}'_{12} \bar{s}_\phi) e^{i\delta} \end{bmatrix} \end{aligned} \quad (161)$$

Identification of this matrix with

$$\begin{aligned} \tilde{U} &= \begin{bmatrix} 1 & 0 & 0 \\ 0 & \tilde{c}_{23} & \tilde{s}_{23} \\ 0 & -\tilde{s}_{23} & \tilde{c}_{23} \end{bmatrix} \begin{bmatrix} \tilde{c}_{13} & 0 & \tilde{s}_{13} e^{-i\tilde{\delta}} \\ 0 & 1 & 0 \\ -\tilde{s}_{13} e^{i\tilde{\delta}} & 0 & \tilde{c}_{13} \end{bmatrix} \begin{bmatrix} \tilde{c}_{12} & \tilde{s}_{12} & 0 \\ -\tilde{s}_{12} & \tilde{c}_{12} & 0 \\ 0 & 0 & 1 \end{bmatrix} \\ &= \begin{bmatrix} \tilde{c}_{12} \tilde{c}_{13} & \tilde{s}_{12} \tilde{c}_{13} & \tilde{s}_{13} e^{-i\tilde{\delta}} \\ -\tilde{s}_{12} \tilde{c}_{23} - \tilde{c}_{12} \tilde{s}_{13} \tilde{s}_{23} e^{i\tilde{\delta}} & \tilde{c}_{12} \tilde{c}_{23} - \tilde{s}_{12} \tilde{s}_{13} \tilde{s}_{23} e^{i\tilde{\delta}} & \tilde{c}_{13} \tilde{s}_{23} \\ \tilde{s}_{12} \tilde{s}_{23} - \tilde{c}_{12} \tilde{s}_{13} \tilde{c}_{23} e^{i\tilde{\delta}} & -\tilde{c}_{12} \tilde{s}_{23} - \tilde{s}_{12} \tilde{s}_{13} \tilde{c}_{23} e^{i\tilde{\delta}} & \tilde{c}_{13} \tilde{c}_{23} \end{bmatrix} , \end{aligned} \quad (162)$$

(up to phases that can be absorbed into redefinitions of the charged lepton fields and the Majorana phases of the neutrinos) yields

$$\begin{aligned} \tilde{\theta}_{13} &\approx \bar{\theta}'_{13} , \\ \tan \tilde{\theta}_{12} &\approx \frac{c_{13}}{\bar{c}'_{13}} \tan \bar{\theta}'_{12} , \\ \tilde{\theta}_{23} &\approx \theta_{23} - \left(\frac{\bar{s}'_{12} \bar{s}_\phi}{\bar{c}'_{13}} \right) \cos \delta , \end{aligned}$$

$$\sin(2\tilde{\theta}_{23}) \sin \tilde{\delta} \approx \sin(2\theta_{23}) \sin \delta , \quad (163)$$

where

$$\bar{s}'_{13} = \sin \bar{\theta}'_{13} , \quad \bar{c}'_{13} = \cos \bar{\theta}'_{13} , \quad \bar{\theta}'_{13} \equiv \theta_{13} + \bar{\phi} . \quad (164)$$

For the $\delta m_{31}^2 > 0$ case (normal hierarchy) with any a , or the $\delta m_{31}^2 < 0$ case (inverted hierarchy) with $a/|\delta m_{31}^2| \leq O(\varepsilon)$, the angle $\bar{\phi}$ is small and the above relations simplify to

$$\begin{aligned} \tilde{\theta}_{13} &\approx \bar{\theta}'_{13} = \theta_{13} + \bar{\phi} , \\ \tilde{\theta}_{12} &\approx \bar{\theta}'_{12} = \theta_{12} + \bar{\varphi} , \\ \tilde{\theta}_{23} &\approx \theta_{23} , \\ \tilde{\delta} &\approx \delta . \end{aligned} \quad (165)$$

For the $\delta m_{31}^2 < 0$ case (inverted hierarchy) with $a/|\delta m_{31}^2| \geq O(1)$, we can approximate

$$\begin{aligned} \tilde{\theta}_{13} &\approx \bar{\theta}'_{13} , \\ \tilde{\theta}_{12} &\approx \frac{c_{13}}{\bar{c}'_{13}} \left(\frac{\delta m_{21}^2}{2a} \right) \sin(2\theta_{12}) , \\ \tilde{\theta}_{23} &\approx \theta_{23} - \frac{\bar{s}_\phi}{\bar{c}'_{13}} \left(\frac{\delta m_{21}^2}{2a} \right) \sin(2\theta_{12}) \cos \delta , \\ \tilde{\delta} &\approx \delta + \frac{\bar{s}_\phi}{\bar{c}'_{13}} \left(\frac{\delta m_{21}^2}{a} \right) \frac{\sin(2\theta_{12})}{\tan(2\theta_{23})} \sin \delta . \end{aligned} \quad (166)$$

The behavior of the angles $\bar{\varphi}$ and $\bar{\phi}$, defined in Eqs. (151) and (156), are plotted in Fig. 12 as functions of $\alpha = \log_{1/\varepsilon}(a/|\delta m_{31}^2|)$ with gray solid lines for the parameter choice of Eq. (140). Approximate values can be obtained from

$$\tan 2\bar{\varphi} \approx -\frac{a \sin 2\theta_{12}}{\delta m_{21}^2 + a \cos 2\theta_{12}} , \quad \tan 2\bar{\phi} \approx -\frac{a \sin 2\theta_{13}}{\delta m_{31}^2 + a \cos 2\theta_{13}} , \quad (167)$$

which are also shown in Fig. 12 with black dashed lines. The accuracy of this approximation is shown in Fig. (13). The approximate values of $\bar{\theta}'_{12} = \theta_{12} + \bar{\varphi}$ and $\bar{\theta}'_{13} = \theta_{13} + \bar{\phi}$ can be calculated from the expressions

$$\tan 2\bar{\theta}'_{12} = \frac{\delta m_{21}^2 \sin 2\theta_{12}}{\delta m_{21}^2 \cos 2\theta_{12} + a} , \quad \tan 2\bar{\theta}'_{13} = \frac{\delta m_{31}^2 \sin 2\theta_{13}}{\delta m_{31}^2 \cos 2\theta_{13} + a} . \quad (168)$$

The accuracy of Eqs. (163), (165), and (166), using Eqs. (167) and (168) as input, is illustrated in Figures 14 through 17 for the parameter set of Eq. (140).

The approximate values for the effective mass-squared eigenvalues are given by

$$\bar{\lambda}_1 \approx \bar{\lambda}''_-$$

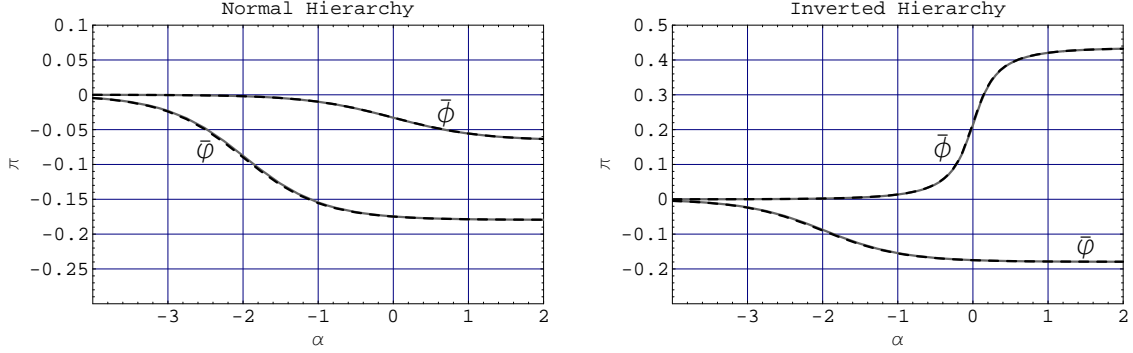


FIG. 12: The exact (gray solid line) and approximate (black dashed line) values of $\bar{\varphi}$ and $\bar{\phi}$ plotted against $\alpha = \log_{1/\varepsilon}(a/|\delta m_{31}^2|)$. The parameter choice was $\tan^2 \theta_{12} = 0.4$, $\sin^2(2\theta_{13}) = 0.16$, $\delta m_{21}^2 = 8.2 \times 10^{-5} \text{eV}^2$ and $|\delta m_{31}^2| = 2.5 \times 10^{-3} \text{eV}^2$.

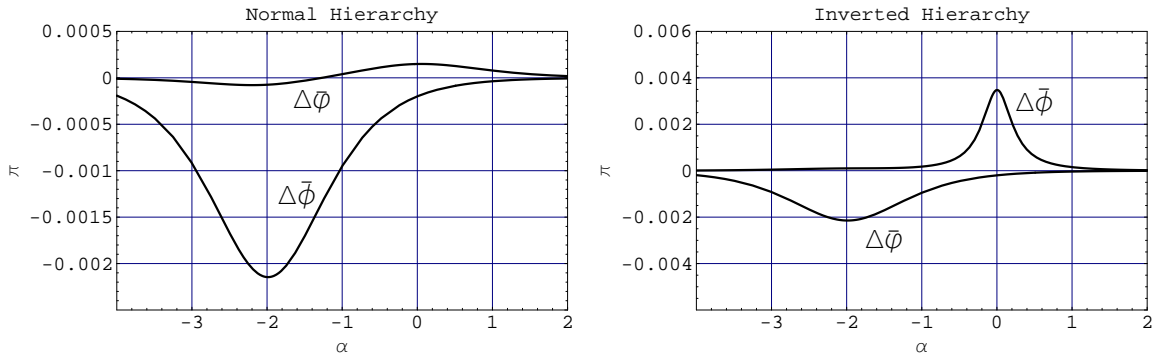


FIG. 13: $\Delta\bar{\varphi} = \bar{\varphi}_{\text{approx}} - \bar{\varphi}_{\text{exact}}$ and $\Delta\bar{\phi} = \bar{\phi}_{\text{approx}} - \bar{\phi}_{\text{exact}}$ plotted against $\alpha = \log_{1/\varepsilon}(a/|\delta m_{31}^2|)$ for the same parameter choice as Fig. 12.

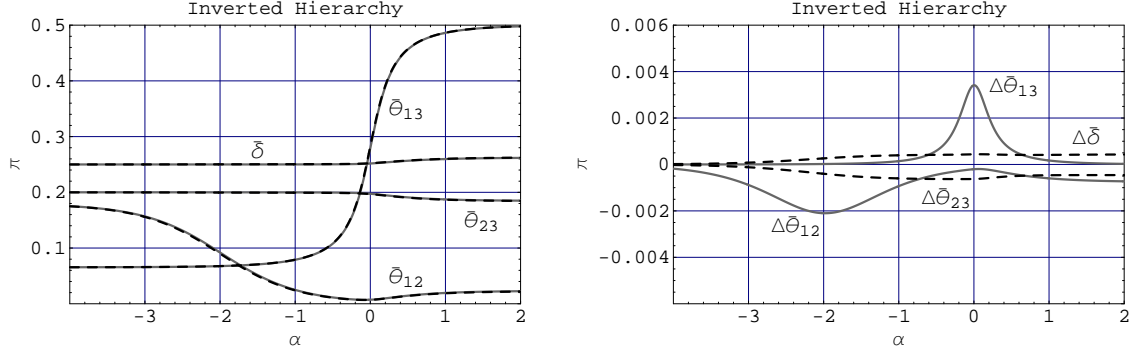


FIG. 14: (a) The exact values of $\tilde{\theta}_{12}$, $\tilde{\theta}_{13}$, $\tilde{\theta}_{23}$, and $\tilde{\delta}$ (gray solid lines) plotted against their approximate values (black dashed lines) obtained using Eq. (163), with Eqs. (167) and (168), as functions of $\alpha = \log_{1/\epsilon}(a/|\delta m_{31}^2|)$. (b) The differences $\Delta\bar{\theta}_{12} = \tilde{\theta}_{12,\text{approx}} - \tilde{\theta}_{12,\text{exact}}$ and $\Delta\bar{\theta}_{13} = \tilde{\theta}_{13,\text{approx}} - \tilde{\theta}_{13,\text{exact}}$ (solid gray lines), and the differences $\Delta\bar{\theta}_{23} = \tilde{\theta}_{23,\text{approx}} - \tilde{\theta}_{23,\text{exact}}$ and $\Delta\bar{\delta} = \tilde{\delta}_{\text{approx}} - \tilde{\delta}_{\text{exact}}$ (black dashed lines) of this approximation plotted against α .

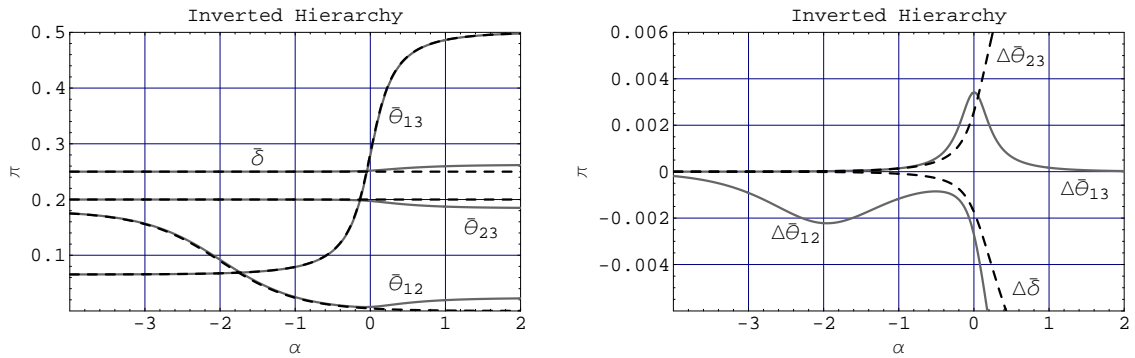


FIG. 15: (a) The exact values of $\tilde{\theta}_{12}$, $\tilde{\theta}_{13}$, $\tilde{\theta}_{23}$, and $\tilde{\delta}$ (gray solid lines) plotted against their approximate values (black dashed lines) obtained using Eq. (165) as functions of $\alpha = \log_{1/\epsilon}(a/|\delta m_{31}^2|)$. (b) $\Delta\bar{\theta}_{12}$ and $\Delta\bar{\theta}_{13}$ (gray solid lines), and $\Delta\bar{\theta}_{23}$ and $\Delta\bar{\delta}$ (black dashed lines) of this approximation plotted as functions of α . This approximation is applicable when $\alpha \lesssim -1$.

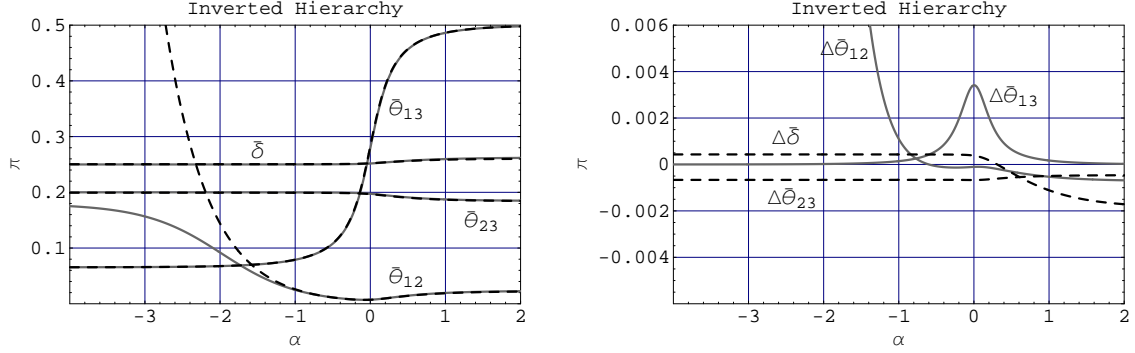


FIG. 16: (a) The exact values of $\tilde{\theta}_{12}$, $\tilde{\theta}_{13}$, $\tilde{\theta}_{23}$, and $\tilde{\delta}$ (gray solid lines) plotted against their approximate values (black dashed lines) obtained using Eq. (166) as functions of $\alpha = \log_{1/\varepsilon}(a/|\delta m_{31}^2|)$. (b) $\Delta\bar{\theta}_{12}$ and $\Delta\bar{\theta}_{13}$ (gray solid lines), and $\Delta\bar{\theta}_{23}$ and $\Delta\bar{\delta}$ (black dashed lines) of this approximation plotted as functions of α . This approximation is applicable when $\alpha \gtrsim 0$.

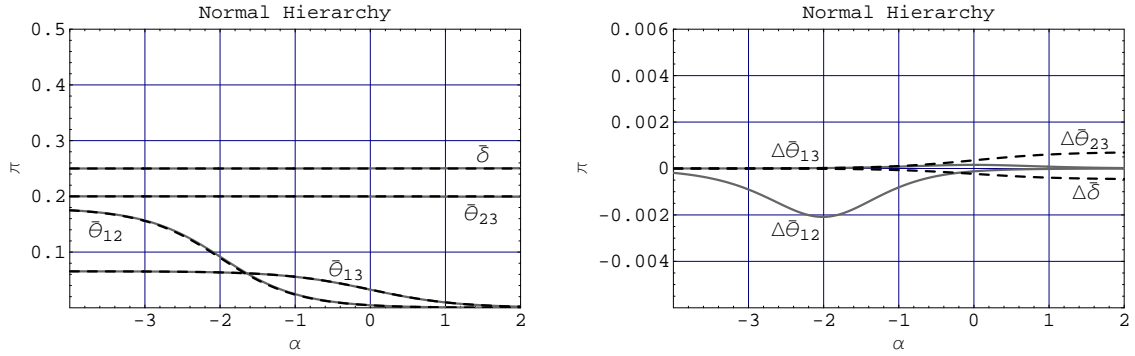


FIG. 17: (a) The exact values of $\tilde{\theta}_{12}$, $\tilde{\theta}_{13}$, $\tilde{\theta}_{23}$, and $\tilde{\delta}$ (gray solid lines) plotted against their approximate values (black dashed lines) obtained using Eq. (165) as functions of $\alpha = \log_{1/\varepsilon}(a/|\delta m_{31}^2|)$ for the normal hierarchy case ($\delta m_{31}^2 > 0$). (b) $\Delta\bar{\theta}_{12}$ and $\Delta\bar{\theta}_{13}$ (gray solid lines), and $\Delta\bar{\theta}_{23}$ and $\Delta\bar{\delta}$ (black dashed lines) of this approximation plotted as functions of α .

$$\begin{aligned}
\bar{\lambda}_2 &\approx \bar{\lambda}'_+, \\
\bar{\lambda}_3 &\approx \bar{\lambda}''_+,
\end{aligned}
\tag{169}$$

for the $\delta m_{31}^2 > 0$ case (normal hierarchy), and

$$\begin{aligned}
\bar{\lambda}_1 &\approx \bar{\lambda}''_+, \\
\bar{\lambda}_2 &\approx \bar{\lambda}'_+, \\
\bar{\lambda}_3 &\approx \bar{\lambda}''_-,
\end{aligned}
\tag{170}$$

for the $\delta m_{31}^2 < 0$ case (inverted hierarchy), where $\bar{\lambda}'_{\pm}$ and $\bar{\lambda}''_{\pm}$ are defined in Eqs. (154) and (159), respectively. The accuracy of this approximation is illustrated in Fig 18 using the parameter values of Eq. (140), where the exact numerically calculated values of $\delta\bar{\lambda}_{21} = \bar{\lambda}_2 - \bar{\lambda}_1$ and $|\delta\bar{\lambda}_{31}| = |\bar{\lambda}_3 - \bar{\lambda}_1|$ are plotted against those obtained from the above approximate expressions. In Fig. 19, we plot the difference between the exact and approximate values of $\delta\bar{\lambda}_{ij}$ normalized to $\delta\bar{\lambda}_{\min,\text{exact}}$:

$$\Delta\bar{\lambda}_{i1} \equiv \frac{\delta\bar{\lambda}_{i1,\text{approx}} - \delta\bar{\lambda}_{i1,\text{exact}}}{\delta\bar{\lambda}_{\min,\text{exact}}}, \quad (i = 2, 3), \tag{171}$$

where

$$\delta\bar{\lambda}_{\min,\text{exact}} \equiv \min(\delta\bar{\lambda}_{21,\text{exact}}, |\delta\bar{\lambda}_{31,\text{exact}}|, |\delta\bar{\lambda}_{32,\text{exact}}|). \tag{172}$$

When either $\delta m_{31}^2 < 0$ (inverted hierarchy) with $\alpha \lesssim -1$, *i.e.* $a/|\delta m_{31}^2| \leq O(\varepsilon)$, or $\delta m_{31}^2 > 0$ (normal hierarchy) with any a , the $\bar{\lambda}$'s can be further approximated by

$$\begin{aligned}
\bar{\lambda}_1 &\approx \frac{(\delta m_{21}^2 - a) - \sqrt{(\delta m_{21}^2 + a)^2 - 4a \delta m_{21}^2 s_{12}^2}}{2}, \\
\bar{\lambda}_2 &\approx \frac{(\delta m_{21}^2 - a) + \sqrt{(\delta m_{21}^2 + a)^2 - 4a \delta m_{21}^2 s_{12}^2}}{2}, \\
\bar{\lambda}_3 &\approx \delta m_{31}^2.
\end{aligned}
\tag{173}$$

For the $\delta m_{31}^2 < 0$ (inverted hierarchy) case with $\alpha \gtrsim -1$, *i.e.* $a/|\delta m_{31}^2| \geq O(\varepsilon)$, we can use

$$\begin{aligned}
\bar{\lambda}_1 &\approx \frac{(\delta m_{31}^2 - a) + \sqrt{(\delta m_{31}^2 + a)^2 - 4a \delta m_{31}^2 s_{13}^2}}{2}, \\
\bar{\lambda}_2 &\approx \delta m_{21}^2 c_{12}^2, \\
\bar{\lambda}_3 &\approx \frac{(\delta m_{31}^2 - a) - \sqrt{(\delta m_{31}^2 + a)^2 - 4a \delta m_{31}^2 s_{13}^2}}{2}.
\end{aligned}
\tag{174}$$

The accuracy of these approximations is illustrated in Figs. 20 and 21 for the $\delta m_{31}^2 < 0$ case, and Fig. 22 for the $\delta m_{31}^2 > 0$ case.

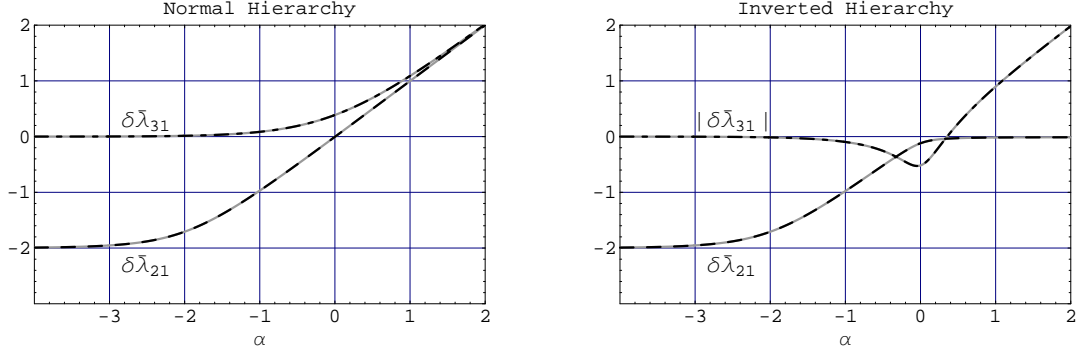


FIG. 18: The exact and approximate values of $\log_{1/\varepsilon}(\delta\bar{\lambda}_{21}/|\delta m_{31}^2|)$ and $\log_{1/\varepsilon}(|\delta\bar{\lambda}_{31}|/|\delta m_{31}^2|)$ for the parameter set of Eq. (140) plotted against $\alpha = \log_{1/\varepsilon}(a/|\delta m_{31}^2|)$. The exact values are in gray solid lines, whereas the approximate values are in black dashed ($\delta\bar{\lambda}_{21}$) and black dot-dashed ($|\delta\bar{\lambda}_{31}|$) lines.

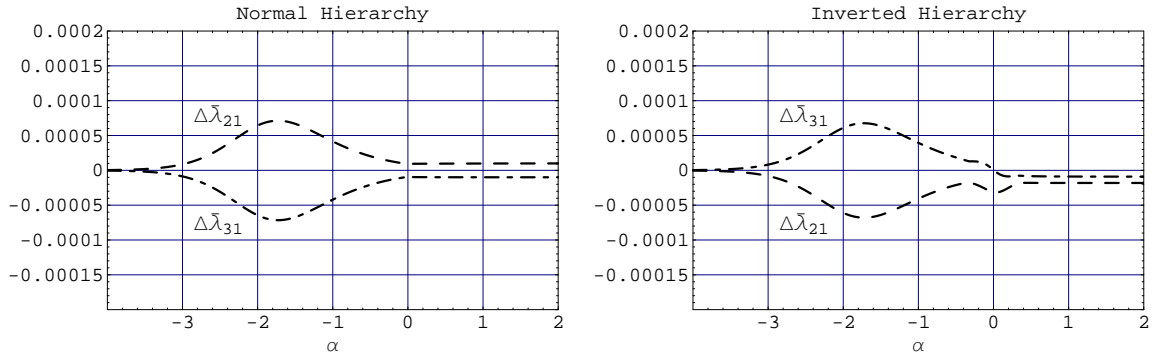


FIG. 19: The rescaled errors $\Delta\bar{\lambda}_{21}$ (dashed) and $\Delta\bar{\lambda}_{31}$ (dot-dashed), as defined in Eq. (171), for the approximation of Fig. 18.

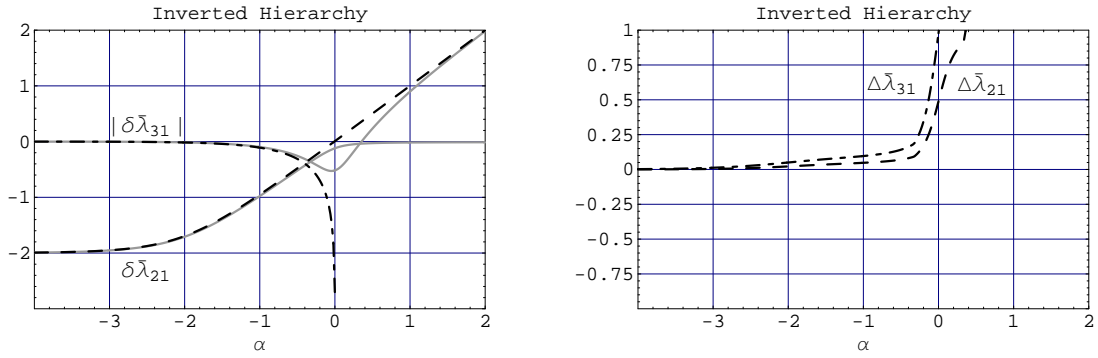


FIG. 20: Comparison of exact and approximate values using Eq. (173) for the inverted hierarchy case. The approximation is applicable when $\alpha \lesssim -1$.

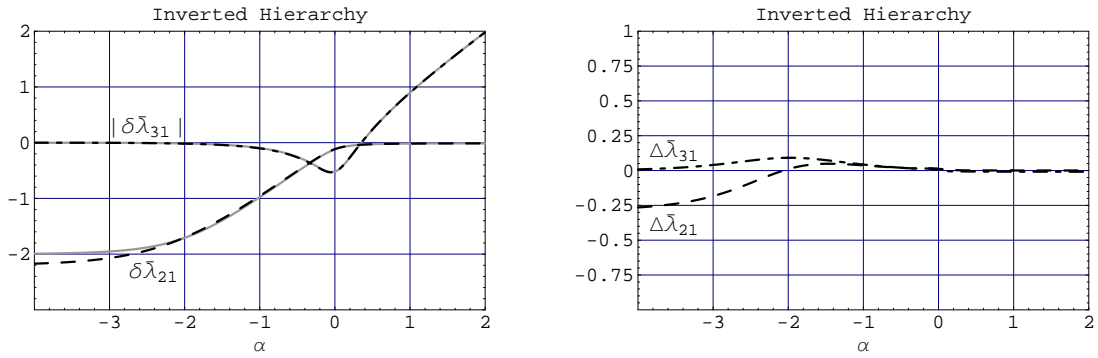


FIG. 21: Comparison of exact and approximate values using Eq. (174) for the inverted hierarchy case. The approximation is applicable when $\alpha \gtrsim -1$.

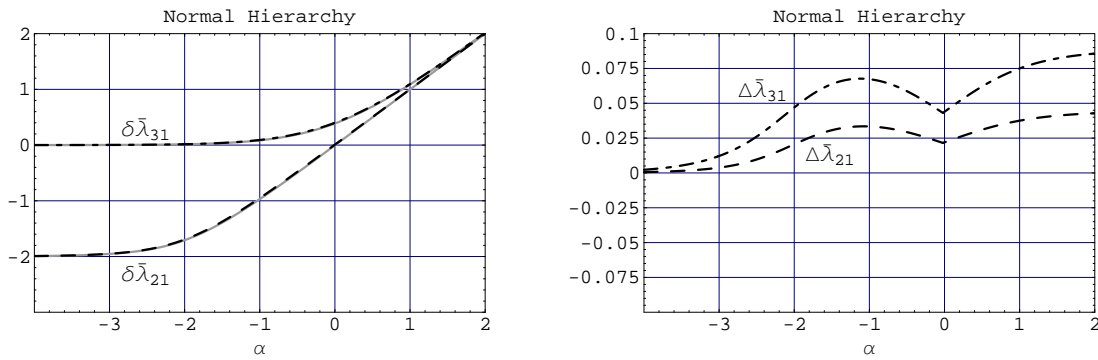


FIG. 22: Comparison of exact and approximate values using Eq. (173) for the normal hierarchy case.

IV. SAMPLE CALCULATION OF OSCILLATION PROBABILITIES

	L (km)	ρ (g/cm ³)	E (GeV)	$\alpha = \log_{1/\varepsilon}(a/ \delta m_{31}^2)$	$ \Delta_{31} $	Reference
T2K (JPARC \rightarrow Super-K)	295	2.6	0.25 \sim 2	-2.3 \sim -1.1	(0.3 \sim 2.4) π	[10]
JPARC \rightarrow Korea	1000	2.7	1 \sim 6	-1.5 \sim -0.4	(0.3 \sim 2.0) π	[15, 16]
BNL \rightarrow Home Stake	2540	3.4	2 \sim 10	-0.9 \sim 0	(0.5 \sim 2.6) π	[11]

TABLE III: The three cases for which we calculate the probabilities for the processes $\nu_\mu \rightarrow \nu_\mu$ and $\nu_\mu \rightarrow \nu_e$. The ranges of α and $|\Delta_{31}|$ were calculated assuming $\delta m_{21}^2 = 8.2 \times 10^{-5} \text{ eV}^2$ and $|\delta m_{31}^2| = 2.5 \times 10^{-3} \text{ eV}^2$. ρ is the average matter density along the baseline calculated using the Preliminary Earth Reference Model (PREM) [26].

The accuracy of our approximation in calculating the effective mixing angles and effective mass-squared differences translates directly into the accuracy in calculating the oscillation probabilities. To illustrate this, we calculate the probabilities for the processes $\nu_\mu \rightarrow \nu_\mu$ and $\nu_\mu \rightarrow \nu_e$ for the three cases listed in Table III. The energy ranges listed include the energies at which $|\Delta_{31}| = \pi$, around where the first oscillation peak occurs. The ranges of the matter effect parameter $\alpha = \log_{1/\varepsilon}(a/|\delta m_{31}^2|)$ for the three cases are roughly $-2 \sim -1$, $-1.5 \sim -0.5$, and $-1 \sim 0$, so together they cover the range $-2 \sim 0$.

Since $\alpha < 0$ for all three cases, the effective mixing angles are well approximated by Eq. (135). For the effective mass-squared differences, we use Eq. (146) which is applicable to $\alpha \lesssim -1$ for the $L = 295 \text{ km}$ case, and Eq. (147) which is applicable to $\alpha \gtrsim -1$ for the $L = 2540 \text{ km}$ case.

The $L = 1000 \text{ km}$ case is a bit problematic since neither Eq. (146) nor (147) can be used throughout the entire range $\alpha = -1.5 \sim -0.5$, Eq. (146) being applicable only to the low energy end, and Eq. (147) being applicable only to the high energy end. Using Eqs. (142) and (143), with Eqs. (49) and (72), which are applicable to all energies, would solve our problem and lead to approximate oscillation probabilities that are virtually indistinguishable from their exact values. However, we would like to illustrate the power (and limitations) of our much simpler expressions in Eqs. (146) and (147). Here, we will use Eq. (146) since the first oscillation peak occurs towards the lower end of the energy range.

In Figs. 23 through 28, we plot the approximate versus the exact oscillation probabilities for both the $\delta m_{31}^2 > 0$ (normal hierarchy) and $\delta m_{31}^2 < 0$ (inverted hierarchy) cases. The vacuum parameters were set to the values listed in Eq. (140) except for the CP violating

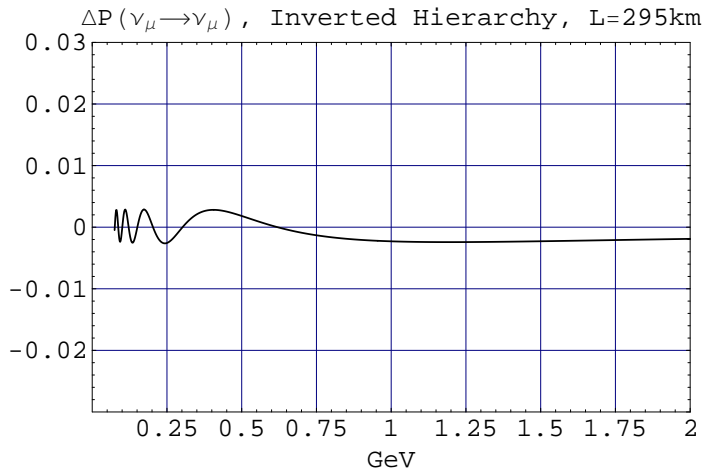
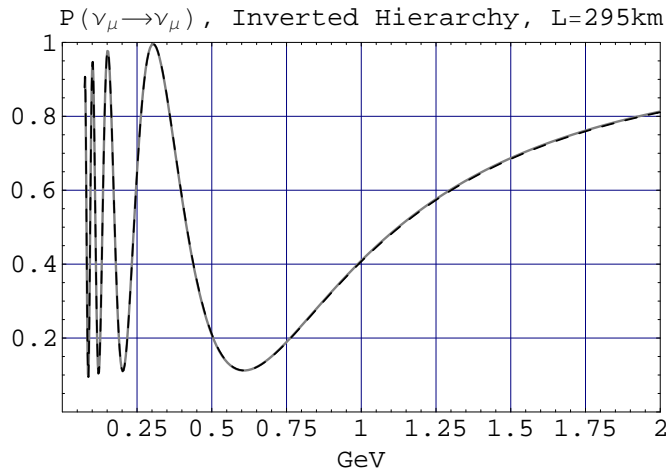
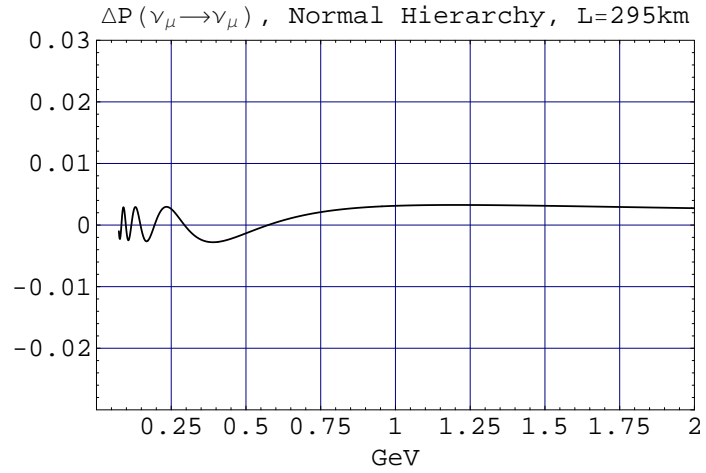
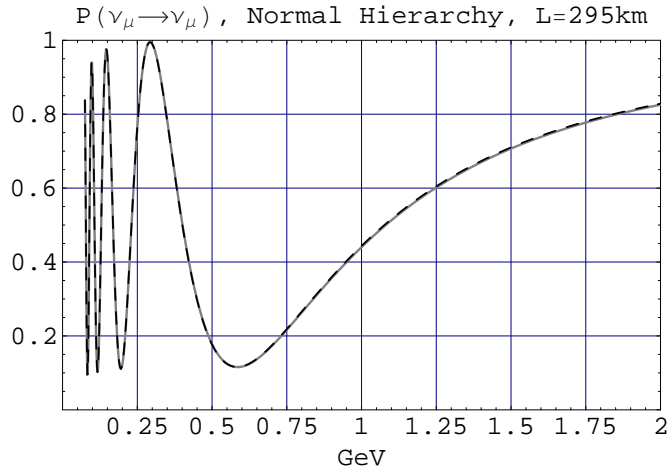


FIG. 23: Comparison of exact (solid gray line) and approximate (black dashed line) values of $P(\nu_\mu \rightarrow \nu_\mu)$ for the $L = 295\text{ km}$ case. The approximate value was calculated using Eq. (135) for the mixing angles, and Eq. (146) for the mass-squared differences. The CP violating phase δ was set to zero. The difference $\Delta P \equiv P_{\text{approx}} - P_{\text{exact}}$ is plotted on the right.

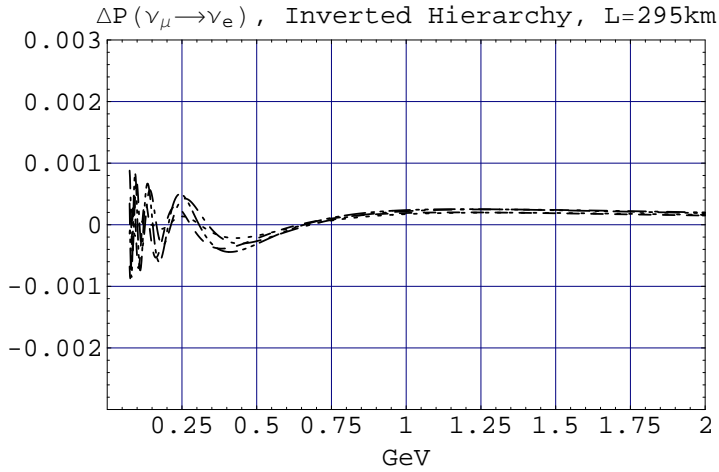
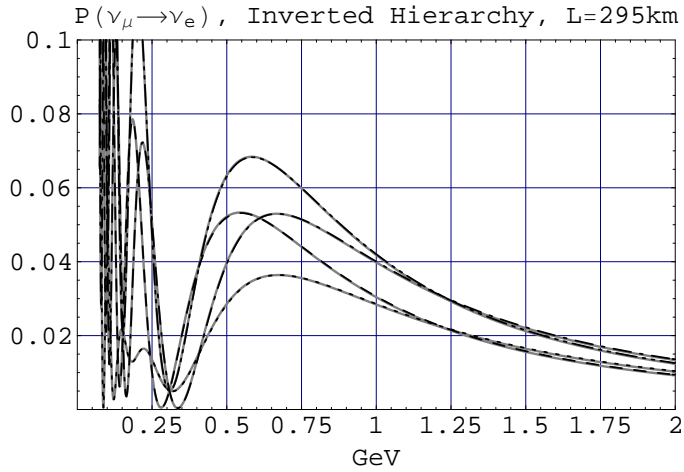
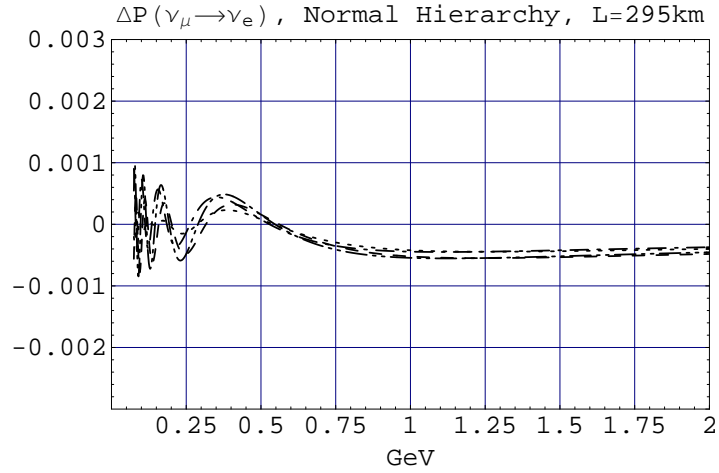
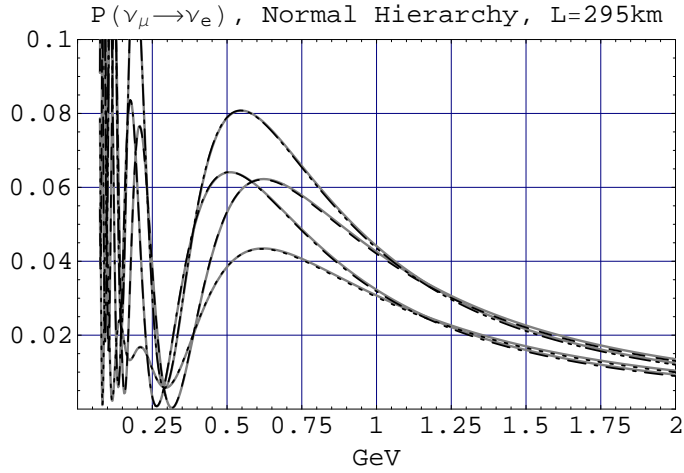


FIG. 24: Comparison of exact and approximate values of $P(\nu_\mu \rightarrow \nu_e)$ for the $L = 295\text{ km}$ case for several different values of the CP violating phase δ . The approximate values were calculated using Eq. (135) for the mixing angles, and Eq. (146) for the mass-squared differences. The exact values are given by the solid gray lines, while the approximate values are the black dashed ($\delta = 0$), dotted ($\delta = \pi/2$), dot-dashed ($\delta = \pi$), and double-dot-dashed ($\delta = 3\pi/2$) lines.

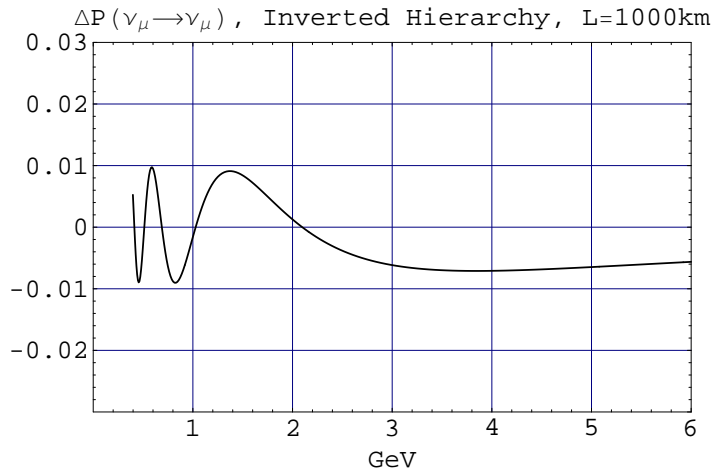
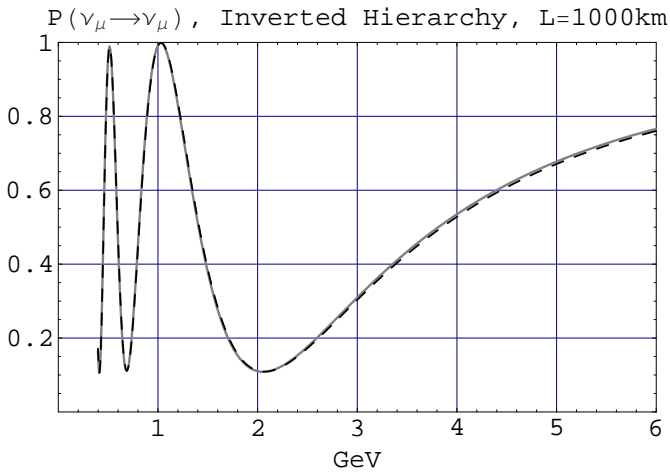
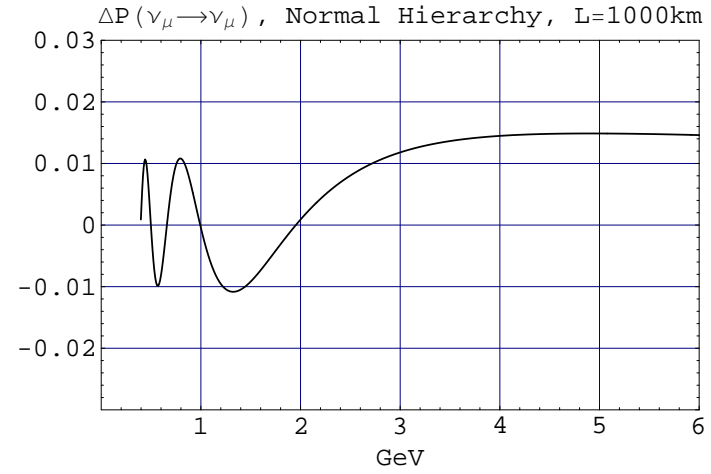
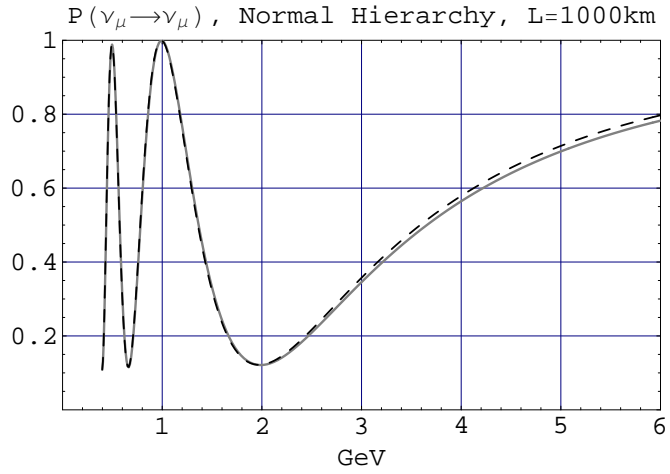


FIG. 25: Comparison of exact (solid gray line) and approximate (black dashed line) values of $P(\nu_\mu \rightarrow \nu_\mu)$ for the $L = 1000\text{km}$ case. The approximate value was calculated using Eq. (135) for the mixing angles, and Eq. (146) for the mass-squared differences. The CP violating phase δ was set to zero. The difference $\Delta P \equiv P_{\text{approx}} - P_{\text{exact}}$ is plotted on the right.

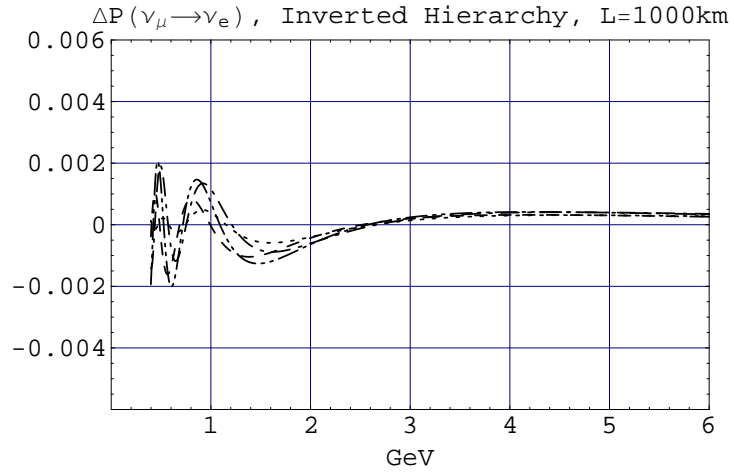
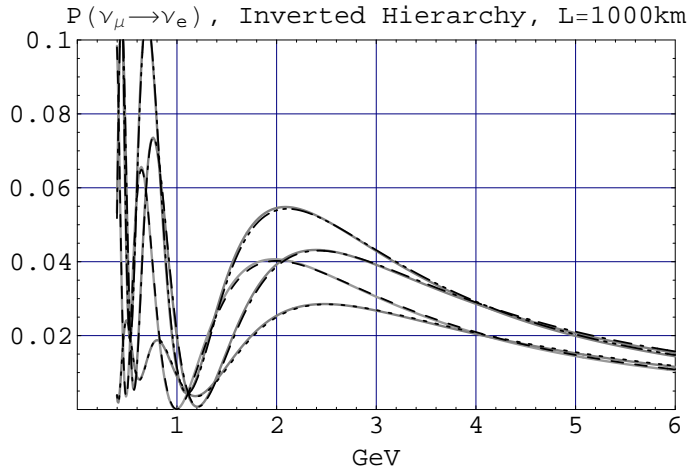
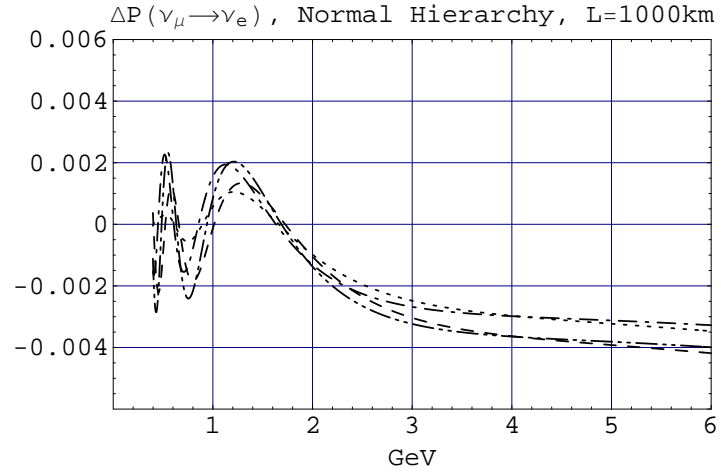
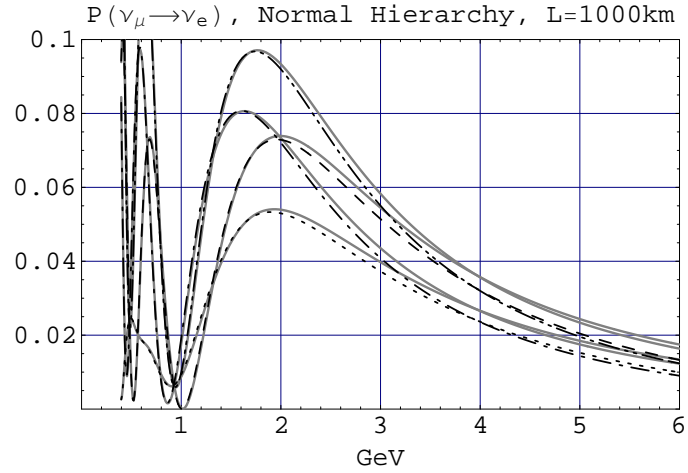


FIG. 26: Comparison of exact and approximate values of $P(\nu_\mu \rightarrow \nu_e)$ for the $L = 1000$ km case for several different values of the CP violating phase δ . The approximate values were calculated using Eq. (135) for the mixing angles, and Eq. (146) for the mass-squared differences. The exact values are given by the solid gray lines, while the approximate values are the black dashed ($\delta = 0$), dotted ($\delta = \pi/2$), dot-dashed ($\delta = \pi$), and double-dot-dashed ($\delta = 3\pi/2$) lines.

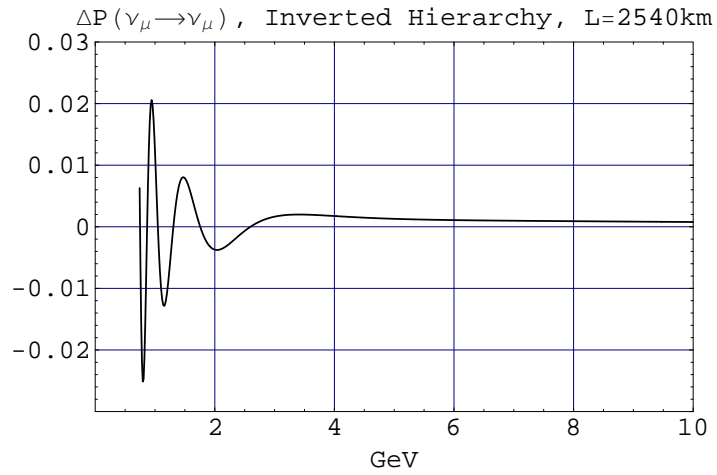
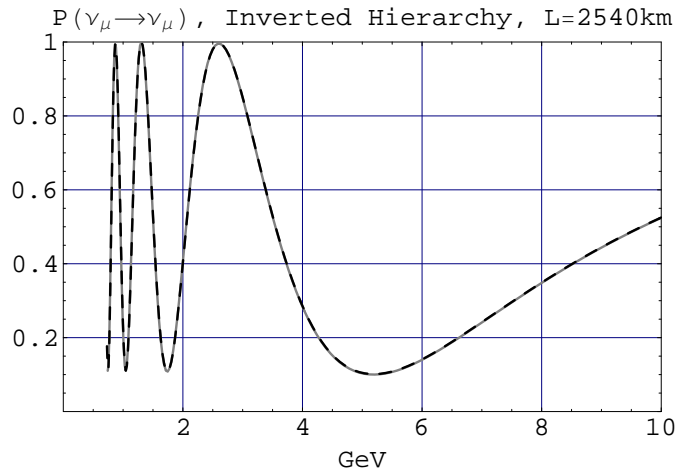
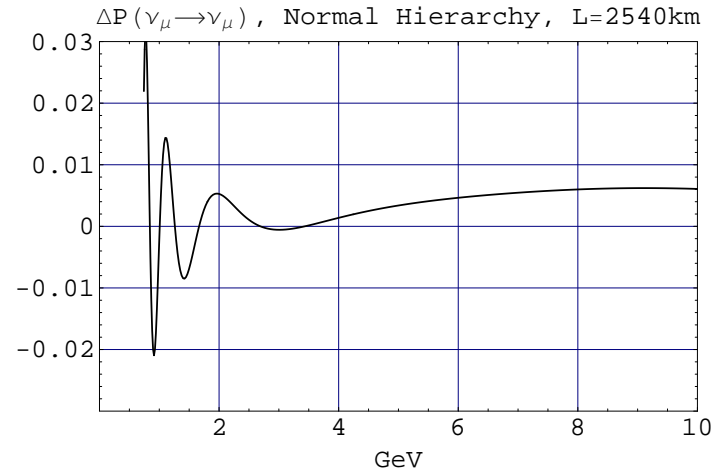
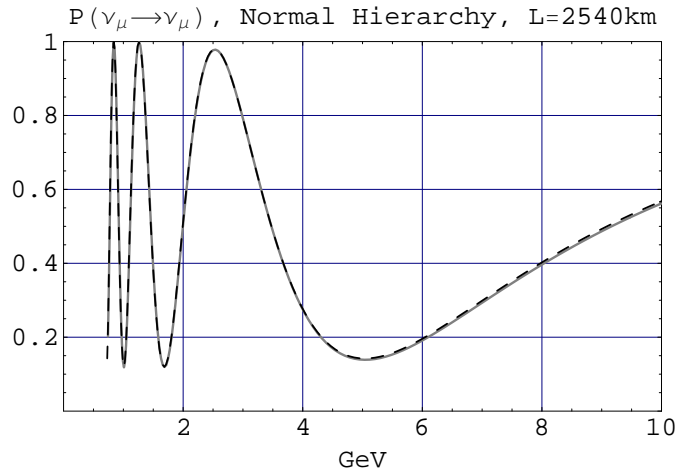


FIG. 27: Comparison of exact (solid gray line) and approximate (black dashed line) values of $P(\nu_\mu \rightarrow \nu_\mu)$ for the $L = 2540\text{km}$ case. The approximate value was calculated using Eq. (135) for the mixing angles, and Eq. (147) for the mass-squared differences. The CP violating phase δ was set to zero.

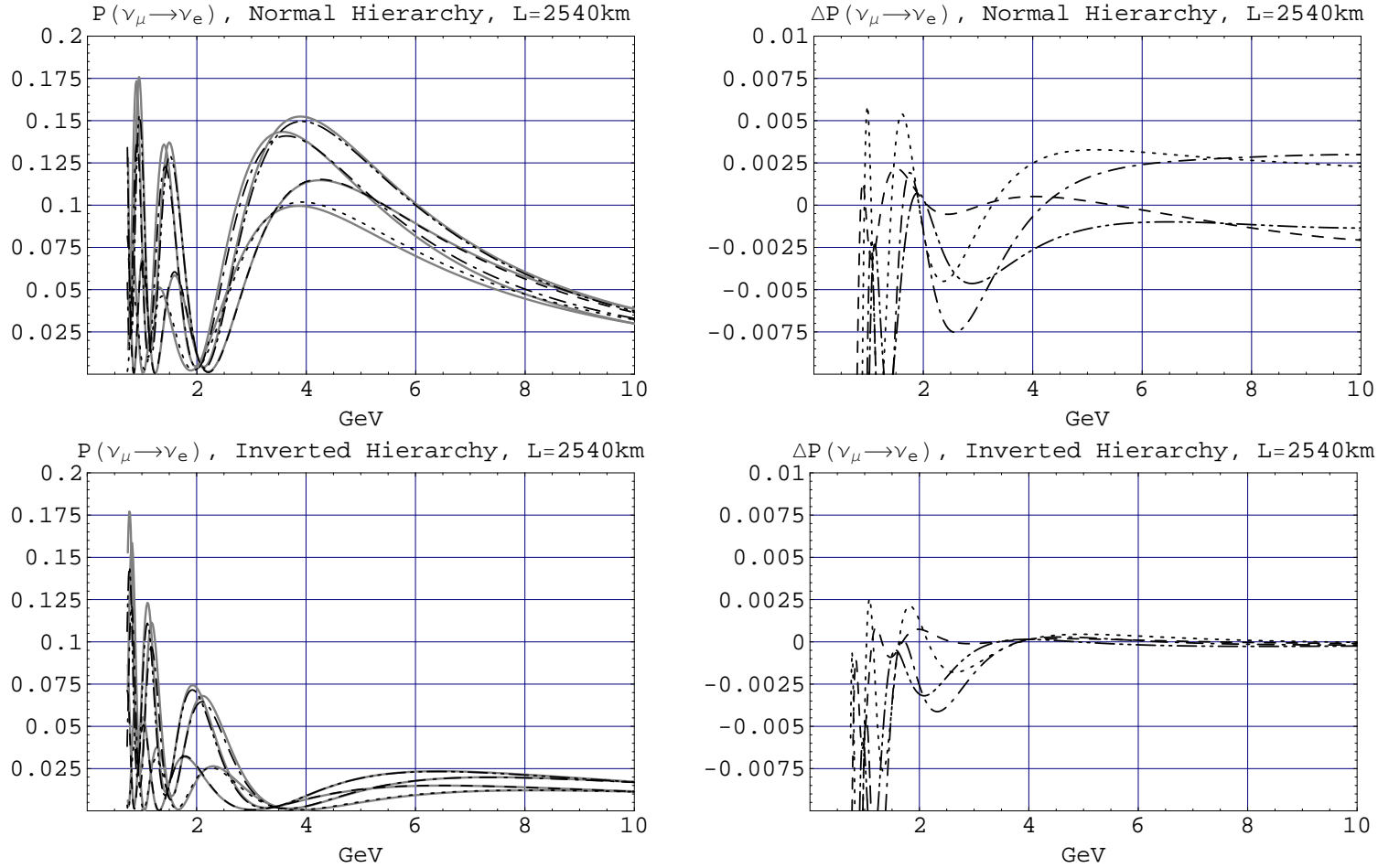


FIG. 28: Comparison of exact and approximate values of $P(\nu_\mu \rightarrow \nu_e)$ for the $L = 2540$ km case for several different values of the CP violating phase δ . The approximate values were calculated using Eq. (135) for the mixing angles, and Eq. (147) for the mass-squared differences. The exact values are given by the solid gray lines, while the approximate values are the black dashed ($\delta = 0$), dotted ($\delta = \pi/2$), dot-dashed ($\delta = \pi$), and double-dot-dashed ($\delta = 3\pi/2$) lines.

phase. For $\nu_\mu \rightarrow \nu_e$, the four cases $\delta = 0, \frac{\pi}{2}, \pi,$ and $\frac{3\pi}{2}$ were plotted. For $\nu_\mu \rightarrow \nu_\mu$, which depends only very weakly on δ , only the $\delta = 0$ case is shown.

The $L = 295$ km case is shown in Figs. 23 and 24. As is clear from the figures, our approximate values are completely indistinguishable from the exact values, the difference being less than a fraction of a percent throughout the energy range considered. For the $L = 1000$ km case shown in Figs. 25 and 26, deviations can be seen toward the high energy end as expected, but the difference is still well under control. For the $L = 2540$ km case shown in Figs. 27 and 28, the difference between the exact and approximate values is again less than a percent in the range $E = 2 \sim 10$ GeV where the approximation is applicable, but becomes large below $E = 2$ GeV.

V. QUALITATIVE ANALYSIS

Let us now use our approximation to see whether we can understand various qualitative features of the oscillation probabilities we plotted.

Since the three cases we considered in the previous section cover the range $\alpha = -2 \sim 0$, let us take the midpoint $\alpha \sim -1$ and further simplify our expressions to those applicable there. The approximations for the effective mixing angles for the neutrinos can be obtained from Eqs. (64), (75), and (135):

$$\begin{aligned}\tilde{\theta}_{12} &\approx \frac{\pi}{2} - \frac{\delta m_{21}^2}{2a} \sin(2\theta_{12}), \\ \tilde{\theta}_{13} &\approx \frac{\theta_{13}}{\left(1 - \frac{a}{\delta m_{31}^2}\right)}, \\ \tilde{\theta}_{23} &\approx \theta_{23}, \\ \tilde{\delta} &\approx \delta.\end{aligned}\tag{175}$$

In Fig. 29 we plot these approximations against the exact values. Though the approximation for θ_{13} breaks down for the normal hierarchy case as $\alpha \rightarrow 0$, these expressions nevertheless capture the essential behavior of the effective mixing angles throughout the range $-2 < \alpha < 0$. They are also numerically accurate for most of this range. In fact, for the inverted hierarchy case, the approximations of $\tilde{\theta}_{13}$, $\tilde{\theta}_{23}$ and $\tilde{\delta}$ are valid for all α . From Eq. (77), the approximations for the effective mass-squared differences are

$$\lambda_1 \approx \delta m_{21}^2 c_{12}^2,$$

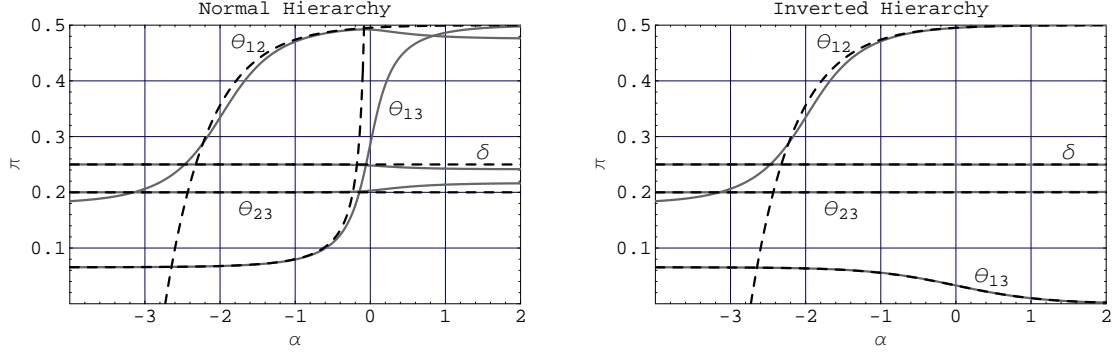


FIG. 29: The exact values of $\tilde{\theta}_{12}$, $\tilde{\theta}_{13}$, $\tilde{\theta}_{23}$, and $\tilde{\delta}$ (solid gray lines) plotted as functions of $\alpha = \log_{1/\varepsilon}(a/|\delta m_{31}^2|)$ against their approximate values (black dashed lines) obtained using Eq. (175). The $\delta m_{31}^2 > 0$ (normal hierarchy) case is shown on the left, and the $\delta m_{31}^2 < 0$ (inverted hierarchy) case is shown on the right. The input parameters are those of Eq. (140).

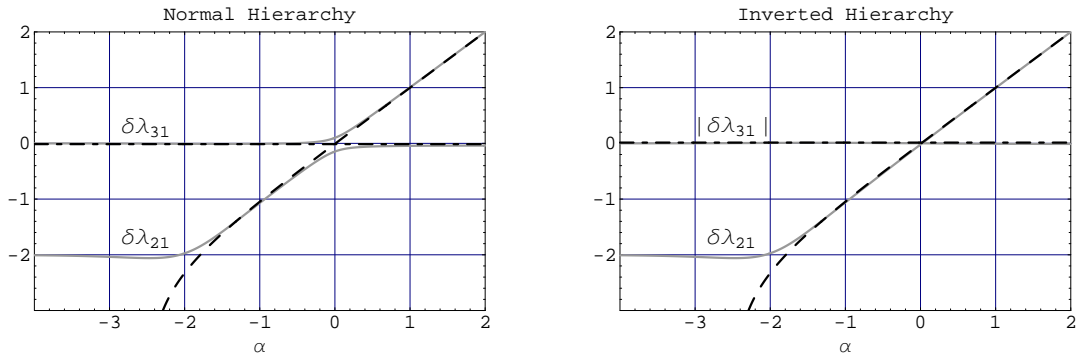


FIG. 30: The exact values of $\log_{1/\varepsilon}(\delta\lambda_{21}/|\delta m_{31}^2|)$ and $\log_{1/\varepsilon}(\delta\lambda_{31}/|\delta m_{31}^2|)$ (solid gray lines) plotted as functions of $\alpha = \log_{1/\varepsilon}(a/|\delta m_{31}^2|)$ against their approximate values (black dashed and dot-dashed lines) obtained using Eq. (176). The input parameters are those of Eq. (140).

$$\begin{aligned}
\lambda_2 &\approx a + \delta m_{21}^2 s_{12}^2, \\
\lambda_3 &\approx \delta m_{31}^2.
\end{aligned}
\tag{176}$$

These expressions are compared against the exact values in Fig. 30, and we can again conclude that they are fairly accurate for most of the range $-2 < \alpha < 0$, except very near the endpoints.

For the anti-neutrinos, the effective mixing angles when $\alpha \sim -1$ are approximated by

$$\begin{aligned}
\tilde{\theta}_{12} &\approx \frac{\delta m_{21}^2}{2a} \sin(2\theta_{12}), \\
\tilde{\theta}_{13} &\approx \frac{\theta_{13}}{\left(1 + \frac{a}{\delta m_{31}^2}\right)}, \\
\tilde{\theta}_{23} &\approx \theta_{23}, \\
\tilde{\delta} &\approx \delta.
\end{aligned}
\tag{177}$$

The accuracy of these expressions is shown in Fig. 31. In contrast to the neutrino case, the approximations for $\tilde{\theta}_{13}$, $\tilde{\theta}_{23}$ and $\tilde{\delta}$ are applicable to all a for the normal hierarchy case, and the approximation for $\tilde{\theta}_{13}$ breaks down as $\alpha \rightarrow 0$ for the inverted hierarchy case. The approximations for the effective mass-squared differences are given by

$$\begin{aligned}
\bar{\lambda}_1 &\approx -a + \delta m_{21}^2 s_{12}^2, \\
\bar{\lambda}_2 &\approx \delta m_{21}^2 c_{12}^2, \\
\bar{\lambda}_3 &\approx \delta m_{31}^2,
\end{aligned}
\tag{178}$$

with the accuracy shown in Fig. (32). As in the neutrino case, we can conclude that these approximations capture the essential behavior of the effective mixing angles and mass squared differences throughout the range $-2 < \alpha < 0$, and are also numerically accurate except near the endpoints.

Let us now apply these approximations to the oscillation probabilities $P(\nu_\mu \rightarrow \nu_\mu)$ and $P(\nu_\mu \rightarrow \nu_e)$ in matter, and their anti-neutrino counterparts. First, recall from Eqs. (20) and (21) that these probabilities in vacuum are given by

$$\begin{aligned}
P(\nu_\mu \rightarrow \nu_\mu) &= 1 - \sin^2(2\theta_{\text{atm}}) \sin^2\left(\frac{\Delta_{31} - \kappa_{\mu\mu}\Delta_{21}}{2}\right) + O(\Delta_{21}^2), \\
P(\nu_\mu \rightarrow \nu_e) &= 4 \sin^2 \theta_{13} \sin^2 \theta_{\text{atm}} \{1 - (B \sin \delta) \Delta_{21}\} \sin^2\left(\frac{\Delta_{31} - \kappa_{\mu e}\Delta_{21}}{2}\right) + O(\Delta_{21}^2),
\end{aligned}
\tag{179}$$

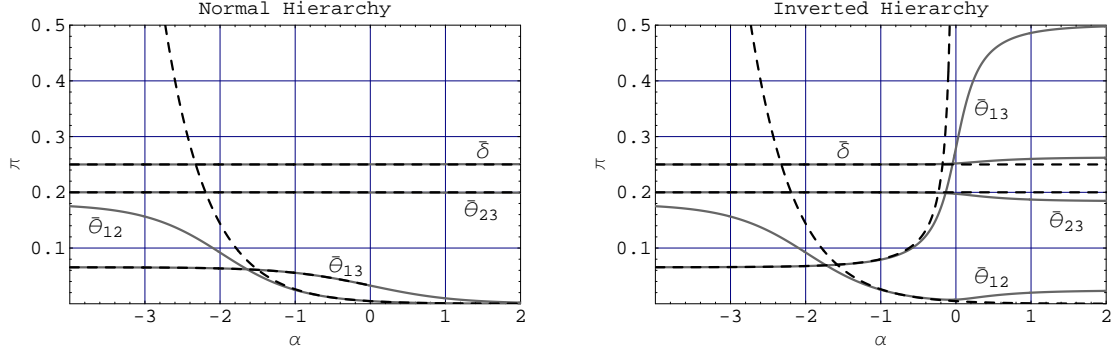


FIG. 31: The exact values of $\tilde{\theta}_{12}$, $\tilde{\theta}_{13}$, $\tilde{\theta}_{23}$, and $\tilde{\delta}$ (solid gray lines) plotted as functions of $\alpha = \log_{1/\varepsilon}(a/|\delta m_{31}^2|)$ against their approximate values (black dashed lines) obtained using Eq. (177). The $\delta m_{31}^2 > 0$ (normal hierarchy) case is shown on the left, and the $\delta m_{31}^2 < 0$ (inverted hierarchy) case is shown on the right. The input parameters are those of Eq. (140).

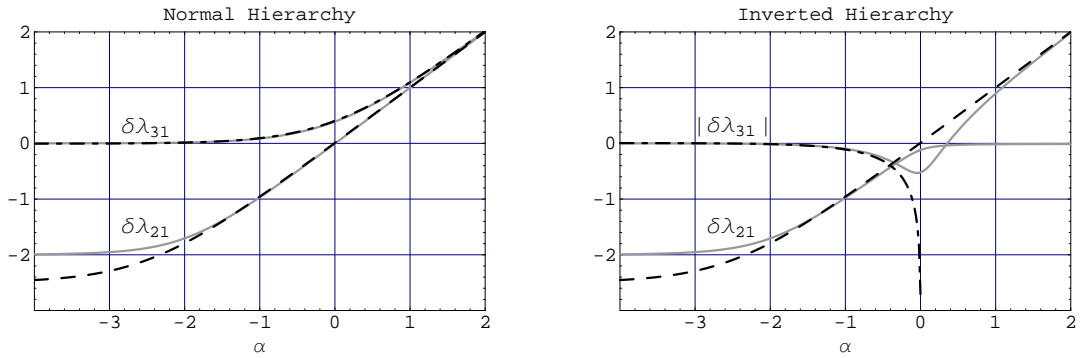


FIG. 32: The exact values of $\log_{1/\varepsilon}(\delta\bar{\lambda}_{21}/|\delta m_{31}^2|)$ and $\log_{1/\varepsilon}(|\delta\bar{\lambda}_{31}|/|\delta m_{31}^2|)$ (solid gray lines) plotted as functions of $\alpha = \log_{1/\varepsilon}(a/|\delta m_{31}^2|)$ against their approximate values (black dashed and dot-dashed lines), obtained using Eq. (178). The input parameters are those of Eq. (140).

where

$$\begin{aligned}
\sin \theta_{\text{atm}} &= s_{23} c_{13} , \\
A &= \frac{1}{8} \sin(2\theta_{12}) \sin(2\theta_{13}) \sin(2\theta_{\text{atm}}) \sqrt{1 - \tan^2 \theta_{13} \tan^2 \theta_{\text{atm}}} \\
&= \frac{1}{8} \times O(1) \times 2O(\varepsilon) \times O(1) \times \sqrt{1 - O(\varepsilon^2)} \\
&= \frac{1}{4} O(\varepsilon) , \\
B &\equiv \frac{A}{\sin^2 \theta_{13} \sin^2 \theta_{\text{atm}}} = \frac{1}{2} O(\varepsilon^{-1}) , \\
\kappa_{\mu\mu} &= c_{12}^2 - \cos(2\theta_{12}) \tan^2 \theta_{13} \tan^2 \theta_{\text{atm}} - \left(\frac{2A}{\cos^2 \theta_{13} \cos^2 \theta_{\text{atm}}} \right) \cos \delta \\
&= \frac{1}{2} O(1) - 2O(\varepsilon^3) - O(\varepsilon) \cos \delta \\
&= \frac{1}{2} O(1) - O(\varepsilon) \cos \delta , \\
\kappa_{\mu e} &= s_{12}^2 - B \cos \delta \\
&= \frac{1}{2} O(1) - \frac{1}{2} O(\varepsilon^{-1}) \cos \delta .
\end{aligned} \tag{180}$$

The oscillation probabilities for the anti-neutrinos are obtained by flipping the sign of $\sin \delta$.

Note that the first oscillation peak occurs at a distance/energy of $|\Delta_{31}| \approx \pi$. Since $\Delta_{21}/|\Delta_{31}| = \delta m_{21}^2/|\delta m_{31}^2| = \varepsilon^2$, the $O(\Delta_{21}^2)$ terms in Eq. (179) are of $O(\pi^2 \varepsilon^4)$ which justifies our dropping them at those distance/energies. Note also that the coefficient of $\cos \delta$ in $\kappa_{\mu e}$ is $B = \frac{1}{2} O(\varepsilon^{-1})$, which when multiplied by Δ_{21} is of $O(\varepsilon)$. The exact same product of parameters, $B\Delta_{21} = O(\varepsilon)$, appears in the coefficient of $\sin \delta$ in the oscillation envelope of $P(\nu_\mu \rightarrow \nu_e)$. Therefore, a measurement of $P(\nu_\mu \rightarrow \nu_e)$ can, in principle, constrain $\cos \delta$ from the position of the peak, and $\sin \delta$ from the height of the peak, provided it is accurate enough to discern these $O(\varepsilon)$ corrections. In contrast, the coefficient of $\cos \delta$ in $\kappa_{\mu\mu}$ is $O(\varepsilon)$, rendering the $\cos \delta$ term in $\kappa_{\mu\mu}\Delta_{21}$ negligible, and we conclude that $P(\nu_\mu \rightarrow \nu_\mu)$ is insensitive to δ .

Of course, actual long-baseline experiments can only measure oscillation probabilities in matter. The effective Δ_{31} 's in matter for the neutrinos and anti-neutrinos are

$$\begin{aligned}
\tilde{\Delta}_{31} &\approx (\Delta_{31} - \Delta_{21} c_{12}^2) , \\
\tilde{\Delta}_{31} &\approx \left(\Delta_{31} + \frac{a}{2E} L - \Delta_{21} s_{12}^2 \right) ,
\end{aligned} \tag{181}$$

respectively, so they are both the same order as Δ_{31} . The effective Δ_{21} 's, on the other hand, are

$$\tilde{\Delta}_{21} \approx \left(\frac{a}{2E} L - \Delta_{21} \cos 2\theta_{12} \right) \approx \frac{a}{2E} L = (\sqrt{2} G_F N_e) L ,$$

$$\tilde{\Delta}_{21} \approx \left(\frac{a}{2E}L + \Delta_{21} \cos 2\theta_{12} \right) \approx \frac{a}{2E}L = (\sqrt{2}G_F N_e)L, \quad (182)$$

so they are enhanced by a factor of $a/\delta m_{21}^2$ relative to Δ_{21} . Therefore, at the first oscillation peak where $|\Delta_{31}| \approx \pi$, we can expect $\tilde{\Delta}_{21}$ and $\tilde{\Delta}_{21}$ to be of order $\pi a/|\delta m_{31}^2|$.

Note that the value of $\tilde{\Delta}_{21} \approx \tilde{\Delta}_{21} \approx (\sqrt{2}G_F N_e)L$ does not depend on the energy E . It is determined solely by the baseline length L , once the matter density ρ is fixed. ($N_e = N_A \rho/2$ where N_A is the Avogadro number.) For the three examples we considered in the previous section, we find

$$(\sqrt{2}G_F N_e)L = \begin{cases} 0.15 & (\rho = 2.6 \text{ g/cm}^3, L = 295 \text{ km}), \\ 0.5 & (\rho = 2.7 \text{ g/cm}^3, L = 1000 \text{ km}), \\ 1.7 & (\rho = 3.4 \text{ g/cm}^3, L = 2540 \text{ km}). \end{cases} \quad (183)$$

Since we would like to use the analog of Eq. (179) to analyze the oscillation probabilities in matter, we would like maintain the condition

$$\tilde{\Delta}_{21}, \tilde{\Delta}_{21} < 1, \quad (184)$$

so that an expansion in $\tilde{\Delta}_{21}$ or $\tilde{\Delta}_{21}$ is justified. The $L = 2540 \text{ km}$ case is clearly problematic and must be treated separately. We will therefore first restrict our attention to the cases in which the $|\Delta_{31}| = \pi$ condition occurs in the region $-2 < \alpha \lesssim -1$, so that $\tilde{\Delta}_{21} \approx \tilde{\Delta}_{21} \lesssim O(\pi\varepsilon) = 0.47 \sim 0.75$.

Even with this restriction, $\tilde{\Delta}_{21}$ and $\tilde{\Delta}_{21}$ can still be enhanced considerably when $|\Delta_{31}| = \pi$ occurs at $\alpha \approx -1$. One may naively anticipate that this enhancement will enhance the coefficients of $\sin \delta$ and $\cos \delta$ in $P(\nu_\mu \rightarrow \mu_e)$, thereby facilitate the detection of δ . At the same time, it could also enhance the $O(\tilde{\Delta}_{21}^2)$ and $O(\tilde{\Delta}_{21}^2)$ terms in the oscillation probabilities and invalidate their complete neglect. However, it turns out that these are not the case.

Let us first look at the ν_μ and $\bar{\nu}_\mu$ survival probabilities in matter which are obtained by replacing all the quantities in the vacuum probability with their tilded and anti-tilded counterparts:

$$\begin{aligned} & \tilde{P}(\nu_\mu \rightarrow \nu_\mu) \\ &= 1 - \sin^2(2\tilde{\theta}_{\text{atm}}) \sin^2 \left(\frac{\tilde{\Delta}_{31} - \tilde{\kappa}_{\mu\mu} \tilde{\Delta}_{21}}{2} \right) \\ & \quad - |\tilde{U}_{\mu 1}|^2 |\tilde{U}_{\mu 2}|^2 \left(1 + \frac{|\tilde{U}_{\mu 3}|^2}{1 - |\tilde{U}_{\mu 3}|^2} \cos \tilde{\Delta}_{31} \right) \tilde{\Delta}_{21}^2 \end{aligned}$$

$$- |\tilde{U}_{\mu 1}|^2 |\tilde{U}_{\mu 2}|^2 |\tilde{U}_{\mu 3}|^2 \left\{ \frac{1 + |\tilde{U}_{\mu 2}|^2 - |\tilde{U}_{\mu 3}|^2}{3(1 - |\tilde{U}_{\mu 3}|^2)^2} \sin \tilde{\Delta}_{31} \right\} \tilde{\Delta}_{21}^3 + O(\tilde{\Delta}_{21}^4), \quad (185)$$

$$\begin{aligned} & \tilde{P}(\bar{\nu}_\mu \rightarrow \bar{\nu}_\mu) \\ &= 1 - \sin^2(2\tilde{\theta}_{\text{atm}}) \sin^2 \left(\frac{\tilde{\Delta}_{31} - \tilde{\kappa}_{\mu\mu} \tilde{\Delta}_{21}}{2} \right) \\ & - |\tilde{U}_{\mu 1}|^2 |\tilde{U}_{\mu 2}|^2 \left(1 + \frac{|\tilde{U}_{\mu 3}|^2}{1 - |\tilde{U}_{\mu 3}|^2} \cos \tilde{\Delta}_{31} \right) \tilde{\Delta}_{21}^2 \\ & - |\tilde{U}_{\mu 1}|^2 |\tilde{U}_{\mu 2}|^2 |\tilde{U}_{\mu 3}|^2 \left\{ \frac{1 + |\tilde{U}_{\mu 2}|^2 - |\tilde{U}_{\mu 3}|^2}{3(1 - |\tilde{U}_{\mu 3}|^2)^2} \sin \tilde{\Delta}_{31} \right\} \tilde{\Delta}_{21}^3 + O(\tilde{\Delta}_{21}^4). \end{aligned} \quad (186)$$

We have kept terms up to $\tilde{\Delta}_{21}^3$ and $\tilde{\Delta}_{21}^3$ explicitly to evaluate their sizes. Using the approximations of Eqs. (175) and (177), the effective MNS matrix elements that appear in these expressions can be evaluated to be

$$\begin{aligned} |\tilde{U}_{\mu 1}|^2 &= |\tilde{s}_{12} \tilde{c}_{23} + \tilde{c}_{12} \tilde{s}_{13} \tilde{s}_{23} e^{i\tilde{\delta}}|^2 = \frac{1}{2} O(1), \\ |\tilde{U}_{\mu 2}|^2 &= |\tilde{c}_{12} \tilde{c}_{23} - \tilde{s}_{12} \tilde{s}_{13} \tilde{s}_{23} e^{i\tilde{\delta}}|^2 \approx O(\varepsilon^2), \\ |\tilde{U}_{\mu 3}|^2 &= (\tilde{c}_{13} \tilde{s}_{23})^2 = \frac{1}{2} O(1). \end{aligned} \quad (187)$$

for the neutrinos, and

$$\begin{aligned} |\tilde{U}_{\mu 1}|^2 &= |\tilde{s}_{12} \tilde{c}_{23} + \tilde{c}_{12} \tilde{s}_{13} \tilde{s}_{23} e^{i\tilde{\delta}}|^2 \approx O(\varepsilon^2), \\ |\tilde{U}_{\mu 2}|^2 &= |\tilde{c}_{12} \tilde{c}_{23} - \tilde{s}_{12} \tilde{s}_{13} \tilde{s}_{23} e^{i\tilde{\delta}}|^2 = \frac{1}{2} O(1), \\ |\tilde{U}_{\mu 3}|^2 &= (\tilde{c}_{13} \tilde{s}_{23})^2 = \frac{1}{2} O(1), \end{aligned} \quad (188)$$

for the anti-neutrinos. This shows that the $\tilde{\Delta}_{21}^2$, $\tilde{\Delta}_{21}^2$ and $\tilde{\Delta}_{21}^3$, $\tilde{\Delta}_{21}^3$ terms are suppressed by $|\tilde{U}_{\mu 2}|^2 = O(\varepsilon^2)$ for the neutrinos, and by $|\tilde{U}_{\mu 1}|^2 = O(\varepsilon^2)$ for the anti-neutrinos, cancelling out the enhancements of $\tilde{\Delta}_{21}$, $\tilde{\Delta}_{21}$ over Δ_{21} , and reducing these higher order terms to $O(\pi^2 \varepsilon^4)$, which is the same order as the $O(\Delta_{21}^2)$ terms that were neglected for the vacuum case. The fact that $\cos \tilde{\Delta}_{31} \approx -1$ and $\sin \tilde{\Delta}_{31} \approx 0$ near the first oscillation peak also helps in suppressing these terms. Therefore, to a very good approximation, we can use the expressions

$$\begin{aligned} \tilde{P}(\nu_\mu \rightarrow \nu_\mu) &= 1 - \sin^2(2\tilde{\theta}_{\text{atm}}) \sin^2 \left(\frac{\tilde{\Delta}_{31} - \tilde{\kappa}_{\mu\mu} \tilde{\Delta}_{21}}{2} \right), \\ \tilde{P}(\bar{\nu}_\mu \rightarrow \bar{\nu}_\mu) &= 1 - \sin^2(2\tilde{\theta}_{\text{atm}}) \sin^2 \left(\frac{\tilde{\Delta}_{31} - \tilde{\kappa}_{\mu\mu} \tilde{\Delta}_{21}}{2} \right). \end{aligned} \quad (189)$$

Looking at the remaining parameters in these expressions, we find

$$\begin{aligned}
\sin \tilde{\theta}_{\text{atm}} &= \tilde{c}_{13} \tilde{s}_{23} = c_{13} s_{23} [1 + O(\varepsilon^3)] \approx \sin \theta_{\text{atm}} , \\
\tilde{A} &= \frac{1}{8} \sin(2\tilde{\theta}_{12}) \sin(2\tilde{\theta}_{13}) \sin(2\tilde{\theta}_{\text{atm}}) \sqrt{1 - \tan^2 \tilde{\theta}_{13} \tan^2 \tilde{\theta}_{\text{atm}}} \\
&\approx \frac{1}{4} \left(\frac{\delta m_{21}^2}{a} \right) \left(1 + \frac{a}{\delta m_{31}^2} \right) \theta_{13} \\
&= \frac{1}{4} O(\varepsilon^2) , \\
\tilde{\kappa}_{\mu\mu} &= \tilde{c}_{12}^2 - \cos(2\tilde{\theta}_{12}) \tan^2 \tilde{\theta}_{13} \tan^2 \tilde{\theta}_{\text{atm}} - \left(\frac{2\tilde{A}}{\cos^2 \tilde{\theta}_{13} \cos^2 \tilde{\theta}_{\text{atm}}} \right) \cos \tilde{\delta} \\
&= O(\varepsilon^2) - O(\varepsilon^2) \cos \delta ,
\end{aligned} \tag{190}$$

for the neutrinos, and

$$\begin{aligned}
\sin \tilde{\theta}_{\text{atm}} &= \tilde{c}_{13} \tilde{s}_{23} = c_{13} s_{23} [1 + O(\varepsilon^3)] \approx \sin \theta_{\text{atm}} , \\
\tilde{A} &\approx \frac{1}{8} \sin(2\tilde{\theta}_{12}) \sin(2\tilde{\theta}_{13}) \sin(2\tilde{\theta}_{\text{atm}}) \sqrt{1 - \tan^2 \tilde{\theta}_{13} \tan^2 \tilde{\theta}_{\text{atm}}} \\
&\approx \frac{1}{4} \left(\frac{\delta m_{21}^2}{a} \right) \left(1 - \frac{a}{\delta m_{31}^2} \right) \theta_{13} = \frac{1}{4} O(\varepsilon^2) , \\
\tilde{\kappa}_{\mu\mu} &= \cos^2 \tilde{\theta}_{12} - \cos(2\tilde{\theta}_{12}) \tan^2 \tilde{\theta}_{13} \tan^2 \tilde{\theta}_{\text{atm}} - \left(\frac{2\tilde{A}}{\cos^2 \tilde{\theta}_{13} \cos^2 \tilde{\theta}_{\text{atm}}} \right) \cos \tilde{\delta} \\
&= O(1) - O(\varepsilon^2) \cos \delta ,
\end{aligned} \tag{191}$$

for the anti-neutrinos. (Recall that $\sin(2\theta_{12}) = 1 - 2O(\varepsilon^2)$ and $\sin(2\theta_{\text{atm}}) = 1 - \frac{1}{2}O(\varepsilon^2)$.) This shows that the coefficient of $\cos \delta$ in $\tilde{\kappa}_{\mu\mu}$ ($\tilde{\kappa}_{\mu\mu}$) is suppressed by one power of ε relative to $\kappa_{\mu\mu}$. Consequently, the ν_μ and $\bar{\nu}_\mu$ survival probabilities remain insensitive to the CP violating phase δ , despite the enhancements of $\tilde{\Delta}_{21}$, $\tilde{\Delta}_{21}$ over Δ_{21} . Looking at the arguments of the sines more carefully, we find

$$\begin{aligned}
\Delta_{31} - \kappa_{\mu\mu} \Delta_{21} &= (\Delta_{31} - c_{12}^2 \Delta_{21}) + O(\varepsilon^3 \Delta_{31}) , \\
\tilde{\Delta}_{31} - \tilde{\kappa}_{\mu\mu} \tilde{\Delta}_{21} &\approx (\Delta_{31} - c_{12}^2 \Delta_{21}) - \tilde{c}_{12}^2 \left(\frac{a}{2E} L - \Delta_{21} \cos 2\theta_{12} \right) \\
&= (\Delta_{31} - c_{12}^2 \Delta_{21}) + O(\varepsilon^3 \Delta_{31}) , \\
\tilde{\Delta}_{31} - \tilde{\kappa}_{\mu\mu} \tilde{\Delta}_{21} &\approx \left(\Delta_{31} + \frac{a}{2E} L - \Delta_{21} s_{12}^2 \right) - \tilde{c}_{12}^2 \left(\frac{a}{2E} L + \Delta_{21} \cos 2\theta_{12} \right) \\
&= \left(\Delta_{31} + \frac{a}{2E} L - \Delta_{21} s_{12}^2 \right) - \left(\frac{a}{2E} L + \Delta_{21} \cos 2\theta_{12} \right) + O(\varepsilon^3 \Delta_{31}) \\
&= (\Delta_{31} - c_{12}^2 \Delta_{21}) + O(\varepsilon^3 \Delta_{31}) .
\end{aligned} \tag{192}$$

Since $\sin(2\theta_{\text{atm}}) \approx \sin(2\tilde{\theta}_{\text{atm}}) \approx \sin(2\tilde{\theta}_{\text{atm}})$, we conclude

$$\tilde{P}(\nu_\mu \rightarrow \nu_\mu) \approx P(\nu_\mu \rightarrow \nu_\mu) = P(\bar{\nu}_\mu \rightarrow \bar{\nu}_\mu) \approx \tilde{P}(\bar{\nu}_\mu \rightarrow \bar{\nu}_\mu) . \tag{193}$$

That is, the ν_μ and $\bar{\nu}_\mu$ survival probabilities are insensitive to matter effects and their values in matter are the same as their values in vacuum. In Fig. 33 we compare the exact numerical values of these probabilities calculated for our example parameter set Eq. (140) with $\delta m_{31}^2 > 0$. As can be seen, the differences among these probabilities are extremely small, and our approximation has allowed us to understand this analytically.

Next, let us consider the $\nu_\mu \rightarrow \nu_e$ and $\bar{\nu}_\mu \rightarrow \bar{\nu}_e$ oscillation probabilities. They are

$$\begin{aligned}
& \tilde{P}(\nu_\mu \rightarrow \nu_e) \\
&= 4 \sin^2 \tilde{\theta}_{13} \sin^2 \tilde{\theta}_{atm} \left[\left\{ 1 - (\tilde{B} \sin \tilde{\delta}) \tilde{\Delta}_{21} \right\} \sin^2 \left(\frac{\tilde{\Delta}_{31} - \tilde{\kappa}_{\mu e} \tilde{\Delta}_{21}}{2} \right) \right. \\
&\quad + \frac{1}{4} \left\{ (\tilde{B} \sin \tilde{\delta})^2 - 2\tilde{\kappa}_{\mu e}(1 - \tilde{\kappa}_{\mu e}) \sin^2 \frac{\tilde{\Delta}_{31}}{2} - (\tilde{B} \sin \tilde{\delta})(1 - 2\tilde{\kappa}_{\mu e}) \sin \tilde{\Delta}_{31} \right\} \tilde{\Delta}_{21}^2 \\
&\quad - \frac{1}{12} \left\{ 3(\tilde{B} \sin \tilde{\delta})\tilde{\kappa}_{\mu e}^2 + 2(\tilde{B} \sin \tilde{\delta})(1 - 3\tilde{\kappa}_{\mu e}^2) \sin^2 \frac{\tilde{\Delta}_{31}}{2} - \tilde{\kappa}_{\mu e}(1 - \tilde{\kappa}_{\mu e}^2) \sin \tilde{\Delta}_{31} \right\} \tilde{\Delta}_{21}^3 \\
&\quad \left. + O(\tilde{\Delta}_{21}^4) \right], \tag{194}
\end{aligned}$$

$$\begin{aligned}
& \tilde{P}(\bar{\nu}_\mu \rightarrow \bar{\nu}_e) \\
&= 4 \sin^2 \tilde{\theta}_{13} \sin^2 \tilde{\theta}_{atm} \left[\left\{ 1 + (\tilde{B} \sin \tilde{\delta}) \tilde{\Delta}_{21} \right\} \sin^2 \left(\frac{\tilde{\Delta}_{31} - \tilde{\kappa}_{\mu e} \tilde{\Delta}_{21}}{2} \right) \right. \\
&\quad + \frac{1}{4} \left\{ (\tilde{B} \sin \tilde{\delta})^2 - 2\tilde{\kappa}_{\mu e}(1 - \tilde{\kappa}_{\mu e}) \sin^2 \frac{\tilde{\Delta}_{31}}{2} + (\tilde{B} \sin \tilde{\delta})(1 - 2\tilde{\kappa}_{\mu e}) \sin \tilde{\Delta}_{31} \right\} \tilde{\Delta}_{21}^2 \\
&\quad + \frac{1}{12} \left\{ 3(\tilde{B} \sin \tilde{\delta})\tilde{\kappa}_{\mu e}^2 + 2(\tilde{B} \sin \tilde{\delta})(1 - 3\tilde{\kappa}_{\mu e}^2) \sin^2 \frac{\tilde{\Delta}_{31}}{2} + \tilde{\kappa}_{\mu e}(1 - \tilde{\kappa}_{\mu e}^2) \sin \tilde{\Delta}_{31} \right\} \tilde{\Delta}_{21}^3 \\
&\quad \left. + O(\tilde{\Delta}_{21}^4) \right], \tag{195}
\end{aligned}$$

From Eq. (190) we obtain

$$\begin{aligned}
\tilde{B} &= \frac{\tilde{A}}{\sin^2 \tilde{\theta}_{13} \sin^2 \tilde{\theta}_{atm}} \approx \frac{1}{2} \left(\frac{\delta m_{21}^2}{a} \right) \left(1 - \frac{a}{\delta m_{31}^2} \right) \frac{1}{\theta_{13}} = \frac{1}{2} O(1), \\
\tilde{\kappa}_{\mu e} &= \tilde{s}_{12}^2 - \tilde{B} \cos \tilde{\delta} \approx 1 - \frac{1}{2} O(1) \cos \delta,
\end{aligned}$$

and from Eq. (191) we obtain

$$\tilde{B} = \frac{\tilde{A}}{\sin^2 \tilde{\theta}_{13} \sin^2 \tilde{\theta}_{atm}} \approx \frac{1}{2} \left(\frac{\delta m_{21}^2}{a} \right) \left(1 + \frac{a}{\delta m_{31}^2} \right) \frac{1}{\theta_{13}} = \frac{1}{2} O(1),$$

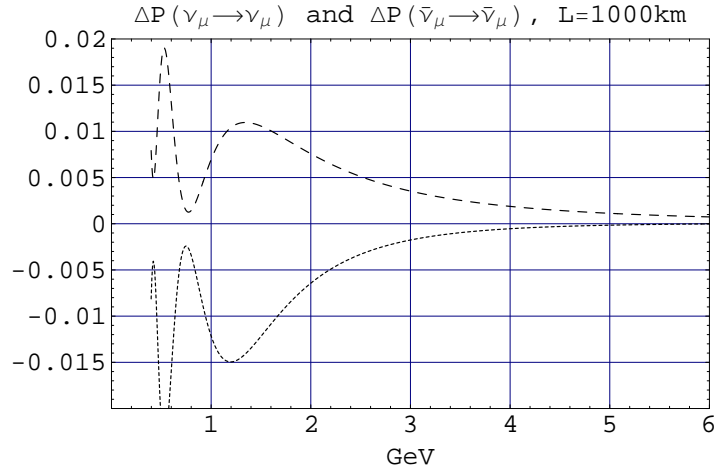
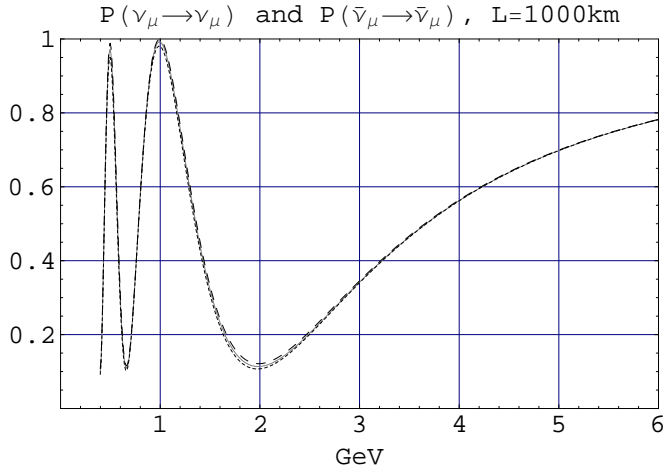
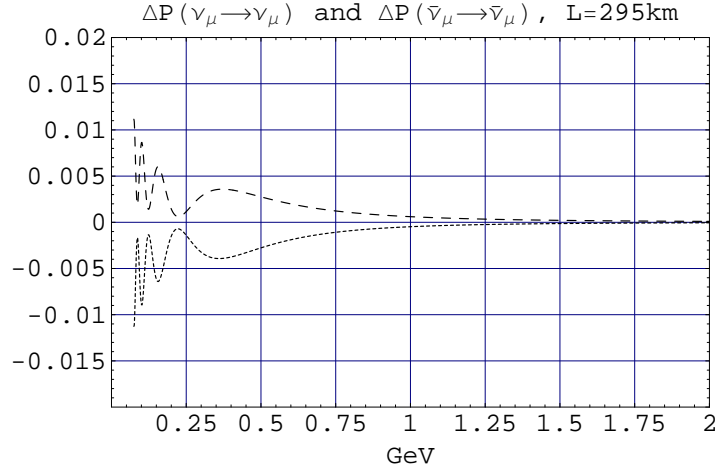
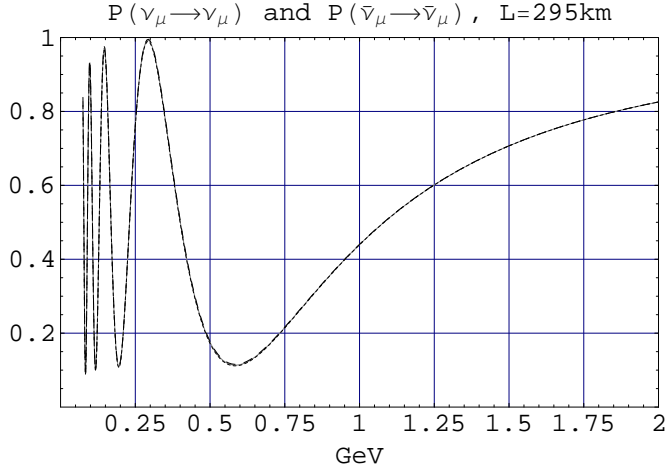


FIG. 33: Comparison of the ν_μ and $\bar{\nu}_\mu$ survival probabilities in vacuum and in matter. On the left, $P(\nu_\mu \rightarrow \nu_\mu) = P(\bar{\nu}_\mu \rightarrow \bar{\nu}_\mu)$ is the solid gray line, $\tilde{P}(\nu_\mu \rightarrow \nu_\mu)$ is the dashed black line, and $\tilde{P}(\bar{\nu}_\mu \rightarrow \bar{\nu}_\mu)$ is the dotted black line. On the right, the difference $\Delta P(\nu_\mu \rightarrow \nu_\mu) = \tilde{P}(\nu_\mu \rightarrow \nu_\mu) - P(\nu_\mu \rightarrow \nu_\mu)$ is the dashed black line, and the difference $\Delta P(\bar{\nu}_\mu \rightarrow \bar{\nu}_\mu) = \tilde{P}(\bar{\nu}_\mu \rightarrow \bar{\nu}_\mu) - P(\bar{\nu}_\mu \rightarrow \bar{\nu}_\mu)$ is the dotted blackline. The input parameters are those listed in Eq. (140) with $\delta m_{31}^2 > 0$.

$$\tilde{\kappa}_{\mu e} = \tilde{s}_{12}^2 - \tilde{B} \cos \tilde{\delta} = \frac{1}{4} O(\varepsilon^2) - \frac{1}{2} O(1) \cos \delta \approx -\frac{1}{2} O(1) \cos \delta .$$

Therefore, the expressions inside the curly brackets in the $\tilde{\Delta}_{21}^2$, $\tilde{\Delta}_{21}^2$ and $\tilde{\Delta}_{21}^3$, $\tilde{\Delta}_{21}^3$ terms are roughly of order one, with factors of 1/4 and 1/12 in front suppressing them. And since the entire expression is multiplied by $\sin^2 \tilde{\theta}_{13} = O(\varepsilon^2)$, $\sin^2 \tilde{\theta}_{13} = O(\varepsilon^2)$ from outside the square brackets, these terms are of $O(\pi^2 \varepsilon^4)$ and are negligible.

Therefore, to a good approximation, we can use the expressions

$$\begin{aligned} \tilde{P}(\nu_\mu \rightarrow \nu_e) &= 4 \sin^2 \tilde{\theta}_{13} \sin^2 \tilde{\theta}_{\text{atm}} \left\{ 1 - (\tilde{B} \sin \tilde{\delta}) \tilde{\Delta}_{21} \right\} \sin^2 \left(\frac{\tilde{\Delta}_{31} - \tilde{\kappa}_{\mu e} \tilde{\Delta}_{21}}{2} \right) , \\ \tilde{P}(\bar{\nu}_\mu \rightarrow \bar{\nu}_e) &= 4 \sin^2 \tilde{\theta}_{13} \sin^2 \tilde{\theta}_{\text{atm}} \left\{ 1 + (\tilde{B} \sin \tilde{\delta}) \tilde{\Delta}_{21} \right\} \sin^2 \left(\frac{\tilde{\Delta}_{31} - \tilde{\kappa}_{\mu e} \tilde{\Delta}_{21}}{2} \right) , \end{aligned} \quad (196)$$

where the arguments of the sine functions are given by

$$\begin{aligned} &\tilde{\Delta}_{31} - \tilde{\kappa}_{\mu e} \tilde{\Delta}_{21} \\ &\approx \tilde{\Delta}_{31} - \left(\tilde{s}_{12}^2 - \tilde{B} \cos \tilde{\delta} \right) \tilde{\Delta}_{21} \\ &\approx (\Delta_{31} - c_{12}^2 \Delta_{21}) - \left\{ 1 - \frac{1}{2} \left(\frac{\delta m_{21}^2}{a \theta_{13}} \right) \left(1 - \frac{a}{\delta m_{31}^2} \right) \cos \delta \right\} \left(\frac{a}{2E} L - \Delta_{21} \cos 2\theta_{12} \right) \\ &= \Delta_{31} \left[1 - \left(\frac{a}{\delta m_{31}^2} \right) + \frac{1}{2\theta_{13}} \left(\frac{\delta m_{21}^2}{\delta m_{31}^2} \right) \cos \delta + O(\varepsilon^2) \right] \\ &= \Delta_{31} \left[1 + \text{sign}(\delta m_{31}^2) \left(-\frac{a}{|\delta m_{31}^2|} + \frac{\varepsilon^2}{2\theta_{13}} \cos \delta \right) + O(\varepsilon^2) \right] , \end{aligned}$$

$$\begin{aligned} &\tilde{\Delta}_{31} - \tilde{\kappa}_{\mu e} \tilde{\Delta}_{21} \\ &\approx \tilde{\Delta}_{31} - \left(\tilde{s}_{12}^2 - \tilde{B} \cos \tilde{\delta} \right) \tilde{\Delta}_{21} \\ &\approx \left(\Delta_{31} + \frac{a}{2E} L - s_{12}^2 \Delta_{21} \right) - \left\{ -\frac{1}{2} \left(\frac{\delta m_{21}^2}{a \theta_{13}} \right) \left(1 + \frac{a}{\delta m_{31}^2} \right) \cos \delta \right\} \left(\frac{a}{2E} L + \Delta_{21} \cos 2\theta_{12} \right) \\ &= \Delta_{31} \left[1 + \left(\frac{a}{\delta m_{31}^2} \right) + \frac{1}{2\theta_{13}} \left(\frac{\delta m_{21}^2}{\delta m_{31}^2} \right) \cos \delta + O(\varepsilon^2) \right] \\ &= \Delta_{31} \left[1 + \text{sign}(\delta m_{31}^2) \left(\frac{a}{|\delta m_{31}^2|} + \frac{\varepsilon^2}{2\theta_{13}} \cos \delta \right) + O(\varepsilon^2) \right] , \end{aligned} \quad (197)$$

while the amplitudes are given by

$$\begin{aligned} &4 \sin^2 \tilde{\theta}_{13} \sin^2 \tilde{\theta}_{\text{atm}} \left\{ 1 - (\tilde{B} \sin \tilde{\delta}) \tilde{\Delta}_{21} \right\} \\ &\approx 2\theta_{13}^2 \left(1 + \frac{2a}{\delta m_{31}^2} \right) \left[1 - \left\{ \frac{1}{2} \left(\frac{\delta m_{21}^2}{a \theta_{13}} \right) \left(1 - \frac{a}{\delta m_{31}^2} \right) \sin \delta \right\} \left(\frac{a}{2E} L - \Delta_{21} \cos 2\theta_{12} \right) \right] \\ &= 2\theta_{13}^2 \left[1 + \frac{2a}{\delta m_{31}^2} - \frac{1}{2\theta_{13}} \left(\frac{\delta m_{21}^2}{\delta m_{31}^2} \right) \Delta_{31} \sin \delta + O(\varepsilon^2) \right] \end{aligned}$$

$$\begin{aligned}
&= 2\theta_{13}^2 \left[1 + \frac{2a}{\delta m_{31}^2} - \frac{\varepsilon^2}{2\theta_{13}} |\Delta_{31}| \sin \delta + O(\varepsilon^2) \right], \\
&4 \sin^2 \tilde{\theta}_{13} \sin^2 \tilde{\theta}_{\text{atm}} \left\{ 1 + (\tilde{B} \sin \tilde{\delta}) \tilde{\Delta}_{21} \right\} \\
&\approx 2\theta_{13}^2 \left(1 - \frac{2a}{\delta m_{31}^2} \right) \left[1 + \left\{ \frac{1}{2} \left(\frac{\delta m_{21}^2}{a\theta_{13}} \right) \left(1 + \frac{a}{\delta m_{31}^2} \right) \sin \delta \right\} \left(\frac{a}{2E} L + \Delta_{21} \cos 2\theta_{12} \right) \right] \\
&= 2\theta_{13}^2 \left[1 - \frac{2a}{\delta m_{31}^2} + \frac{1}{2\theta_{13}} \left(\frac{\delta m_{21}^2}{\delta m_{31}^2} \right) \Delta_{31} \sin \delta + O(\varepsilon^2) \right] \\
&= 2\theta_{13}^2 \left[1 - \frac{2a}{\delta m_{31}^2} + \frac{\varepsilon^2}{2\theta_{13}} |\Delta_{31}| \sin \delta + O(\varepsilon^2) \right]. \tag{198}
\end{aligned}$$

From these simple expressions, we can discern a few facts about ν_e ($\bar{\nu}_e$) appearance experiments.

Roughly speaking, the positions of the oscillation peaks will provide information on the combination

$$\text{sign}(\delta m_{31}^2) \left(\mp \frac{a}{|\delta m_{31}^2|} + \frac{\varepsilon^2}{2\theta_{13}} \cos \delta \right), \tag{199}$$

while the heights of the oscillation peaks will provide information on the combination

$$2\theta_{13}^2 \left[1 \pm \left\{ \text{sign}(\delta m_{31}^2) \frac{2a}{|\delta m_{31}^2|} - \frac{\varepsilon^2}{2\theta_{13}} |\Delta_{31}| \sin \delta \right\} \right], \tag{200}$$

where the upper signs are for the neutrinos, and the lower signs are for the anti-neutrinos.

If the oscillation peaks occur in an energy region in which

$$\frac{a}{|\delta m_{31}^2|} \ll \frac{\varepsilon^2}{2\theta_{13}}, \tag{201}$$

($\alpha \sim -2$) then the $a/|\delta m_{31}^2|$ terms in these expressions can be neglected. Then, measuring the height of the peak (or just the total ν_e or $\bar{\nu}_e$ flux using a narrow band beam) will allow us to constrain $\sin \delta$, provided that θ_{13} is well known from future reactor experiments [27, 28].

If θ_{13} is not well-known, then measuring the peak heights for both the neutrino and anti-neutrino will allow us to constrain both θ_{13} and $\sin \delta$. If one also measures the position of the peaks, either using a wide band beam or by changing the beam energy, then one can also extract information on the product

$$\text{sign}(\delta m_{31}^2) \cos \delta, \tag{202}$$

but neither $\text{sign}(\delta m_{31}^2)$ nor the sign of $\cos \delta$ can be uniquely determined, even if both neutrino and anti-neutrino beams are used [29].

These features are clearly visible in Fig. 24, which shows the probabilities to be probed by the T2K experiment [10]. In phase 2 of T2K, the oscillation event rates for both neutrinos and anti-neutrinos are to be measured, the difference from which we can extract $\sin \delta$. However, this does not provide any information on $\cos \delta$. It was proposed in Ref. [30] to measure the event rates using several beams of different energy, and thereby obtain some information on the peak position of the oscillation spectrum, but the sign of $\cos \delta$ cannot be uniquely determined unless the sign of δm_{31}^2 is known [31]. (These difficulties can be best seen visually by utilizing the Minakata-Nunokawa plot [32].)

On the other hand, if the oscillation peaks occur in an energy region in which

$$\frac{a}{|\delta m_{31}^2|} \approx \frac{\varepsilon^2}{2\theta_{13}}, \quad (203)$$

($\alpha \sim -1$) then the measurement of the peak height by itself may not be able to determine either $\text{sign}(\delta m_{31}^2)$ or $\sin \delta$, even if θ_{13} were accurately known. In particular, there will be a degeneracy between the two cases in which $\text{sign}(\delta m_{31}^2)$ and $\sin \delta$ are both positive, and both negative, as can be clearly seen in Fig. 26. Measuring peak heights for both the neutrino and anti-neutrino will not help use here since they both depend on the same linear combination of $a/\delta m_{31}^2$ and $\sin \delta$, though it will help us in determining θ_{13} . If one also measures the position of the peak, then the degeneracy in $\text{sign}(\delta m_{31}^2)$ and $\cos \delta$ which existed for the previous case can be lifted, except when $\delta \approx 0$ for the neutrino case, and $\delta \approx \pi$ for the anti-neutrino case. Due to these shortcomings in performing a single experiment at either $\alpha \sim -1$ or $\alpha \sim -2$, various scenarios have been suggested which utilize two detectors set up at different baseline lengths [14, 15, 16, 17].

For the $L = 2540$ km case, an expansion in $\tilde{\Delta}_{21}$ is no longer permissible. The approximation we used above for $\tilde{\theta}_{13}$ also breaks down as $\alpha \rightarrow 0$. We can nevertheless simplify the expressions for the oscillation probabilities and understand their behavior analytically. As an example, consider the oscillation probability $\tilde{P}(\nu_\mu \rightarrow \nu_e)$, the full expression of which is

$$\begin{aligned} \tilde{P}(\nu_\mu \rightarrow \nu_e) = & 4 |\tilde{U}_{\mu 2}|^2 |\tilde{U}_{e 2}|^2 \sin^2 \frac{\tilde{\Delta}_{21}}{2} + 4 |\tilde{U}_{\mu 3}|^2 |\tilde{U}_{e 3}|^2 \sin^2 \frac{\tilde{\Delta}_{31}}{2} \\ & + 2 \Re(\tilde{U}_{\mu 3}^* \tilde{U}_{e 3} \tilde{U}_{\mu 2} \tilde{U}_{e 2}^*) \left(4 \sin^2 \frac{\tilde{\Delta}_{21}}{2} \sin^2 \frac{\tilde{\Delta}_{31}}{2} + \sin \tilde{\Delta}_{21} \sin \tilde{\Delta}_{31} \right) \\ & + 4 \tilde{J}_{(\mu, e)} \left(\sin^2 \frac{\tilde{\Delta}_{21}}{2} \sin \tilde{\Delta}_{31} - \sin^2 \frac{\tilde{\Delta}_{31}}{2} \sin \tilde{\Delta}_{21} \right). \end{aligned} \quad (204)$$

Using the approximations in Eq. (175), except the one for $\tilde{\theta}_{13}$, we find

$$\begin{aligned}
|\tilde{U}_{\mu 2}|^2 |\tilde{U}_{e 2}|^2 &\approx s_{23}^2 \tilde{s}_{13}^2 \tilde{c}_{13}^2 - 2\tilde{A} \cos \delta, \\
|\tilde{U}_{\mu 3}|^2 |\tilde{U}_{e 3}|^2 &\approx s_{23}^2 \tilde{s}_{13}^2 \tilde{c}_{13}^2, \\
\Re(\tilde{U}_{\mu 3}^* \tilde{U}_{e 3} \tilde{U}_{\mu 2} \tilde{U}_{e 2}^*) &\approx -s_{23}^2 \tilde{s}_{13}^2 \tilde{c}_{13}^2 + \tilde{A} \cos \delta, \\
\tilde{J}_{(\mu, e)} &\approx \tilde{A} \sin \delta,
\end{aligned} \tag{205}$$

where

$$\tilde{A} \approx \left(\frac{\delta m_{21}^2}{2a} \right) \sin(2\theta_{12}) s_{23} c_{23} \tilde{s}_{13} \tilde{c}_{13}^2. \tag{206}$$

Terms of order $(\delta m_{21}^2/a)^2$ and higher have been neglected. Substituting into Eq. (204), we obtain

$$\begin{aligned}
\tilde{P}(\nu_\mu \rightarrow \nu_e) &\approx 4s_{23}^2 \tilde{s}_{13}^2 \tilde{c}_{13}^2 \sin^2 \frac{\tilde{\Delta}_{32}}{2} + 8\tilde{A} \sin \frac{\tilde{\Delta}_{32}}{2} \sin \frac{\tilde{\Delta}_{21}}{2} \cos \left(\frac{\tilde{\Delta}_{31}}{2} + \delta \right) \\
&\approx \left[s_{23} \sin(2\tilde{\theta}_{13}) \sin \frac{\tilde{\Delta}_{32}}{2} + c_{23} \tilde{c}_{13} \left(\frac{\delta m_{21}^2}{a} \right) \sin(2\theta_{12}) \sin \frac{\tilde{\Delta}_{21}}{2} \cos \left(\frac{\tilde{\Delta}_{31}}{2} + \delta \right) \right]^2 \\
&\approx \frac{1}{2} \left[\sin(2\tilde{\theta}_{13}) \sin \frac{\tilde{\Delta}_{32}}{2} + \tilde{c}_{13} \left(\frac{\delta m_{21}^2}{a} \right) \sin \frac{\tilde{\Delta}_{21}}{2} \cos \left(\frac{\tilde{\Delta}_{31}}{2} + \delta \right) \right]^2,
\end{aligned} \tag{207}$$

where we have used $\sin(2\theta_{12}) = 1 - 2O(\varepsilon)$, and $\sin(2\theta_{23}) = 1 - \frac{1}{2}O(\varepsilon^2)$. Now, the a -dependence of $\tilde{\theta}_{13}$ is different depending on the sign of δm_{31}^2 . If $\delta m_{31}^2 > 0$ (normal hierarchy), $\tilde{\theta}_{13}$ increases monotonically from θ_{13} toward $\frac{\pi}{2}$ as a increases with energy, and passes through $\frac{\pi}{4}$ around $a \approx |\delta m_{31}^2|$. If $\delta m_{31}^2 < 0$ (inverted hierarchy), $\tilde{\theta}_{13}$ decreases monotonically from θ_{13} toward 0 as a increase with energy, and is about $\theta_{13}/2$ around $a \approx |\delta m_{31}^2|$. (cf. Table IV) Therefore, if $\delta m_{31}^2 > 0$, then the coefficient of the first term in the brackets of Eq. (207) is maximized around $a \approx |\delta m_{31}^2|$. If the oscillation peak where $\tilde{\Delta}_{32} \approx \pi$ matches that energy, one can expect a maximum oscillation probability as large as $\frac{1}{2}$. (Note that this maximum probability is determined by θ_{23} and is independent of the value of θ_{13} in vacuum.) On the other hand, if $\delta m_{31}^2 < 0$, then the same coefficient is suppressed to $O(\varepsilon)$, and the oscillation probability will be suppressed by a factor of $O(\varepsilon^2)$. This difference is evident in Fig. 28. (In both cases, the second term in the brackets interferes with the first term giving the probability a weak δ -dependence.) Due to this clear difference, measuring the ν_e appearance probability at the first oscillation peak at a baseline length of $L = 2540$ km has been proposed as an unambiguous method to determine the sign of δm_{31}^2 [11].

$a/ \delta m_{31}^2 $		$O(\varepsilon^3)$	$O(\varepsilon^2)$	$O(\varepsilon)$	$O(1)$	$O(\varepsilon^{-1})$
ν	$\tilde{\theta}_{12}$	$\approx \theta_{12}$	\nearrow	$\approx \frac{\pi}{2}$		
	$\tilde{\theta}_{13}$	$\delta m_{31}^2 > 0$	$\approx \theta_{13}$		\nearrow	$\approx \frac{\pi}{2}$
		$\delta m_{31}^2 < 0$	$\approx \theta_{13}$		\searrow	≈ 0
$\bar{\nu}$	$\tilde{\theta}_{12}$	$\approx \theta_{12}$	\searrow	≈ 0		
	$\tilde{\theta}_{13}$	$\delta m_{31}^2 > 0$	$\approx \theta_{13}$		\searrow	≈ 0
		$\delta m_{31}^2 < 0$	$\approx \theta_{13}$		\nearrow	$\approx \frac{\pi}{2}$

TABLE IV: The dependence of the effective mixing angles on $a/|\delta m_{31}^2|$.

Comparing the $L = 295$ km, $L = 1000$ km, and $L = 2540$ km cases considered above, we can discern a generic trend that the oscillation probability $\tilde{P}(\nu_\mu \rightarrow \nu_e)$ (or $\tilde{P}(\bar{\nu}_\mu \rightarrow \bar{\nu}_e)$) is more sensitive to the CP violating phase δ at lower energies (shorter baselines), and more sensitive to the mass hierarchy (sign of δm_{31}^2) at higher energies (longer baselines). This can be understood as follows. First, the angle $\tilde{\theta}_{13}$, which has a different energy dependence depending on the sign of δm_{31}^2 , enters $\tilde{P}(\nu_\mu \rightarrow \nu_e)$ dominantly in the combination

$$\begin{aligned}
\sin \tilde{\theta}_{13} \sin \tilde{\theta}_{\text{atm}} &= \sin \tilde{\theta}_{13} \cos \tilde{\theta}_{13} \sin \tilde{\theta}_{23} \\
&= \frac{1}{2} \sin(2\tilde{\theta}_{13}) \sin \tilde{\theta}_{23} \\
&\approx \frac{1}{2} \sin(2\tilde{\theta}_{13}) \sin \theta_{23} .
\end{aligned} \tag{208}$$

Therefore, $\sin(2\tilde{\theta}_{13})$ determines the sensitivity of $\tilde{P}(\nu_\mu \rightarrow \nu_e)$ on the behavior of $\tilde{\theta}_{13}$. On the other hand, the size of CP violation is governed by the Jaroskog invariant,

$$\tilde{J} = \tilde{A} \sin \tilde{\delta} , \tag{209}$$

where

$$\begin{aligned}
\tilde{A} &= \tilde{s}_{12} \tilde{c}_{12} \tilde{s}_{13} \tilde{c}_{13}^2 \tilde{s}_{23} \tilde{c}_{23} \\
&= \frac{1}{4} \sin(2\tilde{\theta}_{12}) \sin(2\tilde{\theta}_{23}) \tilde{s}_{13} (1 - \tilde{s}_{13}^2) \\
&\approx \frac{1}{4} \sin(2\tilde{\theta}_{12}) \sin(2\theta_{23}) \tilde{s}_{13} (1 - \tilde{s}_{13}^2) .
\end{aligned} \tag{210}$$

In our convention where the mixing angles are in the first quadrant, \tilde{A} is bounded by

$$0 \leq \tilde{A} \leq \frac{1}{6\sqrt{3}} \equiv A_{\text{max}} . \tag{211}$$

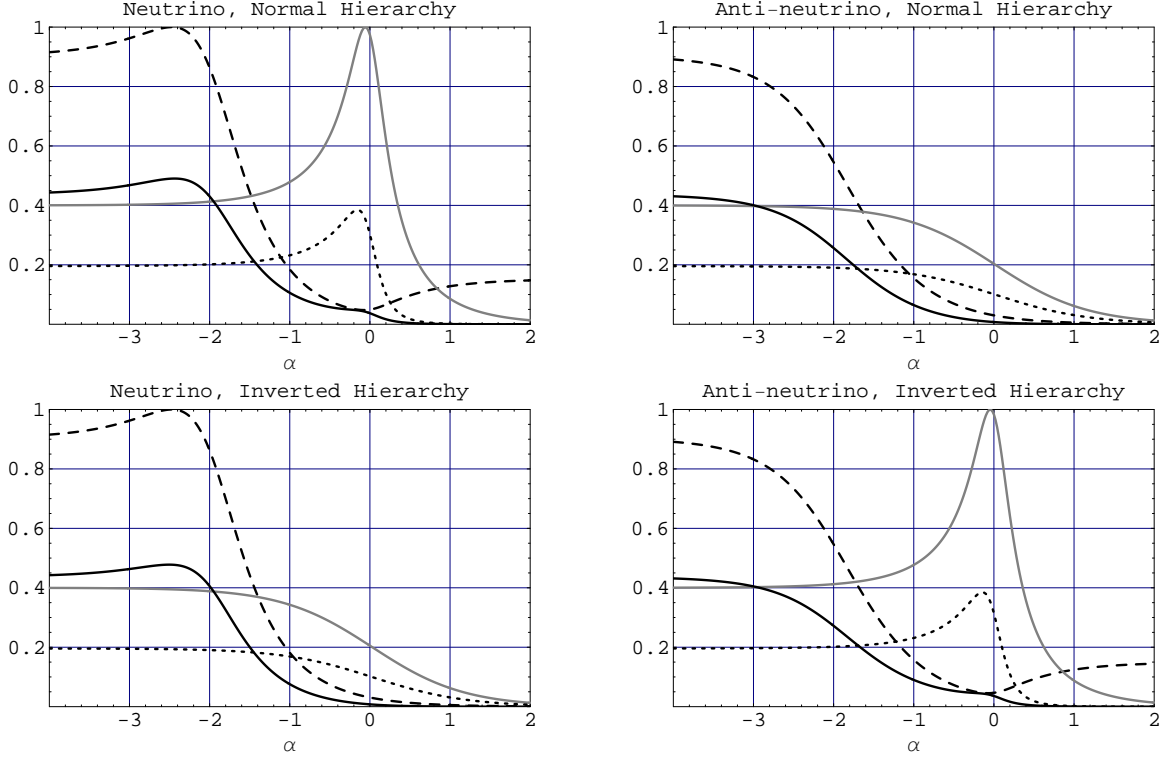


FIG. 34: The dependence of $\sin(2\tilde{\theta}_{13})$, $\sin(2\tilde{\theta}_{12})$ (solid gray lines), $\tilde{s}_{13}(1 - \tilde{s}_{13}^2)$, $\tilde{s}_{13}(1 - \tilde{s}_{13}^2)$ (dotted black lines), and \tilde{A}/A_{\max} , \tilde{A}/A_{\max} (solid black lines) on $\alpha = \log_{1/\varepsilon}(a/|\delta m_{31}^2|)$. The input parameters were those listed in Eq. (140).

In Fig. 34, we plot the α -dependence of $\sin(2\tilde{\theta}_{13})$, $\sin(2\tilde{\theta}_{12})$, $\tilde{s}_{13}(1 - \tilde{s}_{31}^2)$, and \tilde{A}/A_{\max} , and their anti-neutrino counterparts, for the input parameters of Eq. (140). It is clear from the figure that the differences in $\sin(2\tilde{\theta}_{13})$ and $\sin(2\tilde{\theta}_{13})$ between the $\delta m_{31}^2 > 0$ and $\delta m_{31}^2 < 0$ cases is most prominent at $\alpha \approx 0$ where there exists a large peak in one case which is absent in the other. This is due to the fact $\tilde{\theta}_{13}$ ($\tilde{\theta}_{13}$) crosses $\pi/4$ at $a \approx |\delta m_{31}^2|$ when $\delta m_{31}^2 > 0$ ($\delta m_{31}^2 < 0$). (cf. Table IV.) Therefore, experiments that are performed closer to $\alpha = 0$ are more sensitive to $\text{sign}(\delta m_{31}^2)$. On the other hand, the α -dependence of \tilde{A} (\tilde{A}) is dominated by that of $\sin(2\tilde{\theta}_{12})$ ($\sin(2\tilde{\theta}_{12})$) which starts out as a number of $O(1)$ at low α , but drops off quickly toward zero as α is increased from -2 to -1 . Therefore, experiments that are performed at $\alpha \lesssim -2$ are more sensitive to δ than those performed at $\alpha \gtrsim -1$.

VI. SUMMARY

In this paper, we considered the matter effect on neutrino oscillations, and derived simple analytical approximations to the effective mixing angles and effective mass-squared differences in constant density matter. Our results are summarized in Table V. These expressions can be utilized in calculating, analyzing, and understanding the behavior of the oscillation probabilities in LBL neutrino oscillation experiments.

The formalism developed in this paper can be further extended to incorporate matter effects due to the violation of universality in neutral current interactions, or additional matter effects due to new interactions. This will be presented in a subsequent paper [33].

Acknowledgments

We would like to thank Masafumi Koike and Masako Saito for helpful communications. Takeuchi would like to thank the hospitality of the particle theory group at Ochanomizu Women's University, where a major portion of this work was carried out during the summer of 2005. This research was supported in part by the U.S. Department of Energy, grant DE-FG05-92ER40709, Task A (T.T.).

		$\delta m_{31}^2 < 0$ (Inverted Hierarchy)		$\delta m_{31}^2 > 0$ (Normal Hierarchy)	
		$\frac{a}{ \delta m_{31}^2 } \geq O(1)$	$O(\varepsilon) \geq \frac{a}{ \delta m_{31}^2 }$	$\frac{a}{ \delta m_{31}^2 } \leq O(\varepsilon)$	$O(1) \leq \frac{a}{ \delta m_{31}^2 }$
Neutrino Case $\tan 2\varphi = \frac{a \sin 2\theta_{12}}{\delta m_{21}^2 - a \cos 2\theta_{12}}$ $\tan 2\phi = \frac{a \sin 2\theta_{13}}{\delta m_{31}^2 - a \cos 2\theta_{13}}$	$\tilde{\theta}_{13}$	$\theta'_{13} = \theta_{13} + \phi$			
	$\tilde{\theta}_{12}$	$\theta'_{12} = \theta_{12} + \varphi$		$\frac{\pi}{2} - \frac{c_{13}}{c'_{13}} \left(\frac{\delta m_{21}^2}{2a} \right) \sin(2\theta_{12})$	
	$\tilde{\theta}_{23}$	θ_{23}		$\theta_{23} + \frac{s_\phi}{c'_{13}} \left(\frac{\delta m_{21}^2}{2a} \right) \sin(2\theta_{12}) \cos \delta$	
	$\tilde{\delta}$	δ		$\delta - \frac{s_\phi}{c'_{13}} \left(\frac{\delta m_{21}^2}{a} \right) \frac{\sin(2\theta_{12})}{\tan(2\theta_{23})} \sin \delta$	
	λ_1	$\frac{(\delta m_{21}^2 + a) - \sqrt{(\delta m_{21}^2 - a)^2 + 4a\delta m_{21}^2 s_{12}^2}}{2}$		$\delta m_{21}^2 c_{12}^2$	
	λ_2	$\frac{(\delta m_{21}^2 + a) + \sqrt{(\delta m_{21}^2 - a)^2 + 4a\delta m_{21}^2 s_{12}^2}}{2}$		$\frac{(\delta m_{31}^2 + a) - \sqrt{(\delta m_{31}^2 - a)^2 + 4a\delta m_{31}^2 s_{13}^2}}{2}$	
	λ_3	δm_{31}^2		$\frac{(\delta m_{31}^2 + a) + \sqrt{(\delta m_{31}^2 - a)^2 + 4a\delta m_{31}^2 s_{13}^2}}{2}$	
Anti-neutrino Case $\tan 2\bar{\varphi} = -\frac{a \sin 2\theta_{12}}{\delta m_{21}^2 + a \cos 2\theta_{12}}$ $\tan 2\bar{\phi} = -\frac{a \sin 2\theta_{13}}{\delta m_{31}^2 + a \cos 2\theta_{13}}$	$\tilde{\theta}_{13}$	$\bar{\theta}'_{13} = \theta_{13} + \bar{\phi}$			
	$\tilde{\theta}_{12}$	$\frac{c_{13}}{c'_{13}} \left(\frac{\delta m_{21}^2}{2a} \right) \sin(2\theta_{12})$	$\bar{\theta}'_{12} = \theta_{12} + \bar{\varphi}$		
	$\tilde{\theta}_{23}$	$\theta_{23} - \frac{s_\phi}{c'_{13}} \left(\frac{\delta m_{21}^2}{2a} \right) \sin(2\theta_{12}) \cos \delta$	θ_{23}		
	$\tilde{\delta}$	$\delta + \frac{s_\phi}{c'_{13}} \left(\frac{\delta m_{21}^2}{a} \right) \frac{\sin(2\theta_{12})}{\tan(2\theta_{23})} \sin \delta$	δ		
	$\bar{\lambda}_1$	$\frac{(\delta m_{31}^2 - a) + \sqrt{(\delta m_{31}^2 + a)^2 - 4a\delta m_{31}^2 s_{13}^2}}{2}$	$\frac{(\delta m_{21}^2 - a) - \sqrt{(\delta m_{21}^2 + a)^2 - 4a\delta m_{21}^2 s_{12}^2}}{2}$		
	$\bar{\lambda}_2$	$\delta m_{21}^2 c_{12}^2$	$\frac{(\delta m_{21}^2 - a) + \sqrt{(\delta m_{21}^2 + a)^2 - 4a\delta m_{21}^2 s_{12}^2}}{2}$		
	$\bar{\lambda}_3$	$\frac{(\delta m_{31}^2 - a) - \sqrt{(\delta m_{31}^2 + a)^2 - 4a\delta m_{31}^2 s_{13}^2}}{2}$	δm_{31}^2		

TABLE V: The approximate formulae for the effective mixing angles and effective mass-squared differences derived in this paper.

-
- [1] M. B. Smy *et al.* [Super-Kamiokande Collaboration], Phys. Rev. D **69**, 011104 (2004) [arXiv:hep-ex/0309011]. S. N. Ahmed *et al.* [SNO Collaboration], Phys. Rev. Lett. **92**, 181301 (2004) [arXiv:nucl-ex/0309004].
- [2] T. Araki *et al.* [KamLAND Collaboration], Phys. Rev. Lett. **94**, 081801 (2005) [arXiv:hep-ex/0406035].
- [3] Y. Ashie *et al.* [Super-Kamiokande Collaboration], Phys. Rev. Lett. **93**, 101801 (2004) [arXiv:hep-ex/0404034]; Y. Ashie *et al.* [Super-Kamiokande Collaboration], Phys. Rev. D **71**, 112005 (2005) [arXiv:hep-ex/0501064].
- [4] M. Apollonio *et al.* [CHOOZ Collaboration], Phys. Lett. B **466**, 415 (1999) [arXiv:hep-ex/9907037]; M. Apollonio *et al.* [CHOOZ Collaboration], Eur. Phys. J. C **27**, 331 (2003) [arXiv:hep-ex/0301017].
- [5] M. Fukugita and T. Yanagida, Phys. Lett. B **174**, 45 (1986).
- [6] M. H. Ahn *et al.* [K2K Collaboration], Phys. Rev. Lett. **93**, 051801 (2004) [arXiv:hep-ex/0402017], E. Aliu *et al.* [K2K Collaboration], Phys. Rev. Lett. **94**, 081802 (2005) [arXiv:hep-ex/0411038], C. Mariani [K2K Collaboration], arXiv:hep-ex/0505019.
- [7] G. Rosa [OPERA Collaboration], Nucl. Phys. Proc. Suppl. **145**, 98 (2005), H. Pessard [OPERA Collaboration], arXiv:hep-ex/0504033.
- [8] G. S. Tzanakos [MINOS Collaboration], AIP Conf. Proc. **721**, 179 (2004).
- [9] D. Ayres *et al.* [NOvA Collaboration], arXiv:hep-ex/0210005, D. S. Ayres *et al.* [NOvA Collaboration], arXiv:hep-ex/0503053,
- [10] Y. Itow *et al.*, arXiv:hep-ex/0106019; Y. Hayato [T2K Collaboration], Nucl. Phys. Proc. Suppl. **143**, 269 (2005), K. Kaneyuki [T2K Collaboration], Nucl. Phys. Proc. Suppl. **145**, 178 (2005), Y. Hayato [T2K Collaboration], Nucl. Phys. Proc. Suppl. **147**, 9 (2005). See also the JHF Neutrino Working Group's home page, <http://neutrino.kek.jp/jhfnu/>.
- [11] M. V. Diwan *et al.*, Phys. Rev. D **68**, 012002 (2003) [arXiv:hep-ph/0303081].
- [12] N. Okamura, M. Aoki, K. Hagiwara, Y. Hayato, T. Kobayashi, T. Nakaya and K. Nishikawa, arXiv:hep-ph/0104220; M. Aoki, K. Hagiwara, Y. Hayato, T. Kobayashi, T. Nakaya, K. Nishikawa and N. Okamura, Phys. Rev. D **67**, 093004 (2003) [arXiv:hep-ph/0112338].
- [13] H. S. Chen *et al.* [VLBL Study Group H2B-1], arXiv:hep-ph/0104266, Y. F. Wang, K. Whis-

- nant, Z. H. Xiong, J. M. Yang and B. L. Young [VLBL Study Group H2B-4], Phys. Rev. D **65**, 073021 (2002) [arXiv:hep-ph/0111317].
- [14] H. Minakata and H. Nunokawa, Phys. Lett. B **413**, 369 (1997) [arXiv:hep-ph/9706281]; V. Barger, D. Marfatia and K. Whisnant, Phys. Lett. B **560**, 75 (2003) [arXiv:hep-ph/0210428].
- [15] M. Ishitsuka, T. Kajita, H. Minakata and H. Nunokawa, Phys. Rev. D **72**, 033003 (2005) [arXiv:hep-ph/0504026].
- [16] K. Hagiwara, N. Okamura and K. i. Senda, arXiv:hep-ph/0504061.
- [17] O. Mena Requejo, S. Palomares-Ruiz and S. Pascoli, Phys. Rev. D **72**, 053002 (2005) [arXiv:hep-ph/0504015]; O. Mena and S. Parke, Phys. Rev. D **72**, 053003 (2005) [arXiv:hep-ph/0505202]; O. Mena, S. Palomares-Ruiz and S. Pascoli, arXiv:hep-ph/0510182.
- [18] L. Wolfenstein, Phys. Rev. D **17**, 2369 (1978); R. R. Lewis, Phys. Rev. D **21**, 663 (1980); V. D. Barger, K. Whisnant, S. Pakvasa and R. J. N. Phillips, Phys. Rev. D **22**, 2718 (1980); S. P. Mikheyev and A. Yu. Smirnov, Yad. Fiz. **42**, 1441 (1985), [Sov. J. Nucl. Phys. **42**, 913 (1986)]; S. P. Mikheyev and A. Yu. Smirnov, Nuovo Cimento **C9**, 17 (1986).
- [19] P. Lipari, Phys. Rev. D **61**, 113004 (2000) [arXiv:hep-ph/9903481]; V. D. Barger, S. Geer, R. Raja and K. Whisnant, Phys. Lett. B **485**, 379 (2000) [arXiv:hep-ph/0004208].
- [20] K. Kimura, A. Takamura and H. Yokomakura, J. Phys. G **29**, 1839 (2003); K. Kimura, A. Takamura and H. Yokomakura, Phys. Rev. D **66**, 073005 (2002) [arXiv:hep-ph/0205295]; K. Kimura, A. Takamura and H. Yokomakura, Phys. Lett. B **537**, 86 (2002) [arXiv:hep-ph/0203099].
- [21] J. Arafune, M. Koike and J. Sato, Phys. Rev. D **56**, 3093 (1997) [Erratum-ibid. D **60**, 119905 (1999)] [arXiv:hep-ph/9703351].
- [22] M. Freund, Phys. Rev. D **64**, 053003 (2001) [arXiv:hep-ph/0103300].
- [23] Z. Maki, M. Nakagawa and S. Sakata, Prog. Theor. Phys. **28**, 870 (1962).
- [24] “Neutrino mass, mixing, and flavor change”, B. Kayser, in the *Review of Particle Physics*, Phys. Lett. B **592** (2004) 1.
- [25] K. Hagiwara and N. Okamura, Nucl. Phys. B **548**, 60 (1999) [arXiv:hep-ph/9811495].
- [26] A. M. Dziewonski and D. L. Anderson, Physics of the Earth and Planetary Interiors, **25** (1981) 297–356.
- [27] F. Ardellier *et al.* [Double-Chooz Collaboration], arXiv:hep-ex/0405032; F. Dalnoki-Veress

- [Double-Chooz Collaboration], arXiv:hep-ex/0406070.
- [28] F. Suekane [KASKA Collaboration], arXiv:hep-ex/0407016.
- [29] V. Barger, D. Marfatia and K. Whisnant, Phys. Rev. D **65**, 073023 (2002) [arXiv:hep-ph/0112119].
- [30] M. Aoki, K. Hagiwara and N. Okamura, Phys. Lett. B **554**, 121 (2003) [arXiv:hep-ph/0208223].
- [31] K. Hagiwara, Nucl. Phys. Proc. Suppl. **137**, 84 (2004) [arXiv:hep-ph/0410229].
- [32] H. Minakata and H. Nunokawa, JHEP **0110**, 001 (2001) [arXiv:hep-ph/0108085].
- [33] M. Honda, N. Okamura, and T. Takeuchi, in preparation.